UNIVERSITY OF OKLAHOMA

GRADUATE COLLEGE

CASIMIR EFFECT: AN AVATAR OF THE QUANTUM VACUUM

A DISSERTATION

SUBMITTED TO THE GRADUATE FACULTY

in partial fulfillment of the requirements for the

Degree of

DOCTOR OF PHILOSOPHY

By

KULOTH V. SHAJESH
Norman, Oklahoma
2008

CASIMIR EFFECT: AN AVATAR OF THE QUANTUM VACUUM

A DISSERTATION APPROVED FOR THE
HOMER L. DODGE DEPARTMENT OF PHYSICS AND ASTRONOMY

BY

Kimball A. Milton, Chair

David Branch

Leonid Dickey

Ronald Kantowski

Chung Kao

©Copyright by KULOTH V. SHAJESH 2008
All Rights Reserved.

I dedicate this thesis to my father, V. Karunan, my mother, K. Yeshoda, and my sister, K. V. Shamna, for their unconditional love and support. I also extend this dedication to my brother-in-law, Krishnan Digvijay, and my nephews, Krishank and Kaushik.

Acknowledgements

First and foremost I would like to thank my thesis adviser, Kimball A. Milton, for giving me ample amount of independence during this project. I have had a very productive and a very rich learning experience under Kim's guidance. Kim's constructive criticisms almost always led me into regions of thought which would not have been explored otherwise. The field theoretical techniques I have learned from Kim, as part of Schwinger's legacy, are precious and will greatly benefit my work in the future.

Most of the work reported here evolved during the innumerable presentations and discussions that took place in the group meetings attended by Kim, Inés Cavero-Peláez, Prachi Parashar, Jef Wagner, and Archana Anandakrishnan. I would like to thank each of the group members for their invaluable input. Since Fall 2005 at least one of the group members have been attending the meetings virtually using the VRVS (Virtual Room Videoconferencing System) and lately using the EVO (Enabling Virtual Organizations) system. I would like to take this opportunity to thank the VRVS team for making these meetings feasible.

My work has benefited from the Quantum Vacuum meeting, which is an annual workshop attended by my collaborators in this region of the country, and the workshop on Quantum Field Theory Under the Influence of External conditions (QFEXT). I would like to particularly thank Iver Brevik, Simen Ellingsen, Steve Fulling, Lev

Kaplan, Klaus Kirsten, Zhonghai Liu, and Justin Wilson for discussions, constructive comments, and suggestions at various stages of this project. Without listing the names I thank everyone who contributed to the knowledge to make this project achievable.

I thank my committee members David Branch, Leonid Dickey, Ronald Kantowski, and Chung Kao for their time and support. I acknowledge Pravin Chaubey, Joe Regan, Milinda Rupasinghe, and Priyangika Wickramarachchi, for their kind company while I was compiling this thesis.

Last but not the least, I would like to thank Phyllis and Jack Edwards, Sandy and John Furneaux, the complete Hendley family, Margarita and Kim Milton, and Elissa and O'Tar Norwood, for their warm support during my stay in Norman.

Contents

Acknowledgements iv
Abstract x

1 Vacuum energy **1**
1.1 Scalar field interacting with a background potential 2
1.2 Casimir energy 7
1.3 Energy momentum tensor 8
1.4 Energy density 11
1.5 Casimir force 14

2 Green's function **16**
2.1 Inhomogeneous differential equations 16
2.1.1 Illustrative example 18
2.2 Reciprocal symmetry of Green's function 26
2.3 Green's function for δ-function potentials 27
2.3.1 Green's function for a single plate 27
2.3.2 Green's function for parallel plates 31
2.3.3 Green's function for a single cylinder 33
2.3.4 Green's function for two concentric cylinders 35
2.4 Derivatives of the Green's function 37

3 Casimir plates **40**
3.1 Single semitransparent plate 42
3.2 Parallel semitransparent plates 44

4 How does Casimir energy fall? **50**
4.1 Rindler Coordinates 52
4.2 Formalism 55
4.2.1 Single plate falling in a constant gravitational field 59
4.2.2 Parallel plates falling in a constant gravitational field 61
4.3 Weak gravity approximation 63
4.4 Interpretations and conclusions 66

4.4.1 Gravitational force on a single particle 68
4.4.2 Renormalization 69

5 Inertial forces on vacuum energy **71**
5.1 Force in the local Lorentz coordinates 73
5.1.1 Rindler metric 75
5.2 Rotating Casimir apparatus 76
5.2.1 Centripetal force 79
5.2.2 Centripetal force on a single plate 81
5.2.3 Parallel plates 81
5.3 Orientation independence of centripetal force 83

6 Lateral Casimir force **86**
6.1 Statement of the problem 88
6.1.1 Casimir energy contributing to the lateral force 91
6.1.2 Formal series expansion 93
6.2 Leading order contribution 94
6.2.1 Second order perturbation in Casimir energy due to corrugations 94
6.2.2 Comparison of our leading order result with earlier results in the literature 98
6.2.3 Sinusoidal corrugations: Leading order 101
6.3 Next-to-leading-order contribution 105
6.3.1 Fourth order perturbation in Casimir energy due to corrugations 106
6.3.2 Sinusoidal corrugations: Next-to-leading order 114
6.4 Proximity force approximation 120
6.5 Analysis and discussion 123

Conclusions **133**

List of Figures

2.1 Description of the regions in the $z - z'$ domain on which the Green's function for a single plate is defined. 28

2.2 Description of the regions in the $z - z'$ domain on which the Green's function for parallel plates is defined. 31

5.1 Casimir apparatus rotating with constant angular speed ω about the $\bar{x}$ axis. The plane of the plates are chosen to be perpendicular to the radial direction. We have $r_a = r_0 - \frac{a}{2}$, and $r_b = r_0 + \frac{a}{2}$. 77

5.2 A Casimir apparatus oriented at an angle α with respect to the tangent to the circle of radius r_0 and rotating with constant angular speed ω about the $\bar{x}$ axis. We have $r_a \cos\alpha = r_0 \cos\alpha - \frac{a}{2}$, $r_b \cos\alpha = r_0 \cos\alpha + \frac{a}{2}$, $r_0 = (r_a + r_b)/2$, and $a = (r_b - r_a)\cos\alpha$. 84

6.1 Parallel plates with sinusoidal corrugations. 100

6.2 Dirichlet limit: Plot of $A_D^{(1,1)}(k_0 a)$ versus $k_0 a$. 102

6.3 Weak coupling limit: Plot of $A_W^{(2)}(k_0 a) = e^{-k_0 a} e_2(k_0 a)$ versus $k_0 a$. . . 104

6.4 Dirichlet limit: Plot of $A_D^{(3,1)}(k_0 a)$ and $A_D^{(2,2)}(k_0 a)$ versus $k_0 a$. The dashed curve represents $A_D^{(1,1)}(k_0 a)$ which is plotted here for reference. 117

6.5 Weak coupling limit: Plot of $A_W^{(4)}(k_0 a)$ and $A_W^{(4)}(2k_0 a)$ versus $k_0 a$. The dashed curve represents $A_W^{(2)}(k_0 a)$ which is plotted here for reference. 119

6.6 Dirichlet limit: The plots on the left show $\mathcal{F}_D^{[\infty,4]}$ versus $k_0 a$ for various values of $k_0 y_0$. The dashed curve represents $\mathcal{F}_D^{[\infty,2]}$ which is plotted here for reference. In each plot the higher values of $k_0 h$ deviate more from the reference. The plots on the right show the fractional correction in the next-to-leading order contribution. In each plot the higher values of $k_0 h$ have larger corrections. 125

6.7 Weak coupling limit: The plots on the left show $\mathcal{F}_D^{[\infty,\infty]}$ versus $k_0 a$ for various values of $k_0 y_0$ at $k_0 h = 0.3$. The dashed curves represents $\mathcal{F}_D^{[\infty,2]}$ and $\mathcal{F}_D^{[\infty,4]}$ which is plotted here for reference. In each plot the exact value is greater than the value estimated by $\mathcal{F}_D^{[\infty,4]}$. The plots on the right show the fractional error in the perturbative result. In each plot the higher values of $k_0 h$ have larger errors. 127
6.8 Weak coupling limit: Fractional error in PFA is plotted as the dashed curve. The corresponding error in the perturbative result is plotted as the bold curve and is described by the axis on the right. 131
6.9 Weak coupling limit: On the left the PFA is shown as the dashed curve. The exact results for higher values of $k_0 a$ are seen to deviate from the dashed curve. On the right the fractional error in PFA is shown to increase with higher values of $k_0 a$. 132

Abstract

In this dissertation we study the Casimir effect, which is demonstrated to be a manifestation of the quantum vacuum. We confine our study to the case of scalar fields which serves as a toy model to the experimentally relevant case of electrodynamics. The boundary conditions are imposed by constructing δ-function potentials, so-called semitransparent boundaries. The coupling to the δ-function potential reduces to the Dirichlet boundary condition in the strong coupling limit. In the case of electrodynamics the strong coupling limit corresponds to metallic plates, and the weak coupling limit corresponds to tenuous dielectrics.

In chapter 1 we derive the expression for the vacuum energy in the presence of a background for the case of scalar fields. The vacuum energy, or the Casimir energy, is expressed in terms of the trace of the logarithm of Green's functions. Thus the problem is reduced to solving a second order differential equation for the Green's function in the presence of a background potential. The Casimir energy is compared to the alternate expression derived from the energy-momentum tensor associated with the field in the presence of a background. The Casimir force is interpreted as the force between two objects arising due to the change in energy when the distance between their center of masses is varied. The Casimir force is also identified in terms of the divergence of the energy-momentum tensor.

In Chapter 2 we study the differential equations satisfied by Green's function and present solutions to the Green's functions which will be used in this thesis.

Using the expressions derived in chapters 1 and 2 we derive the Casimir energy associated with a single plate, and two parallel plates, in chapter 3. The infinite energy associated with the vacuum in the absence of a potential, or the plates, which is a divergent quantity, is isolated. The Casimir energy associated with a single plate is shown to be divergent. The Casimir energy for two parallel plates is written as a sum of three terms. Two of these terms correspond to the energy associated with the two single plates constituting the parallel plates, each of which is divergent. The third term which is finite is interpreted to arise due to the interaction between the two plates. The Casimir force on a single plate is evaluated to be zero. This is expected because we do not change the energy by shifting a single plate due to translational symmetry. The same argument applies for the two divergent terms associated with the single plates forming the parallel plates. But the third finite term does contribute to a change in the energy when the distance between the plates is changed. We derive an explicit expression for the Casimir force between parallel plates for arbitrary couplings to the δ-function potentials. In the strong coupling limit we recover the Casimir force in the Dirichlet limit for the case of scalar fields.

Even though the divergent terms in the total energy associated with the single plates constituting two parallel plates do not contribute to the Casimir force, the situation still appears unsatisfactory. Any form of energy acts as a 'source' in the Einstein's equation and thus "falls" under gravity. The classic example is that of bending of light around a planet. How do the divergent terms associated with single plates interact with gravity? In chapter 4 we consider parallel plates falling in a weak gravitational field described by a space-time given in terms of Rindler coordinates.

For the case of parallel plates we show that all the three terms contributing to the total energy interact with a weak gravitational field exactly like a conventional mass. We interpret this as meaning that the divergent terms associated with the single plates serve to renormalize the bare masses of the single plates.

In chapter 5 we generalize our results for other inertial forces. In particular we demonstrate that the results of chapter 4 hold for the case of two parallel plates rotating with a constant angular speed. We show that exactly as in the case of Rindler acceleration, the Casimir energy, including its divergent parts, experiences a centripetal force exactly like a conventional mass. In chapter 4 our analysis is restricted to the case when the direction of the Rindler acceleration is in a direction perpendicular to the plane containing the plates. In chapter 5 we generalize this result for the case when the parallel plates makes an arbitrary angle with respect to the tangent to the circle of rotation. We show that the centripetal force is independent of the orientation of the parallel plates in a frame in which the center of inertia is at the origin.

In chapter 6 we study parallel plates with sinusoidal corrugations. The energy associated with the parallel plates when the corrugations are absent, which includes two divergent contributions from the single plates and the interaction energy contributing to the Casimir force between uncorrugated plates, is treated as a background and separated from the outset. The lateral force arising due to the change in energy due to a relative lateral shift in a direction parallel to the plates is calculated perturbatively for the case when the mean amplitude of the corrugations is small in comparison to the wavelength associated with the corrugations. The lateral force is calculated to the leading—and next-to-leading—order in perturbation. The corresponding next-to-leading-order results for the case of electrodynamics will reduce

the error in the theoretical prediction sufficiently for comparison with the current experiments. It should be noted that once the required accuracy is met in the measurement of Casimir forces they can be used to infer knowledge of new physics. Very recently (June 2008) it has been reported that an accuracy of 0.1% between theory and experiment has been met for the case of dielectric gratings.

Chapter 1

Vacuum energy

Casimir in 1948 [1] theoretically demonstrated that two uncharged parallel conducting plates attract. This force of attraction can be attributed to the quantum vacuum energy associated with the electromagnetic field between the conducting plates. Experimental measurements of this force since 1997 [2] and the plausible dominance of this force in the nano-scale regime have attracted the attention of physicists from various research area to the subject recently. These observations being invoked as an evidence of zero-point energy of the vacuum has been questioned in [3]. In this thesis we demonstrate that the Casimir energy is indeed a manifestation of the quantum vacuum starting from Schwinger's source techniques, which is often used to argue the other point of view.

We shall concentrate on the interaction of a scalar field through a background potential. Study of this simplified model sheds light on the more physical problem of electrodynamics.

In this chapter we give a derivation of the Casimir energy in the quantum field theoretical setting. We derive an expression for the quantum vacuum energy, or the

Casimir energy, in terms of the Green's function in the presence of a background potential. These ideas were explicit in the work of Schwinger [4] who played a very dominant role in developing and honing the formalism of quantum field theory as we know it today. Most recently these ideas have been highlighted in [5], [6], and references therein.

1.1 Scalar field interacting with a background potential

Let us consider a scalar field, $\phi(x)$, interacting with a scalar background potential, $V(x)$, described by the Lagrangian density

$$\mathcal{L}(\phi(x)) = -\frac{1}{2}\,\partial_\mu\phi(x)\partial^\mu\phi(x) - \frac{1}{2}\,V(x)\,\phi(x)^2. \tag{1.1}$$

In terms of the source function, $K(x)$, corresponding to the scalar field, we write the action for this description to be

$$W[\phi;K] = \int d^4x\Big[K(x)\phi(x) + \mathcal{L}(\phi(x))\Big]. \tag{1.2}$$

The vacuum to vacuum persistence amplitude,

$$Z[K] = \langle 0_+|0_-\rangle^K, \tag{1.3}$$

which generates the amplitudes for all the physical processes, satisfies the Schwinger's quantum action principle, (refer to [7, 8, 9, 10], and to [11, 12, 13, 14, 15, 16, 17]),

$$\delta Z[K] = i \langle 0_+ | \, \delta W[\phi; K] \, | 0_- \rangle^K. \tag{1.4}$$

Our immediate task will be to get a formal solution for the vacuum amplitude, $Z[K]$, in the form

$$Z[K] = e^{i\,W[K]}, \tag{1.5}$$

where $W[K]$, which is not an action anymore, is dependent only on the source function. Note that the action, $W[\phi; K]$ in eq. (1.2), which satisfied the action principle, was described in terms of both the (operator) scalar field and the source function.

Schwinger's quantum action principle is basically a statement of the calculus satisfied by the vacuum amplitude. It dictates how the vacuum amplitude deviates due to a small variation in the action. The variation in the action can be generated due to a variable or a function. For our purpose we shall find it suitable to study the variation of the action due to the source function, $K(x)$, the operator field, $\phi(x)$, and the background potential, $V(x)$.

Variation with respect to the source function, $K(x)$, in the quantum action principle, in eq. (1.4), leads to

$$\delta Z[K] = i \int d^4x \, \delta K(x) \, \langle 0_+ | \, \phi(x) \, | 0_- \rangle^K, \tag{1.6}$$

which allows us to write

$$\varphi(x) \equiv \frac{1}{Z[K]} \frac{1}{i} \frac{\delta Z[K]}{\delta K(x)} = \frac{\langle 0_+ | \, \phi(x) \, | 0_- \rangle^K}{Z[K]}, \tag{1.7}$$

where the redefined scalar field, on the left of the above expression, is an effective field. This will be used to replace operator fields with functional derivatives with respect to the sources.

Variation with respect to the scalar field, $\phi(x)$, leaves the action stationary using the stationary action principle which states that there is no change in the action due to a variation in a dynamical field for variations which vanish on the boundary. To study the consequence of this principle we begin by noting, using eq. (1.1), that

$$\int d^4x\, \delta\mathcal{L}(\phi(x)) = \int d^4x\, \delta\phi(x)\, [\partial^2 - V(x)]\, \phi(x), \tag{1.8}$$

where we have integrated by parts and defined the variations on the surface of integration to be zero. Using the above variation in the Lagrangian in the quantum action principle, in eq. (1.4), we have

$$\delta Z[K] = i \int d^4x\, \langle 0_+|\, \delta\phi(x) \Big[[\partial^2 - V(x)]\phi(x) + K(x) \Big]\, |0_-\rangle^K. \tag{1.9}$$

Choosing the variations, $\delta\phi(x)$, to be classical number variations, which presumably is not a necessary restriction (refer to [11, 12, 13, 14, 15, 16, 17]), and then using eq. (1.7) to replace the operator field with functional derivatives with respect to the source function, and finally invoking the stationary action principle, we conclude

$$-\Big[\partial^2 - V(x)\Big]\, \frac{1}{i} \frac{\delta Z[K]}{\delta K(x)} = K(x) Z[K]. \tag{1.10}$$

The above differential equation can be immediately inverted and rewritten in the

form, after identifying the effective field using eq. (1.7),

$$\varphi(x) = \frac{1}{Z[K]} \frac{1}{i} \frac{\delta Z[K]}{\delta K(x)} = \int d^4x' G(x, x') K(x'), \tag{1.11}$$

where we defined the inverse of the differential operator, the Green's function, as

$$-\Big[\partial^2 - V(x)\Big] G(x, x') = \delta^{(4)}(x - x'). \tag{1.12}$$

The solution to eq. (1.11) is a Gaussian in the functional sense, and when written in the desired form in eq. (1.5), lets us identify

$$W[K] = Q[V] + \frac{1}{2} \int d^4x \int d^4x' K(x) G(x, x') K(x'), \tag{1.13}$$

where $Q[V]$ is a functional of the background potential alone.

For the case when the background potential is switched off, described by $V = 0$, we have

$$Z_0[K] = e^{iW_0[K]}, \tag{1.14}$$

where

$$W_0[K] = Q_0[0] + \frac{1}{2} \int d^4x \int d^4x' K(x) G_0(x, x') K(x'), \tag{1.15}$$

where quantities with subscript 0 are the corresponding quantities for the case $V = 0$. In particular $G_0(x, x')$ is the corresponding Green's function in eq. (1.12) for the case when $V = 0$ given as

$$-\partial^2 G_0(x, x') = \delta^{(4)}(x - x'). \tag{1.16}$$

Now, in the absence of a source function, and for the case $V = 0$, the vacuum should

not decay, which amounts to the statement $\langle 0_+|0_-\rangle^{K=0}$ is a pure phase. Further requiring the ground state energy to be zero implies that $W_0[0] = 0$, which when used in eq. (1.15) lets us conclude that $Q_0[0] = 0$.

Variation with respect to the background potential, $V(x)$, in eq. (1.4) yields

$$\delta Z[K] = -\frac{i}{2}\int d^4x\, \delta V(x)\, \langle 0_+|\, \phi(x)\phi(x)\, |0_-\rangle, \tag{1.17}$$

where we can replace the operator fields with functional derivatives using eq. (1.7) to rewrite

$$\frac{\delta Z[K]}{\delta V(x)} = -\frac{i}{2}\frac{1}{i}\frac{\delta}{\delta K(x)}\frac{1}{i}\frac{\delta}{\delta K(x)} Z[K] \tag{1.18}$$

and then write the formal solution as

$$Z[K] = e^{-\frac{i}{2}\int d^4x\, V(x)\frac{1}{i}\frac{\delta}{\delta K(x)}\frac{1}{i}\frac{\delta}{\delta K(x)}} e^{\frac{i}{2}\int d^4x \int d^4x' K(x) G_0(x,x') K(x')}. \tag{1.19}$$

Using the standard identity, we have

$$W[K] = -\frac{i}{2}\,\mathrm{Tr}\ln GG_0^{-1} + \frac{1}{2}\int d^4x \int d^4x' K(x) G(x,x') K(x'), \tag{1.20}$$

which uses

$$G = (1 + G_0 V)^{-1} G_0. \tag{1.21}$$

Using eq. (1.20) in eq. (1.5) we observe that in the presence of a background the vacuum to vacuum transition amplitude is not zero, instead it evaluates to

$$\langle 0_+|0_-\rangle^{K=0} = e^{iW[0]} = e^{\frac{1}{2}\,\mathrm{Tr}\ln GG_0^{-1}}. \tag{1.22}$$

1.2 Casimir energy

For the case when the process under investigation is time independent, denoting τ to be the time associated with the physical process, we can evolve the vacuum state using the Hamiltonian of the system and thus conclude

$$\langle 0_+|0_-\rangle^{K=0} = \langle 0_-|e^{-iH\tau}|0_-\rangle = e^{-iE\tau}, \tag{1.23}$$

where we assumed the vacuum to be an eigenstate of the Hamiltonian. Comparing the two forms, eq. (1.22) and eq. (1.23), we thus identify the energy of the vacuum in the presence of a background to be

$$E = \frac{i}{2\tau}\,\mathrm{Tr}\ln GG_0^{-1}, \tag{1.24}$$

which serves as the central formula for calculating the Casimir energy.

Further, for the case of a time independent situation, making a Fourier transformation in the time variable and using translational independence in time, we can write

$$G(x,x') = \int_{-\infty}^{\infty} \frac{d\omega}{2\pi}\, e^{-i\omega(t-t')}\bar{G}(\mathbf{x},\mathbf{x}';\omega), \tag{1.25}$$

which when substituted in eq. (1.12) leads to the differential equation

$$-\Big[\omega^2 + \nabla^2 - V(x)\Big]\,\bar{G}(\mathbf{x},\mathbf{x}';\omega) = \delta^{(3)}(x-x') \tag{1.26}$$

for the Fourier transformed Green's function, $\bar{G}(\mathbf{x},\mathbf{x}';\omega)$. The above equation can be

immediately inverted to yield, in symbolic notation,

$$\bar{G}^{-1} = [-\omega^2 - \nabla^2 + V]. \tag{1.27}$$

Using the above form in eq. (1.24) we have

$$E = \frac{i}{2}\int_{-\infty}^{\infty}\frac{d\omega}{2\pi}\,\mathrm{Tr}\ln\bar{G}\bar{G}_0^{-1} = -\frac{1}{2}\int_{-\infty}^{\infty}\frac{d\zeta}{2\pi}\,\mathrm{Tr}\ln\bar{G}\bar{G}_0^{-1}, \tag{1.28}$$

where we note that because of time independence in the problem the ω integral commutes with the logarithm. We have also made a Euclidean rotation and switched to imaginary frequencies using the prescription $\omega \to i\zeta$. The trace now is only over the spatial coordinates. Thus, we have

$$E = \frac{1}{2}\int_{-\infty}^{\infty}\frac{d\zeta}{2\pi}\,\mathrm{Tr}\ln\Big[\zeta^2 - \nabla^2 + V\Big] - \frac{1}{2}\int_{-\infty}^{\infty}\frac{d\zeta}{2\pi}\,\mathrm{Tr}\ln\Big[\zeta^2 - \nabla^2\Big]. \tag{1.29}$$

Integrating by parts and throwing away the boundary terms we derive

$$E = -\frac{1}{2}\int\frac{d\zeta}{2\pi}\,2\zeta^2\int d^3x\,\bar{G}(\mathbf{x},\mathbf{x}) + \frac{1}{2}\int\frac{d\zeta}{2\pi}\,2\zeta^2\int d^3x\,\bar{G}_0(\mathbf{x},\mathbf{x}), \tag{1.30}$$

which is an alternate expression to eq. (1.24) for evaluating the Casimir energy.

1.3 Energy momentum tensor

A class of variations in the field is generated by infinitesimal general coordinate transformations in space time,

$$x^\alpha \to x^\alpha - \delta x^\alpha, \tag{1.31}$$

which leads to the variation in the field

$$\delta\phi = -\delta x^{\lambda}\partial_{\lambda}\phi(x). \tag{1.32}$$

The above variational statement generated by coordinate transformations in space time can be interpreted as the definition of the scalar field. The corresponding variational statement for the source function is derived by requiring the source term in the action, in eq. (1.2), to be invariant under infinitesimal general coordinate transformation in space-time. Thus we require

$$\int d^4x\, \delta\Big[K(x)\phi(x)\Big] = 0, \tag{1.33}$$

which lets us derive

$$\begin{aligned}\int d^4x\, \phi(x)\delta K(x) &= -\int d^4x\, \delta\phi(x)\, K(x) \\ &= \int d^4x\, \delta x^{\lambda}\big[\partial_{\lambda}\phi(x)\big]\, K(x) \\ &= -\int d^4x\, \phi(x)\, \partial_{\lambda}\big[\delta x^{\lambda}K(x)\big],\end{aligned} \tag{1.34}$$

where we have used eq. (1.32) and integrated by parts and assumed the variation on the surface of integration to be zero, to conclude

$$\delta K(x) = -\partial_{\lambda}\big[\delta x^{\lambda}K(x)\big]. \tag{1.35}$$

The variation in the Lagrangian density in eq. (1.1) due to an infinitesimal general

coordinate transformation when written in the form

$$\delta\mathcal{L} = -\partial^{\lambda}\left[\delta x_{\lambda}\mathcal{L}\right] + \left(\partial^{\alpha}\delta x^{\beta}\right) t_{\alpha\beta}(x) \tag{1.36}$$

lets us identify the energy-momentum tensor, or the stress tensor, for the scalar field as

$$t_{\alpha\beta}(x) = \partial_{\alpha}\phi(x)\partial_{\beta}\phi(x) + g_{\alpha\beta}\mathcal{L}(\phi(x)) \tag{1.37}$$

which is symmetric, $t_{\alpha\beta} = t_{\beta\alpha}$. This is the prescription used to define the stress tensor in the absence of gravity. Under the more general setup where gravity is treated as the dynamics of the metric field $g_{\alpha\beta}(x)$, the stress tensor is identified, and defined, as the right hand side (source) of the Einstein's equation which is gotten by requiring the action (when gravity is included) to be stationary under an arbitrary variation in the metric field. Identification of the stress tensor using the prescription in eq. (1.36) is unique only up to an additive term that identically satisfies $\partial^{\beta}t_{\alpha\beta} = 0$. This arbitrariness is incorporated into the stress tensor by redefining

$$t_{\alpha\beta}(x) = \partial_{\alpha}\phi(x)\partial_{\beta}\phi(x) + g_{\alpha\beta}\mathcal{L}(\phi(x)) - \theta\left\{\partial_{\alpha}\partial_{\beta} - g_{\alpha\beta}\partial^{2}\right\}\phi(x)^{2} \tag{1.38}$$

by adding a term, with an arbitrary coefficient θ, which explicitly satisfies $\partial^{\beta}t_{\alpha\beta} = 0$. The added term is called the conformal term in the stress tensor and θ is called the conformal coupling constant. The trace of the stress tensor is evaluated to be

$$t(x) = g^{\alpha\beta}t_{\alpha\beta}(x) = 3\left(\theta - \frac{1}{6}\right)\partial^{2}\left[\phi(x)^{2}\right] - V(x)\phi(x)^{2} - K(x)\phi(x), \tag{1.39}$$

where we have used the equation of motion for the field. The particular choice,

$\theta = \frac{1}{6}$, which renders the stress tensor traceless in the absence of the source and the background, is called the conformal choice. Using the equation of motion for the field we can also deduce

$$\partial^{\alpha} t_{\alpha\beta}(x) = -K(x)\partial_{\beta}\phi(x) - \frac{1}{2}\phi(x)^2 \partial_{\beta} V(x), \tag{1.40}$$

which is the local statement of conservation of energy and momentum in the absence of the source and the background.

1.4 Energy density

The physics of a fluid is described by the energy-momentum tensor associated with a fluid. Analogously, the physical quantities associated with the scalar field are determined by the energy-momentum tensor in eq. (1.38). The four-momentum of a small volume containing the field at the spatial point $\mathbf{x}$ at time t is defined in terms of the energy-momentum tensor as

$$P^{\mu}(x) = d\Sigma_{\nu}(x)\, t^{\nu\mu}(x), \tag{1.41}$$

where $d\Sigma_{\nu}(x)$ is the spatial volume element constructed out of three linearly independent space-like vectors

$$d\Sigma_{\nu}(x) = \epsilon_{\nu\alpha\beta\sigma}\, \delta_1 x^{\alpha}\, \delta_2 x^{\beta}\, \delta_3 x^{\sigma}. \tag{1.42}$$

In the particular Lorentz frame in which the above spatial volume element has only a time component we have

$$P^{\mu}(x) = d^3x\, t^{0\mu}(x). \tag{1.43}$$

The energy associated with the field is interpreted as the time-component of the four-momentum. Thus using eq. (1.43) the energy density of the field is defined to be the $t^{00}(x)$ component of the stress tensor which can be read off from eq. (1.38), and after using the field equation of motion in the absence of sources

$$-\Big[\partial^2 - V(x)\Big]\phi(x) = 0 \tag{1.44}$$

takes the form

$$t^{00}(x) = \frac{1}{2}\frac{\partial\phi}{\partial t}\frac{\partial\phi}{\partial t} - \frac{1}{2}\phi\frac{\partial^2}{\partial t^2}\phi + (1-4\theta)\,\frac{1}{4}\,\boldsymbol{\nabla}\cdot\boldsymbol{\nabla}\left[\phi^2\right]. \tag{1.45}$$

The energy density in eq. (1.45) has been defined in terms of the field operators. To define the effective energy density in the spirit of eq. (1.7) we define the effective bilinear product of field operators as

$$\begin{aligned}
\langle\phi(x)\phi(y)\rangle^K &= \frac{\langle 0_+|\phi(x)\phi(y)|0_-\rangle^K}{Z[K]} \\
&= \frac{1}{Z[K]}\frac{1}{i}\frac{\delta}{\delta K(x)}\frac{1}{i}\frac{\delta}{\delta K(y)}Z[K] \\
&= -i\frac{\delta}{\delta K(x)}\frac{\delta}{\delta K(y)}W[K] + \frac{\delta W[K]}{\delta K(x)}\frac{\delta W[K]}{\delta K(y)}.
\end{aligned} \tag{1.46}$$

Using eq. (1.13) in the above expression we thus derive the following correspondence

between the Green's function, $G(x, x')$, and the bilinear product of fields

$$\langle \phi(x)\phi(x') \rangle = \frac{1}{i} G(x, x'). \tag{1.47}$$

Thus, in terms of the Green's function the effective energy density can be written as

$$\langle t^{00}(x) \rangle = \mathcal{E}_{\rm vol}(x) + (1 - 4\theta)\, \mathcal{E}_{\rm sur}(x) \tag{1.48}$$

where we have introduced the definitions

$$\mathcal{E}_{\rm vol}(x) = \frac{1}{2i} \left\{ \left(\frac{\partial}{\partial t} \frac{\partial}{\partial t'} - \frac{\partial^2}{\partial t^2} \right) G(x, x') \right\}_{x=x'} \tag{1.49}$$

$$\mathcal{E}_{\rm sur}(x) = \frac{1}{4i} \boldsymbol{\nabla} \cdot \boldsymbol{\nabla}\, G(x, x). \tag{1.50}$$

We shall use the notation in which a curly letter, $\mathcal{E}(x)$, will denote energy density, and a capital letter, E, will be the corresponding total energy gotten by integrating the energy density over the total spatial volume, $E = \int d^3x\, \mathcal{E}(x)$. The energy density, $t^{00}(x)$, when integrated over the complete spatial volume, $\int d^3x\, t^{00}(x)$, is defined to be the total energy. This immediately lets us define the total energy as

$$E_{\rm tot} = E_{\rm vol} + (1 - 4\theta)\, E_{\rm sur}. \tag{1.51}$$

One expects the total surface energy, $E_{\rm sur} = \int d^3x\, \mathcal{E}_{\rm sur}(x)$, to evaluate to zero using the divergence theorem. The surface energy density, $\mathcal{E}_{\rm sur}(x)$, given in eq. (1.50), involves the gradient of the Green's function, $\boldsymbol{\nabla} G(x, x)$, which in general has jump discontinuities. But, since the divergence theorem is applicable for any piecewise continuous function, the total surface energy does indeed evaluate to zero. Thus

$E_{\rm sur} = 0$. Using this in eq. (1.51) leads to

$$E_{\rm tot} = E_{\rm vol}. \tag{1.52}$$

For the particular case when the potential $V(x)$ is independent of time we can use eq. (1.25) in eq. (1.49) and thus evaluate eq. (1.52) to yield

$$E_{\rm tot} = -\frac{1}{2}\int_{-\infty}^{\infty}\frac{d\zeta}{2\pi}\,2\zeta^2\int d^3x\,\bar{G}(\mathbf{x},\mathbf{x}), \tag{1.53}$$

which is exactly the first term in eq. (1.30). The second term in eq. (1.30) corresponds to the total energy in the absence of the background which is often termed the bulk energy.

1.5 Casimir force

The force density on the vacuum generated by the background is defined to be, see eq. (1.40),

$$f^\mu(x) = -\,\partial_\nu t^{\nu\mu}(x) = \frac{1}{2}\phi(x)^2\,\partial^\mu V(x) \tag{1.54}$$

in the absence of sources.

In terms of the correspondence between the fields and the Green's function in eq. (1.47) the force density in eq. (1.54) takes the form

$$\langle f^\mu(x)\rangle = \frac{1}{2i}\,G(x,x)\,\partial^\mu V(x). \tag{1.55}$$

For time independent situations we can use eq. (1.25) to write

$$\begin{aligned}\langle f^{\mu}(x)\rangle &= \frac{1}{2i}\int \frac{d\omega}{2\pi}\,\bar{G}(\mathbf{x},\mathbf{x};\omega)\,\partial^{\mu}V(x)\\ &= \frac{1}{2}\int \frac{d\zeta}{2\pi}\,\bar{G}(\mathbf{x},\mathbf{x};\omega)\,\partial^{\mu}V(x).\end{aligned} \tag{1.56}$$

The force density integrated over a spatial volume leads to the total force as

$$\begin{aligned}F^{\mu} = \int_{\text{vol}} d^3x\,\langle f^{\mu}(x)\rangle &= \frac{1}{2i}\int_{\text{vol}} d^3x\,G(x,x)\partial^{\mu}V(x)\\ &= -\frac{1}{2i}\int_{\text{vol}} d^3x\,V(x)\,\partial^{\mu}G(x,x),\end{aligned} \tag{1.57}$$

where we have integrated by parts to arrive at the final form by assuming that the volume is bounded by a surface on which the potential vanishes. The spatial components of the above vector gives the physical force. The time-component is interpreted as the change in energy per unit time. For the case when the potential is independent of time we can use eq. (1.25) in eq. (1.57) and write

$$\begin{aligned}F^{\mu} &= \frac{1}{2}\int_{-\infty}^{\infty}\frac{d\zeta}{2\pi}\int_{\text{vol}} d^3x\,\bar{G}(\mathbf{x},\mathbf{x};\omega)\,\partial^{\mu}V(x)\\ &= -\frac{1}{2}\int_{-\infty}^{\infty}\frac{d\zeta}{2\pi}\int_{\text{vol}} d^3x\,V(x)\,\partial^{\mu}\bar{G}(\mathbf{x},\mathbf{x};\omega).\end{aligned} \tag{1.58}$$

In writing the final form we have again assumed that the volume is bounded by a surface on which the potential vanishes.

Chapter 2

Green's function

In chapter 1 we derived expressions for the Casimir energy and the Casimir force, for configurations described by a general background potential, in terms of the corresponding Green's functions. In this chapter we shall describe the Green's function technique and find solutions for a few specific configurations which will then be used in the following chapters.

2.1 Inhomogeneous differential equations

An inhomogeneous linear differential equation can be written in the form

$$L\,x(t) = F(t), \tag{2.1}$$

where L is a polynomial of order n in $\frac{d}{dt}$ with coefficients that are functions of time. $F(t)$ is a prior given function which is also called the 'source'. The corresponding

homogeneous linear differential equation is

$$L\, x_0(t) = 0. \tag{2.2}$$

The general solution $x_0(t)$ to eq. (2.2) is given as a linear superposition of n independent solutions to eq. (2.2) with n arbitrary constants corresponding to the n integration constants, which are fixed by the boundary conditions. If we can determine any one solution $x_1(t)$ which satisfies eq. (2.1) the general solution to eq. (2.1) is given as

$$x(t) = x_0(t) + x_1(t), \tag{2.3}$$

where $x_0(t)$, in this context, is called the homogeneous solution to eq. (2.1) and $x_1(t)$ in this situation is called the particular solution to eq. (2.1). One worries if another choice of the particular solution would lead to another solution. If $x_1(t)$ and $x_2(t)$ are two independent particular solutions that satisfy eq. (2.1), by subtracting the two equations we get

$$L\, [x_1(t) - x_2(t)] = 0. \tag{2.4}$$

Thus, the arbitrariness in the general solution, $x(t)$, due to the choice of the particular solution, is of the form $x_0(t)$.

The Green's function method is a particular technique used for solving an inhomogeneous linear differential equation. The Green's function corresponding to eq. (2.1) satisfies an inhomogeneous linear differential equation

$$L\, g(t, t') = \delta(t - t'), \tag{2.5}$$

in which the source is a δ-function.

2.1.1 Illustrative example

For our discussion we shall consider the following differential equation satisfied by $x(t)$

$$-\left(\frac{d^2}{dt^2}+\omega^2\right)x(t)=F(t), \tag{2.6}$$

where $F(t)$ is a prior given source, and the initial conditions are, $x(0)=-A$, and $\dot{x}(0)=0$. The corresponding differential equation for the Green's function, $g(t,t')$, is

$$-\left(\frac{d^2}{dt^2}+\omega^2\right)g(t,t')=\delta(t-t'). \tag{2.7}$$

Integrating eq. (2.7) over an infinitesimal region around the point t' lets us extract the information pertaining to the continuity of the derivative of the Green's function at $t=t'$. This reads as

$$-\left\{\frac{d}{dt}g(t,t')\right\}\Big|_{t=t'+\epsilon}+\left\{\frac{d}{dt}g(t,t')\right\}\Big|_{t=t'-\epsilon}=1. \tag{2.8}$$

We also observe that using equations (2.7) and (2.8) we can learn about the continuity of the Green's function at $t=t'$. We note that eq. (2.8) can be satisfied with either the Green's function being finitely discontinuous at $t=t'$, or it being continuous at the point $t=t'$. In particular we ask, can equations (2.7) and (2.8) accommodate a finite discontinuity in the Green's function? With a finite discontinuity in the Green's function at $t=t'$ the $\frac{d^2}{dt^2}g(t,t')$ term in eq. (2.7) will contribute a term involving the derivative of a delta function, which is not the required quantity on the right hand side of the equation. On the contrary, with a Green's function continuous at $t=t'$ the $\frac{d^2}{dt^2}g(t,t')$ term in eq. (2.7) will contribute a delta function, as required to balance

the right hand side. Thus we conclude that

$$-\,g(t,t')|_{t=t'+\epsilon} + g(t,t')|_{t=t'-\epsilon} = 0. \tag{2.9}$$

Thus, eq. (2.7), the differential equation for the Green's function, inherently enforces two continuity conditions, given in equations (2.8) and (2.9), on the Green's function at $t = t'$.

Solving for the Green's function

The homogeneous differential equation corresponding to Eq. (2.7) is

$$-\left(\frac{d^2}{dt^2} + \omega^2\right) g_0(t,t') = 0 \tag{2.10}$$

where $g_0(t,t')$ is the corresponding homogeneous solution. For all points, except $t = t'$, the differential equation (2.7) has no source term and thus reads like the equation for $g_0(t,t')$ in eq. (2.10). This equation has oscillatory solutions, which could have different behaviors at $t < t'$ and $t > t'$, except for the constraint imposed by the continuity conditions in eqs. (2.8) and (2.9). In terms of four arbitrary functions A, B, C, and D, which depend on t' we can write

$$g(t,t') = \begin{cases} A(t')\,e^{i\omega t} + B(t')\,e^{-i\omega t} & \text{if } t < t', \\ C(t')\,e^{i\omega t} + D(t')\,e^{-i\omega t} & \text{if } t > t'. \end{cases} \tag{2.11}$$

Imposing the continuity conditions in eqs. (2.8) and (2.9) we get the following equations constraining $A(t')$, $B(t')$, $C(t')$, and $D(t')$:

$$[C(t') - A(t')]\, e^{i\omega t'} + [D(t') - B(t')]\, e^{-i\omega t'} = 0, \tag{2.12a}$$

$$[C(t') - A(t')]\, e^{i\omega t'} - [D(t') - B(t')]\, e^{-i\omega t'} = \frac{i}{\omega}. \tag{2.12b}$$

From the structure of the above constraints we note that the solutions can be sought in combinations of A and C, and B and D. This lets us solve for $g(t, t')$ in the following four forms:

$$g(t,t') = A(t')\, e^{i\omega t} + B(t')\, e^{-i\omega t} + \bar{g}_R(t - t') \tag{2.13a}$$

$$= C(t')\, e^{i\omega t} + D(t')\, e^{-i\omega t} + \bar{g}_A(t - t') \tag{2.13b}$$

$$= A(t')\, e^{i\omega t} + D(t')\, e^{-i\omega t} + \bar{g}_F(t - t') \tag{2.13c}$$

$$= C(t')\, e^{i\omega t} + B(t')\, e^{-i\omega t} + \bar{g}_W(t - t'), \tag{2.13d}$$

where

$$\bar{g}_R(t-t') = -\frac{1}{\omega}\frac{1}{2i}\left[+\theta(t-t')\, e^{i\omega(t-t')} - \theta(t-t')\, e^{-i\omega(t-t')}\right]$$

$$= -\frac{1}{\omega}\,\theta(t-t')\,\sin\omega(t-t'), \tag{2.14a}$$

$$\bar{g}_A(t-t') = -\frac{1}{\omega}\frac{1}{2i}\left[-\theta(t'-t)\, e^{i\omega(t-t')} + \theta(t'-t)\, e^{-i\omega(t-t')}\right]$$

$$= +\frac{1}{\omega}\,\theta(t'-t)\,\sin\omega(t-t'), \tag{2.14b}$$

$$\bar{g}_F(t-t') = -\frac{1}{\omega}\frac{1}{2i}\left[+\theta(t-t')\, e^{i\omega(t-t')} + \theta(t'-t)\, e^{-i\omega(t-t')}\right], \tag{2.14c}$$

$$\bar{g}_W(t-t') = -\frac{1}{\omega}\frac{1}{2i}\left[-\theta(t'-t)\, e^{i\omega(t-t')} - \theta(t-t')\, e^{-i\omega(t-t')}\right], \tag{2.14d}$$

and the subscripts has been chosen to stand for retarded, advanced, Feynman, and Wheeler, respectively. It is easy to recognize that the above four forms are special cases of the following general expression for $\bar{g}(t-t')$

$$\begin{aligned}\bar{g}(t-t') = &-\frac{1}{\omega}\frac{1}{2i}\left[\,a\,\theta(t-t') - b\,\theta(t'-t)\right]\,e^{i\omega(t-t')} \\ &+\frac{1}{\omega}\frac{1}{2i}\left[\,c\,\theta(t-t') - d\,\theta(t'-t)\right]\,e^{-i\omega(t-t')}\end{aligned} \tag{2.15}$$

where the numerical constants a, b, c, and d, are arbitrary to the extent that they obey the constraints $a+b=1$, and $c+d=1$. The special cases, $a=1$, $c=1$, corresponds to $\bar{g}_R$; $a=0$, $c=0$, corresponds to $\bar{g}_A$; $a=1$, $c=0$, corresponds to $\bar{g}_F$; and $a=0$, $c=1$, corresponds to $\bar{g}_W$, respectively.

Using eq. (2.15) in eq. (2.13) we can write the Green's function in the form

$$g(t,t') = g_0(t,t') + \bar{g}(t-t'), \tag{2.16}$$

where

$$g_0(t,t') = A_0(t')e^{i\omega t} + B_0(t')e^{-i\omega t}, \tag{2.17}$$

and $\bar{g}(t-t')$ is given by eq. (2.15).

We also said that the difference between any two particular solutions will be a homogeneous solution. This can be illustrated by making finite changes in a and c given as, $a' = a+\delta_1$, and $c' = c+\delta_2$, and studying for the variation in $\bar{g}(t-t')$ due

to this change. We get the variation in the Green's function to be

$$\begin{aligned}\Delta\bar{g}(t-t') &= -\frac{1}{\omega}\frac{1}{2i}\left[\,\delta_1\,\theta(t-t') + \,\delta_1\,\theta(t'-t)\right]\,e^{i\omega(t-t')} \\ &\quad + \frac{1}{\omega}\frac{1}{2i}\left[\,\delta_2\,\theta(t-t') + \,\delta_2\,\theta(t'-t)\right]\,e^{-i\omega(t-t')} \\ &= -\frac{\delta_1}{\omega}\frac{1}{2i}\,e^{i\omega(t-t')} + \frac{\delta_2}{\omega}\frac{1}{2i}\,e^{-i\omega(t-t')}, \end{aligned} \tag{2.18}$$

which indeed can be absorbed into the homogeneous part of the solution.

Solution to $x(t)$ in terms of $g(t,t')$

We substitute $t \to t'$ in eq. (2.6), multiply it by $g(t,t')$ and integrate it with respect to t'; independently, we multiply eq. (2.7) with $x(t')$ and integrate it with respect to t'; and subsequently subtract the modified equations to get

$$x(t) = x_{\bar{g}_0}(t) + \bar{x}(t) \tag{2.19}$$

where the contribution to $x(t)$ from the homogeneous part of the Green's function in eq. (2.16) is captured in

$$x_{\bar{g}_0}(t) = \int_{-\infty}^{\infty} dt' \bar{g}_0(t,t')F(t') + \int_{-\infty}^{\infty} dt' \Big[\bar{g}_0(t,t')\frac{d^2}{dt'^2}x(t') - x(t')\frac{d^2}{dt^2}\bar{g}_0(t,t')\Big] \tag{2.20}$$

which evaluates to zero when we use equations (2.6) and (2.10). Thus the homogeneous part of the Green's function, when written in the form of eq. (2.16), does not

contribute to $x(t)$. The second term in eq. (2.19) reads

$$\begin{aligned}\bar{x}(t) &= \int_{-\infty}^{+\infty} dt' \bar{g}(t-t') F(t') + \int_{-\infty}^{+\infty} dt' \frac{d}{dt'} \left[\bar{g}(t-t') \dot{x}(t') - x(t') \frac{d}{dt'} \bar{g}(t-t') \right] \\ &= \int_{-\infty}^{+\infty} dt' \bar{g}(t-t') F(t') + \lim_{\tau_2 \to +\infty} \left(\dot{x}(\tau_2) - x(\tau_2) \frac{d}{d\tau_2} \right) \bar{g}(t-\tau_2) \\ &\quad - \lim_{\tau_1 \to -\infty} \left(\dot{x}(\tau_1) - x(\tau_1) \frac{d}{d\tau_1} \right) \bar{g}(t-\tau_1), \end{aligned} \tag{2.21}$$

where we isolated the surface terms using integration by parts. The limiting variables are assumed to satisfy $\tau_1 < \{t, t'\} < \tau_2$. We note that the surface terms satisfy the homogeneous equation corresponding to eq. (2.6)

$$- \left(\frac{d^2}{dt^2} + \omega^2 \right) \left(\dot{x}(\tau) - x(\tau) \frac{d}{d\tau} \right) \bar{g}(t-\tau) = 0, \tag{2.22}$$

because the surface points, denoted by τ, never equals the variable t, i.e. $\tau \neq t$.

Let us define the functions

$$S_{\pm}(\tau) = \frac{1}{\omega} \frac{1}{2i} \left(\dot{x}(\tau) - x(\tau) \frac{d}{d\tau} \right) e^{\pm i\omega\tau} \tag{2.23}$$

in terms of which we can write the surface terms in eq. (2.21) as

$$\lim_{\tau_2 \to +\infty} \left(\dot{x}(\tau_2) - x(\tau_2) \frac{d}{d\tau_2} \right) \bar{g}(t-\tau_2) = +\, b\, S_-(+\infty) e^{+i\omega t} - \, d\, S_+(+\infty) e^{-i\omega t}, \tag{2.24a}$$

$$\lim_{\tau_1 \to -\infty} \left(\dot{x}(\tau_1) - x(\tau_1) \frac{d}{d\tau_1} \right) \bar{g}(t-\tau_1) = -\, a\, S_-(-\infty) e^{+i\omega t} + \, c\, S_+(-\infty) e^{-i\omega t}. \tag{2.24b}$$

Using eq. (2.24) in eq. (2.21) and subsequently using it with eq. (2.20) into eq. (2.19) we can write

$$x(t) = \int_{-\infty}^{\infty} dt' \bar{g}(t-t') F(t') + \alpha_0\, e^{i\omega t} + \beta_0\, e^{-i\omega t}, \tag{2.25}$$

where

$$\alpha_0 = +\,a\,S_-(-\infty) +\; b\,S_-(+\infty) \tag{2.26a}$$

$$\beta_0 = -\,c\,S_+(-\infty) -\; d\,S_+(+\infty). \tag{2.26b}$$

In summary, the homogeneous part of the Green's function when expressed in the form of eq. (2.16) does not contribute to $x(t)$. The homogeneous part of $x(t)$ gets its contribution from $x(\tau)$ and $\bar{g}(t-\tau)$, where τ is evaluated at the surfaces at $\pm\infty$.

Solution to $x(t)$

Using the expression for $\bar{g}(t-t')$, given in eq. (2.15), into eq. (2.25) and subjecting it to the initial conditions $x(0) = -A$ and $\dot{x}(0) = 0$ we get

$$\begin{aligned}\alpha_0 + \beta_0 = -A &+ \frac{1}{2i\omega}\int_{-\infty}^{0} dt' F(t') \left[a\, e^{-i\omega t'} - c\, e^{i\omega t'}\right] \\ &- \frac{1}{2i\omega}\int_{0}^{+\infty} dt' F(t') \left[b\, e^{-i\omega t'} - d\, e^{i\omega t'}\right], \end{aligned} \tag{2.27}$$

$$\begin{aligned}\alpha_0 - \beta_0 = -0 &+ \frac{1}{2i\omega}\int_{-\infty}^{0} dt' F(t') \left[a\, e^{-i\omega t'} + c\, e^{i\omega t'}\right] \\ &- \frac{1}{2i\omega}\int_{0}^{+\infty} dt' F(t') \left[b\, e^{-i\omega t'} + d\, e^{i\omega t'}\right], \end{aligned} \tag{2.28}$$

where the differentiations with respect to the limits on the integrals, arising due to step functions in eq. (2.15), contributes to

$$\frac{1}{\omega}\frac{1}{2i} F(0)\left[(a+b) - (c+d)\right] = 0, \tag{2.29}$$

because $a+b=c+d=1$. Solving for α_0 and β_0 in the above equations gives us

$$\alpha_0 = -\frac{A}{2} + a\,\frac{1}{\omega}\frac{1}{2i}\int_{-\infty}^{0} dt' F(t') e^{-i\omega t'} - b\,\frac{1}{\omega}\frac{1}{2i}\int_{0}^{+\infty} dt' F(t') e^{-i\omega t'}, \quad (2.30a)$$

$$\beta_0 = -\frac{A}{2} - c\,\frac{1}{\omega}\frac{1}{2i}\int_{-\infty}^{0} dt' F(t') e^{+i\omega t'} + d\,\frac{1}{\omega}\frac{1}{2i}\int_{0}^{+\infty} dt' F(t') e^{+i\omega t'}. \quad (2.30b)$$

The eqs. (2.26) and (2.30) relate the coefficients (a, c) with the surface terms $S_{\pm}(\pm\infty)$. We note that the surface terms in eq. (2.23) are determined in terms of the solution $x(t)$ and thus are unknowns until the problem is solved. Thus the above equation should be interpreted as a constraint equation relating (a, c) and $S_{\pm}(\pm\infty)$.

We can proceed by working in terms of α_0 and β_0. Using the expressions for α_0 and β_0 in eq. (2.30) into eq. (2.25) we get

$$\begin{aligned} x(t) &= -A\cos\omega t - (a+b)\frac{1}{2i\omega}\int_0^t dt' F(t') e^{i\omega(t-t')} + (c+d)\frac{1}{2i\omega}\int_0^t dt' F(t') e^{-i\omega(t-t')} \\ &= -A\cos\omega t - \frac{1}{\omega}\int_0^t dt' F(t')\sin\omega(t-t'), \end{aligned} \quad (2.31)$$

where we used $a+b=1$ and $c+d=1$. Differentiating the above expression with t gives us

$$\dot{x}(t) = +\omega A\sin\omega t - \int_0^t dt' F(t')\cos\omega(t-t'), \quad (2.32)$$

where the differentiation with respect to the integration limit in eq. (2.31) contributed zero.

Once the solution is known we note that

$$S_{\pm}(\tau) = \pm\frac{A}{2} - \frac{1}{\omega}\frac{1}{2i}\int_0^{\tau} dt' F(t') e^{\pm i\omega t'}, \quad (2.33)$$

where we used eqs. (2.31) and (2.32) for the evaluation.

2.2 Reciprocal symmetry of Green's function

Let us consider the differential equation

$$-\left[\frac{\partial^2}{\partial z^2} - V(z)\right] g(z, z') = \delta(z - z'). \tag{2.34}$$

The statement of reciprocal symmetry of Green's function is very general, but we shall prove it for the above differential equation only, because that is what we will need in the following sections.

We begin by rewriting eq. (2.34) in the form

$$-\left[\frac{\partial^2}{\partial z^2} - V(z)\right] g(z, z'') = \delta(z - z''). \tag{2.35}$$

Multiplying eqs. (2.34) and (2.35) with $g(z, z'')$ and $g(z, z')$ respectively and integrating with respect to z in each leads to

$$-\int dz\, g(z, z'') \left[\frac{\partial^2}{\partial z^2} - V(z)\right] g(z, z') = g(z', z''), \tag{2.36a}$$

$$-\int dz\, g(z, z') \left[\frac{\partial^2}{\partial z^2} - V(z)\right] g(z, z'') = g(z'', z'). \tag{2.36b}$$

Subtracting the two equations in eqs. (2.36) yields

$$\begin{aligned} g(z', z'') - g(z'', z') &= -\int dz\, g(z, z'') \frac{\partial^2}{\partial z^2} g(z, z') + \int dz\, g(z, z') \frac{\partial^2}{\partial z^2} g(z, z'') \\ &= 0, \end{aligned} \tag{2.37}$$

where we have integrated by parts and assumed that the Green's function vanishes at infinity to arrive at the second equality. Thus, we have proved

$$g(z', z'') = g(z'', z') \tag{2.38}$$

which is the statement of reciprocal symmetry in the Green's function and is obvious physically, for example using eq. (1.47).

2.3 Green's function for δ-function potentials

In this section we shall concentrate on evaluating the solutions to Green's function for specific background potentials. We shall consider background potentials described by δ-functions. In particular we shall consider configurations consisting of δ-functions describing a single plate, parallel plates, and concentric cylinders.

The δ-function potentials, the so-called semitransparent plates, simulates physical materials in electrodynamics [18]. When the coupling (the permittivity) to the potential is very large it simulates a conductor, and when the coupling is very weak it simulates a dilute dielectric material.

2.3.1 Green's function for a single plate

A single plate positioned at $z = a_1$ is mathematically designed using the potential

$$V(z) = \lambda_1 \delta(z - a_1), \tag{2.39}$$

where λ_1 is the coupling parameter which has the dimensions of inverse length. Since the potential depends only on the z variable, the Green's function, which is a solution

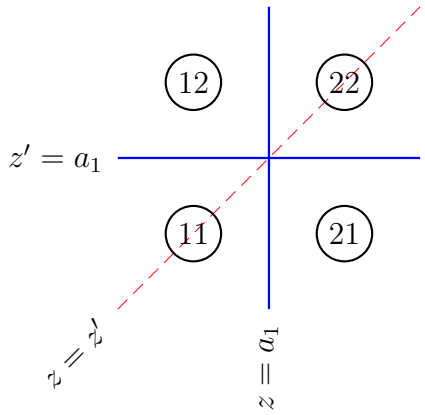

Figure 2.1: Description of the regions in the $z - z'$ domain on which the Green's function for a single plate is defined.

to eq. (1.12), can be written as

$$G(\mathbf{x}, t, \mathbf{x}', t') = \int \frac{d\omega}{2\pi} e^{-i\omega(t-t')} \int \frac{dk_x}{2\pi} e^{ik_x(x-x')} \int \frac{dk_y}{2\pi} e^{ik_y(y-y')} g(z, z'; \kappa), \qquad (2.40)$$

where $\kappa^2 = k_x^2 + k_y^2 - \omega^2$, where $k_{x,y}$ and ω are the Fourier variables corresponding to the space-time coordinates x, y and t respectively. Substituting eq. (2.40) into the differential equation for the Green's function in eq. (1.12) we learn that the reduced Green's function, $g(z, z'; \kappa)$, satisfies the differential equation

$$-\left[\frac{\partial^2}{\partial z^2} - \kappa^2 - \lambda_1 \delta(z - a_1)\right] g(z, z'; \kappa) = \delta(z - z'). \qquad (2.41)$$

Our goal in this section will be to find an explicit solution for the above differential equation.

We begin by noting that the δ-functions in eq. (2.41) divides each of the z and z' variables into three distinct regions. These regions are described in the $z - z'$ domain in Figure 2.1. We next note that in the absence of the potential, achieved

by setting $\lambda_1 = 0$, eq. (2.41) reduces to eq. (2.7), if we replace $\omega \to i\kappa$ and make the corresponding Euclidean rotation. We shall denote the Green's function in the absence of the potential by a subscript 0, see eq. (1.16). Thus, using the Feynman Green's function, $a = 1$ and $c = 0$, by choosing eq. (2.14c) out of the possible alternatives, which amounts to the so-called causal or Feynman boundary conditions, which requires the Green's function to vanish at infinity, we can write

$$g_0(z, z'; \kappa) = \frac{1}{2\kappa}\, e^{-\kappa|z-z'|}. \tag{2.42}$$

Using the reciprocal symmetry (see eq. (2.38)) we further learn that it is enough to solve for the region $z > z'$. The solution in the other regions is gotten by using the reciprocal symmetry. Using these observations and the requirement that the Green's function should vanish at infinity we can write, for $z' > z$,

$$g_{11}(z, z'; \kappa) = \frac{1}{2\kappa}\, e^{+\kappa z - \kappa z'} + A_{11}^{++}\, e^{+\kappa z + \kappa z'}, \tag{2.43a}$$

$$g_{12}(z, z'; \kappa) = A_{12}^{+-}\, e^{+\kappa z - \kappa z'}, \tag{2.43b}$$

$$g_{22}(z, z'; \kappa) = \frac{1}{2\kappa}\, e^{+\kappa z - \kappa z'} + A_{22}^{--}\, e^{-\kappa z - \kappa z'} \tag{2.43c}$$

in terms of the coefficients $A_{ij}^{\pm\pm}$, where the subscripts denote the regions they are defined in and the superscripts are chosen to denote the function they go with. The superscripts are redundant for the case of single plate. At each of the boundaries in Figure 2.1 the Green's function is required to satisfy continuity conditions imposed on it analogous to those derived in eq. (2.8) and eq. (2.9) for the case of no background. For a single plate only three of these continuity conditions are independent. In general for n plates we will have $n(n+1)$ independent continuity conditions for the Green's

function, and $n(n+1)-1$ conditions for the continuity of the derivatives of the Green's functions. These continuity conditions for the single plate under consideration are

$$g_{11}(a_1, a_1) = g_{12}(a_1, a_1), \tag{2.44a}$$

$$g_{12}(a_1, a_1) = g_{22}(a_1, a_1), \tag{2.44b}$$

$$\Big[\frac{\partial}{\partial a_1} g_{22}(a_1, z')\Big]\Big|_{z'=a_1} - \Big[\frac{\partial}{\partial a_1} g_{12}(a_1, z')\Big]\Big|_{z'=a_1} = \lambda_1 g_{12}(a_1, a_1), \tag{2.44c}$$

which leads to the equations

$$A_{12}^{+-} - e^{2\kappa a_1} A_{11}^{++} = \frac{1}{2\kappa}, \tag{2.45a}$$

$$A_{12}^{+-} - e^{-2\kappa a_1} A_{22}^{--} = \frac{1}{2\kappa}, \tag{2.45b}$$

$$\Big(1 + \frac{\lambda_1}{\kappa}\Big) A_{12}^{+-} + e^{-2\kappa a_1} A_{22}^{--} = \frac{1}{2\kappa}, \tag{2.45c}$$

and can be solved to yield

$$A_{12}^{+-} = \frac{1}{\lambda_1 + 2\kappa}, \tag{2.46a}$$

$$A_{11}^{++} = -\frac{1}{2\kappa} \frac{\lambda_1}{\lambda_1 + 2\kappa} e^{-2\kappa a_1}, \tag{2.46b}$$

$$A_{22}^{--} = -\frac{1}{2\kappa} \frac{\lambda_1}{\lambda_1 + 2\kappa} e^{+2\kappa a_1}. \tag{2.46c}$$

These functions in conjunction with eq. (2.43) determine the Green's function. For the present case of single plate we can further write the Green's function as

$$g(z, z'; \kappa) = \frac{1}{2\kappa} e^{-\kappa|z-z'|} - \frac{\lambda_1}{\lambda_1 + 2\kappa} e^{-\kappa|z-a_1|} e^{-\kappa|z'-a_1|}. \tag{2.47}$$

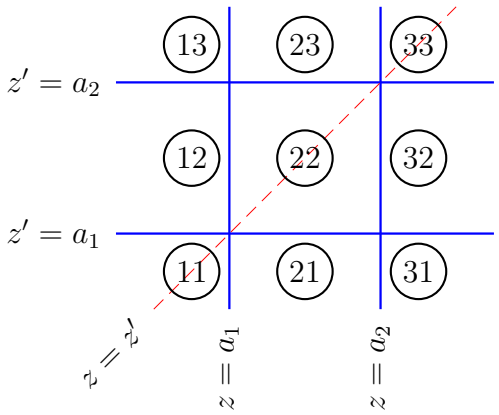

Figure 2.2: Description of the regions in the $z - z'$ domain on which the Green's function for parallel plates is defined.

2.3.2 Green's function for parallel plates

Parallel plates positioned at $z = a_1$ and $z = a_2$, such that $a = a_2 - a_1 > 0$, are described by the potential

$$V(z) = \lambda_1 \, \delta(z - a_1) + \lambda_2 \, \delta(z - a_2), \tag{2.48}$$

where $\lambda_{1,2}$ are the coupling constants associated with the plates. Since the potential is dependent only on the z variable, we can write the background Green's function, satisfying eq. (1.12), in the form of eq. (2.40), where the reduced Green's function, $g(z, z'; \kappa)$, now satisfies the differential equation

$$-\left[\frac{\partial^2}{\partial z^2} - \kappa^2 - \lambda_1 \delta(z - a_1) - \lambda_2 \delta(z - a_2)\right] g(z, z'; \kappa) = \delta(z - z'). \tag{2.49}$$

We note that the δ-functions in eq. (2.49) divide each of the z and z' variables into four regions. These regions are described in Figure 2.2. Requiring the Green's function to vanish at infinity we can write the Green's function in terms of the following

piecewise-defined functions:

$$g_{11}(z,z';\kappa) = \frac{1}{2\kappa}\, e^{-\kappa|z-z'|} + A_{11}^{++}\, e^{\kappa(z+z')}, \tag{2.50a}$$

$$g_{22}(z,z';\kappa) = \frac{1}{2\kappa}\, e^{-\kappa|z-z'|} + A_{22}^{++}\, e^{\kappa(z+z')} + A_{22}^{--}\, e^{-\kappa(z+z')} + A_{22}^{+-}\, e^{\kappa(z-z')} + A_{22}^{-+}\, e^{-\kappa(z-z')}, \tag{2.50b}$$

$$g_{33}(z,z';\kappa) = \frac{1}{2\kappa}\, e^{-\kappa|z-z'|} + A_{33}^{--}\, e^{-\kappa(z+z')}, \tag{2.50c}$$

$$g_{12}(z,z';\kappa) = A_{12}^{+-}\, e^{\kappa(z-z')} + A_{12}^{++}\, e^{\kappa(z+z')}, \tag{2.50d}$$

$$g_{13}(z,z';\kappa) = A_{13}^{+-}\, e^{\kappa(z-z')}, \tag{2.50e}$$

$$g_{23}(z,z';\kappa) = A_{23}^{+-}\, e^{\kappa(z-z')} + A_{23}^{--}\, e^{-\kappa(z+z')}, \tag{2.50f}$$

where the coefficients are determined using 6 continuity conditions involving the Green's functions and 5 continuity conditions involving the derivatives of the Green's functions. These continuity conditions determine the 11 coefficients in eq. (2.50) to be,

$$A_{11}^{++} = -\frac{1}{\Delta}\frac{1}{2\kappa}\left[\frac{\lambda_1}{2\kappa}\, e^{-2\kappa a_1} + \frac{\lambda_2}{2\kappa}\, e^{-2\kappa a_2} - \frac{\lambda_1}{2\kappa}\frac{\lambda_2}{2\kappa}\Big(e^{-2\kappa a_2} - e^{-2\kappa a_1}\Big)\right], \tag{2.51a}$$

$$A_{22}^{++} = -\frac{1}{\Delta}\frac{1}{2\kappa}\frac{\lambda_2}{2\kappa}\Big(1+\frac{\lambda_1}{2\kappa}\Big)\, e^{-2\kappa a_2}, \qquad A_{22}^{--} = -\frac{1}{\Delta}\frac{1}{2\kappa}\frac{\lambda_1}{2\kappa}\Big(1+\frac{\lambda_2}{2\kappa}\Big)\, e^{2\kappa a_1}, \tag{2.51b}$$

$$A_{22}^{+-} = A_{22}^{-+} = \frac{1}{\Delta}\frac{1}{2\kappa}\frac{\lambda_1}{2\kappa}\frac{\lambda_2}{2\kappa}\, e^{-2\kappa a}, \tag{2.51c}$$

$$A_{33}^{--} = -\frac{1}{\Delta}\frac{1}{2\kappa}\left[\frac{\lambda_1}{2\kappa}\, e^{2\kappa a_1} + \frac{\lambda_2}{2\kappa}\, e^{2\kappa a_2} - \frac{\lambda_1}{2\kappa}\frac{\lambda_2}{2\kappa}\Big(e^{2\kappa a_1} - e^{2\kappa a_2}\Big)\right], \tag{2.51d}$$

$$A_{12}^{+-} = \frac{1}{\Delta}\frac{1}{2\kappa}\Big(1+\frac{\lambda_2}{2\kappa}\Big), \qquad A_{12}^{++} = -\frac{1}{\Delta}\frac{1}{2\kappa}\frac{\lambda_2}{2\kappa}\, e^{2\kappa a_2}, \tag{2.51e}$$

$$A_{13}^{+-} = \frac{1}{\Delta}\frac{1}{2\kappa}, \tag{2.51f}$$

$$A_{23}^{+-} = \frac{1}{\Delta}\frac{1}{2\kappa}\Big(1+\frac{\lambda_1}{2\kappa}\Big), \qquad A_{23}^{--} = -\frac{1}{\Delta}\frac{1}{2\kappa}\frac{\lambda_1}{2\kappa}\, e^{-2\kappa a_1}, \tag{2.51g}$$

where

$$\Delta = 1 + \frac{\lambda_1}{2\kappa} + \frac{\lambda_2}{2\kappa} + \frac{\lambda_1}{2\kappa}\frac{\lambda_2}{2\kappa}\left(1 - e^{-2\kappa a}\right). \tag{2.52}$$

Using the reciprocal symmetry of the Green's function we further have $g_{21}(z, z'; \kappa) = g_{12}(z', z; \kappa)$, $g_{31}(z, z'; \kappa) = g_{13}(z', z; \kappa)$, and $g_{32}(z, z'; \kappa) = g_{23}(z', z; \kappa)$.

2.3.3 Green's function for a single cylinder

A single cylinder of radius a_1 centered at the origin is described by the potential

$$V(r) = \lambda_1 \, \delta(r - a_1), \tag{2.53}$$

where r is the radial coordinate in the $x - y$ plane given by $r^2 = x^2 + y^2$. Since the potential for a cylinder depends only on the radial coordinate, the background Green's function satisfying eq. (1.12) can be written in the form

$$G(\mathbf{x}, t, \mathbf{x}', t') = \int \frac{d\omega}{2\pi} \, e^{-i\omega(t-t')} \int \frac{dk_z}{2\pi} \, e^{ik_z(z-z')} \sum_{m=-\infty}^{\infty} \frac{1}{2\pi} \, e^{im(\theta-\theta')} \, g_m(r, r'; \kappa), \tag{2.54}$$

where $\kappa^2 = k_z^2 - \omega^2$. Substituting eq. (2.54) into the differential equation for the Green's function in eq. (1.12) we find that the reduced Green's function, $g_m(r, r'; \kappa)$, satisfies the differential equation

$$-\left[\frac{1}{r}\frac{\partial}{\partial r} r \frac{\partial}{\partial r} - \frac{m^2}{r^2} - \kappa^2 - \lambda_1 \delta(r - a_1)\right] g_m^{(0)}(r, r'; \kappa) = \frac{\delta(r - r')}{r}. \tag{2.55}$$

For the case when the background potential is switched off, $\lambda_1 = 0$, choosing the causal or Feynman boundary conditions, like in eq. (2.14c), the solution to eq. (2.55)

is given in terms of the modified Bessel functions as

$$(g_0)_m(r,r';\kappa) = I_m(\kappa r_<)K_m(\kappa r_>), \tag{2.56}$$

where $r_< = \mathrm{Min}(r,r')$ and $r_> = \mathrm{Max}(r,r')$.

We note that the δ-functions divide the r and r' variables into three regions. Note that $r \geq 0$. In terms of the notations introduced in Figure 2.1 we can thus write

$$(g_m)_{11}(r,r';\kappa) = I_m(\kappa r_<)K_m(\kappa r_>) + B_{11}^{++}\, I_m(\kappa r)I_m(\kappa r'), \tag{2.57a}$$

$$(g_m)_{12}(r,r';\kappa) = B_{12}^{+-}\, I_m(\kappa r)K_m(\kappa r'), \tag{2.57b}$$

$$(g_m)_{22}(r,r';\kappa) = I_m(\kappa r_<)K_m(\kappa r_>) + B_{22}^{--}\, K_m(\kappa r)K_m(\kappa r'), \tag{2.57c}$$

where

$$B_{11}^{++} = \frac{\lambda_1 a_1 K_1^2}{1+\lambda_1 a_1 I_1 K_1}, \tag{2.58a}$$

$$B_{12}^{+-} = \frac{1}{1+\lambda_1 a_1 I_1 K_1}, \tag{2.58b}$$

$$B_{22}^{--} = \frac{\lambda_1 a_1 I_1^2}{1+\lambda_1 a_1 I_1 K_1}, \tag{2.58c}$$

where we have used the notation $I_{1,2} \equiv I_m(\kappa a_{1,2})$ and $K_{1,2} \equiv K_m(\kappa a_{1,2})$. The variable a_2 which has not yet appeared will be defined as the radius of the second cylinder in the next section. In the other regions not quoted above the solution is determined by using the reciprocal symmetry, $g_m^{(0)}(r,r';\kappa) = g_m^{(0)}(r',r;\kappa)$, in the Green's function.

A cylinder with very large radius, such that $a_1 \to \infty$, will simulate a plate in the region of small variations in the angle ($\theta \to 0$). This corresponds to $m \to \infty$, such that m/a_1 is finite. These limits are compatible with the leading uniform asymptotic

approximants to the modified Bessel functions for large orders, see for eg. [19],

$$I_m(mz) \sim \sqrt{\frac{t}{2\pi m}}\, e^{m\eta(z)} \qquad \text{and} \qquad K_m(mz) \sim \sqrt{\frac{\pi t}{2m}}\, e^{-m\eta(z)}, \qquad m \to \infty, \tag{2.59}$$

where

$$t = \frac{1}{\sqrt{1+z^2}} \qquad \text{and} \qquad \eta(z) = \sqrt{1+z^2} + \ln\frac{z}{1+\sqrt{1+z^2}}. \tag{2.60}$$

Using the above asymptotic behaviors in eq. (2.57), and after interpreting $m/a_1 \to k_y$, $k_z \leftrightarrow k_x$, we can reproduce the solution in eq. (2.47) for a single plate.

2.3.4 Green's function for two concentric cylinders

Two concentric cylinders of radii $a_{1,2}$, such that $a = a_2 - a_1 > 0$, are described by the potential

$$V(r) = \lambda_1\, \delta(r - a_1) + \lambda_2\, \delta(r - a_2). \tag{2.61}$$

Since the potential depends only on the radial coordinate, the background Green's function satisfying eq. (1.12) can be written in the form of eq. (2.54). Substituting eq. (2.54) into the differential equation for the Green's function in eq. (1.12) we find that the reduced Green's function, $g_m(r, r'; \kappa)$, satisfies the differential equation

$$-\left[\frac{1}{r}\frac{\partial}{\partial r} r \frac{\partial}{\partial r} - \frac{m^2}{r^2} - \kappa^2 - \lambda_1 \delta(r - a_1) - \lambda_2 \delta(r - a_2)\right] g_m(r, r'; \kappa) = \frac{\delta(r - r')}{r}. \tag{2.62}$$

In terms of the notations introduced in Figure 2.2 we can write the solution to

eq. (2.62) in the form

$$(g_m)_{11}(r,r';\kappa) = I_m(\kappa r_<)K_m(\kappa r_>) + B_{11}^{++}\, I_m(\kappa r)I_m(\kappa r') \tag{2.63a}$$

$$\begin{aligned}(g_m)_{22}(r,r';\kappa) = {} & I_m(\kappa r_<)K_m(\kappa r_>) + B_{22}^{++}\, I_m(\kappa r)I_m(\kappa r') + B_{22}^{--}\, K_m(\kappa r)K_m(\kappa r') \\ & + B_{22}^{+-}\, I_m(\kappa r)K_m(\kappa r') + B_{22}^{-+}\, K_m(\kappa r)I_m(\kappa r'),\end{aligned} \tag{2.63b}$$

$$(g_m)_{33}(r,r';\kappa) = I_m(\kappa r_<)K_m(\kappa r_>) + B_{33}^{--}\, K_m(\kappa r)K_m(\kappa r'), \tag{2.63c}$$

$$(g_m)_{12}(r,r';\kappa) = B_{12}^{+-}\, I_m(\kappa r)K_m(\kappa r') + B_{12}^{++}\, I_m(\kappa r)I_m(\kappa r'), \tag{2.63d}$$

$$(g_m)_{13}(r,r';\kappa) = B_{13}^{+-}\, I_m(\kappa r)K_m(\kappa r'), \tag{2.63e}$$

$$(g_m)_{23}(r,r';\kappa) = B_{23}^{+-}\, I_m(\kappa r)K_m(\kappa r') + B_{23}^{--}\, K_m(\kappa r)K_m(\kappa r'), \tag{2.63f}$$

where the coefficients are determined using the continuity conditions to be

$$B_{11}^{++} = -\frac{1}{\Delta}\Big[\lambda_1 a_1 \lambda_2 a_2\, K_1K_2\,\big(I_2K_1 - I_1K_2\big) + \lambda_1 a_1\, K_1^2 + \lambda_2 a_2\, K_2^2\Big], \tag{2.64a}$$

$$B_{22}^{++} = -\frac{1}{\Delta}\lambda_2 a_2\, K_2^2\,\big(1 + \lambda_1 a_1\, I_1K_1\big), \qquad B_{22}^{--} = -\frac{1}{\Delta}\lambda_1 a_1\, I_1^2\,\big(1 + \lambda_2 a_2\, I_2K_2\big), \tag{2.64b}$$

$$B_{22}^{+-} = B_{22}^{-+} = \frac{1}{\Delta}\lambda_1 a_1 \lambda_2 a_2\, I_1^2K_2^2, \tag{2.64c}$$

$$B_{33}^{--} = -\frac{1}{\Delta}\Big[\lambda_1 a_1 \lambda_2 a_2\, I_1I_2\,\big(I_2K_1 - I_1K_2\big) + \lambda_1 a_1\, I_1^2 + \lambda_2 a_2\, I_2^2\Big], \tag{2.64d}$$

$$B_{12}^{+-} = \frac{1}{\Delta}\Big[1 + \lambda_2 a_2\, I_2K_2\Big], \qquad B_{12}^{++} = -\frac{1}{\Delta}\lambda_2 a_2\, K_2^2, \tag{2.64e}$$

$$B_{13}^{+-} = \frac{1}{\Delta}, \tag{2.64f}$$

$$B_{23}^{+-} = \frac{1}{\Delta}\Big[1 + \lambda_1 a_1\, I_1K_1\Big], \qquad B_{23}^{--} = -\frac{1}{\Delta}\lambda_1 a_1\, I_1^2, \tag{2.64g}$$

where

$$\Delta = 1 + \lambda_1 a_1\, I_1K_1 + \lambda_2 a_2\, I_2K_2 + \lambda_1 a_1 \lambda_2 a_2\, I_1K_2\,\big(I_2K_1 - I_1K_2\big). \tag{2.65}$$

2.4 Derivatives of the Green's function

Derivatives of Green's functions involves evaluating a function at a point where it has jump discontinuities. We shall confine our discussion in this section for the case of parallel plates for simplicity.

It is of relevance to observe that the Green's function represented above is continuous everywhere in the z, z' domain while its first derivatives have simple (jump) discontinuities along the lines, $z = z'$, $z = a_1$, $z = a_2$, $z' = a_1$, and $z' = a_2$. Thus for evaluating expressions involving taking derivatives of the Green's function at the lines of discontinuity, a definite prescription for the evaluation of the derivatives is called for. For this purpose, we interpret the value of a function at the point where it has a jump discontinuity to be the average of all the possible limiting values. For example, the derivative of the Green's function at the point $(z = a_2, z' = a_1)$ in Figure 2.2 takes on four different values when approached from the four regions 21, 22, 31, and 32. The value of the derivative is defined as the average of these four values.

Evaluation of the derivatives using the averaging prescription is made convenient when we define the Green's function around a point as the average of the suitable

piecewise functions. Thus, we evaluate

$$
\begin{aligned}
g(a_1,a_2;\kappa) &= \frac{1}{4}\Big[g_{22}(a_1,a_2;\kappa)+g_{12}(a_1,a_2;\kappa)+g_{13}(a_1,a_2;\kappa)+g_{23}(a_1,a_2;\kappa)\Big] \\
&= \frac{1}{\Delta}\frac{1}{2\kappa}\,e^{-\kappa a}, && \text{(2.66a)} \\
g(a_2,a_1;\kappa) &= \frac{1}{4}\Big[g_{22}(a_2,a_1;\kappa)+g_{21}(a_2,a_1;\kappa)+g_{31}(a_2,a_1;\kappa)+g_{32}(a_2,a_1;\kappa)\Big] \\
&= \frac{1}{\Delta}\frac{1}{2\kappa}\,e^{-\kappa a}, && \text{(2.66b)} \\
g(a_1,a_1;\kappa) &= \frac{1}{4}\Big[g_{11}(a_1,a_1;\kappa)+g_{22}(a_1,a_1;\kappa)+g_{12}(a_1,a_1;\kappa)+g_{21}(a_1,a_1;\kappa)\Big] \\
&= \frac{1}{\Delta}\frac{1}{2\kappa}\left[1+\frac{\lambda_2}{2\kappa}\Big(1-e^{-2\kappa a}\Big)\right], && \text{(2.66c)} \\
g(a_2,a_2;\kappa) &= \frac{1}{4}\Big[g_{22}(a_2,a_2;\kappa)+g_{33}(a_2,a_2;\kappa)+g_{23}(a_2,a_2;\kappa)+g_{32}(a_2,a_2;\kappa)\Big] \\
&= \frac{1}{\Delta}\frac{1}{2\kappa}\left[1+\frac{\lambda_1}{2\kappa}\Big(1-e^{-2\kappa a}\Big)\right]. && \text{(2.66d)}
\end{aligned}
$$

The first derivatives evaluate to be

$$
\begin{aligned}
\partial_z\, g(z,z';\kappa)\big|_{z=a_1,z'=a_2} &= \partial_{z'}\, g(z,z';\kappa)\big|_{z=a_2,z'=a_1} = \frac{1}{\Delta}\frac{\kappa}{2\kappa}\Big(1+\frac{\lambda_1}{2\kappa}\Big)\,e^{-\kappa a}, && \text{(2.67a)} \\
\partial_{z'}\, g(z,z';\kappa)\big|_{z=a_1,z'=a_2} &= \partial_{z}\, g(z,z';\kappa)\big|_{z=a_2,z'=a_1} = -\frac{1}{\Delta}\frac{\kappa}{2\kappa}\Big(1+\frac{\lambda_2}{2\kappa}\Big)\,e^{-\kappa a}, && \text{(2.67b)} \\
\partial_z\, g(z,z';\kappa)\big|_{z=a_1,z'=a_1} &= \partial_{z'}\, g(z,z';\kappa)\big|_{z=a_1,z'=a_1} = -\frac{1}{\Delta}\frac{\kappa}{2\kappa}\frac{\lambda_2}{2\kappa}\,e^{-\kappa a}, && \text{(2.67c)} \\
\partial_z\, g(z,z';\kappa)\big|_{z=a_2,z'=a_2} &= \partial_{z'}\, g(z,z';\kappa)\big|_{z=a_2,z'=a_2} = \frac{1}{\Delta}\frac{\kappa}{2\kappa}\frac{\lambda_1}{2\kappa}\,e^{-\kappa a}. && \text{(2.67d)}
\end{aligned}
$$

where $\partial_{z,z'}$ is derivative with respect to z, z'. The second derivatives involving two

distinct variables evaluate to be

$$\begin{aligned}
\partial_z \partial_{z'}\, g(z,z';\kappa)\big|_{z=a_1,z'=a_2} &= \partial_z \partial_{z'}\, g(z,z';\kappa)\big|_{z=a_2,z'=a_1} \\
&= -\frac{1}{\Delta}\frac{\kappa^2}{2\kappa}\Big(1+\frac{\lambda_1}{2\kappa}\Big)\Big(1+\frac{\lambda_2}{2\kappa}\Big)\, e^{-\kappa a}, \qquad (2.68a) \\
\partial_z \partial_{z'}\, g(z,z';\kappa)\big|_{z=a_1,z'=a_1} &= -\frac{1}{\Delta}\frac{\kappa^2}{2\kappa}\left[\Big(1+\frac{\lambda_1}{2\kappa}\Big)\Big(1+\frac{\lambda_2}{2\kappa}\Big)+\frac{\lambda_2}{2\kappa}\, e^{-2\kappa a}\right], \qquad (2.68b) \\
\partial_z \partial_{z'}\, g(z,z';\kappa)\big|_{z=a_2,z'=a_2} &= -\frac{1}{\Delta}\frac{\kappa^2}{2\kappa}\left[\Big(1+\frac{\lambda_1}{2\kappa}\Big)\Big(1+\frac{\lambda_2}{2\kappa}\Big)+\frac{\lambda_1}{2\kappa}\, e^{-2\kappa a}\right]. \qquad (2.68c)
\end{aligned}$$

The second derivatives involving the same variables evaluate to

$$\partial_z^2 g(z,z';\kappa) = \kappa^2\, g(z,z';\kappa) \qquad (2.69)$$

which when compared with eq. (2.41) tells us that the averaging prescription practically throws away the delta function contributions in eq. (2.41). A more detailed study of this issue is being sought. Since the second derivative returns the Green's function back, all higher order derivatives are obtained in terms of the above expressions.

Steve Fulling suggests that our averaging prescription can be justified from a distributional interpretation of the Green function and its differential equation. He suspects that it may even be related to the "fat points" that he studied with Estrada in [20].

Chapter 3

Casimir plates

In chapter 1 we derived expressions for Casimir energy and Casimir force for a general geometric configuration in terms of the Green's functions for the scalar case. In chapter 2 we evaluated the Green's functions for parallel plates and concentric cylinders. In this chapter we shall unite these to derive explicit expressions for the Casimir energy and Casimir force for a single plate and for parallel plate configuration. This should serve as a demonstration of our techniques which will be employed with much more vigor in the later chapters.

The Casimir force between parallel plates described by δ-function potentials was studied in 1992 [18] [also see references to even earlier articles in Russian there]. Reexamination of this study by the MIT group in [21] led to discussions in which "more heat than light was generated" [22] and thus further clarified in [22].

When the plates are chosen to be parallel to the $x-y$ plane the potentials describing the plates have dependence only on the z variable. Thus we can write the Green's function in the form of eq. (2.40) in terms of the reduced Green's function, $g(z, z'; \kappa)$. Further, inserting the Green's function in eq. (2.40) into the expression for

the Casimir force in eq. (1.58) we have the total force per area acting on the potential to be

$$\frac{F}{A} = \frac{1}{2}\int_{-\infty}^{\infty}\frac{d\zeta}{2\pi}\int\frac{d^2k_\perp}{(2\pi)^2}\int_{\frac{\text{vol}}{A}} dz\, g(z,z;\kappa)\frac{\partial}{\partial z}V(z), \tag{3.1}$$

where we have used $A = \int dx \int dy$ to represent the total area of the plates. The integration limit vol/A for the z integration symbolically specifies the body on which the force is being evaluated. For example, for parallel plates situated at $z = a_{1,2}$, the force on the plate at a_1 will be evaluated by integrating from $z = a_1 - \epsilon$ to $z = a_1 + \epsilon$ and then taking the limit $\epsilon \to 0$. Also, integrating from $-\infty$ to $+\infty$ evaluates the force per area on both the plates which in general evaluates to zero unless there is another source of interaction.

Similarly substituting the expression for the Green's function in eq. (2.40) into the expression for Casimir energy in eq. (1.53) we have the total energy per area to be

$$\frac{E_{\text{tot}}}{A} = -\frac{1}{2}\int_{-\infty}^{\infty}\frac{d\zeta}{2\pi}\int\frac{d^2k_\perp}{(2\pi)^2}\,2\zeta^2\int_{-\infty}^{\infty} dz\, g(z,z;\kappa). \tag{3.2}$$

We have thus described a formalism to evaluate the force per area on the plates, and total energy per area. Evaluations of these quantities for specific potentials requires the solution for the reduced Green's function which has been given for specific cases of interest in chapter 2. More specifically, the problem involves integrating over ζ, $k_\perp$, and z. Our strategy will be to evaluate the z integral first which is immediate for the case of δ-function potentials when evaluating the force per area after integration by parts in eq. (3.1). In performing the ζ and $k_\perp$ integrals it will be convenient to exploit the relation $\kappa^2 = \mathbf{k}_\perp^2 + \zeta^2$ which follows from the relation introduced after eq. (2.40) using the fact that $\omega \to i\zeta$. Using spherical polar coordinates we will thus be

able to evaluate

$$\frac{1}{2}\int_{-\infty}^{\infty}\frac{d\zeta}{2\pi}\int\frac{d^2k_\perp}{(2\pi)^2}\to\frac{1}{4\pi^2}\int_0^\infty\kappa^2 d\kappa, \tag{3.3}$$

and

$$\frac{1}{2}\int_{-\infty}^{\infty}\frac{d\zeta}{2\pi}\int\frac{d^2k_\perp}{(2\pi)^2}\frac{\zeta^2}{\kappa^2}\to\frac{1}{3}\frac{1}{4\pi^2}\int_0^\infty\kappa^2 d\kappa, \tag{3.4}$$

where the factor of one third in the second situation comes from the angular integration in spherical polar coordinates.

3.1 Single semitransparent plate

We begin by recalling that a single semitransparent plate positioned at $z = a_1$ is mathematically described using the potential in eq. (2.39). In this particular case the only contribution to the z integration in the expression for the force in eq. (3.1) comes when $z = a_1$. Thus, after integrating by parts in z in the expression for force in eq. (3.1), and with the observation that the δ-function in the potential contributes only at the position of the plate, we can write

$$\frac{F_1}{A} = -\frac{\lambda_a}{2}\int_{-\infty}^{\infty}\frac{d\zeta}{2\pi}\int\frac{d^2k_\perp}{(2\pi)^2}\left\{\frac{\partial}{\partial z}g(z,z;\kappa)\right\}_{z=a_1}. \tag{3.5}$$

For a single plate we evaluated the solution to the reduced Green's function, $g(z, z; \kappa)$, in eq. (2.47). The force per area on the plate is given in terms of eq. (3.5) which is determined in terms of $g(z, z'; \kappa)$ when evaluated at $z = z'$, which is read off from the solution in eq. (2.47) to be

$$g(z,z;\kappa) = \frac{1}{2\kappa} - \frac{\lambda_1}{\lambda_1 + 2\kappa}\frac{1}{2\kappa}\,e^{-2\kappa|z-a_1|}. \tag{3.6}$$

The first derivative of the Green's function computed after evaluating the function at $z = z'$ is

$$\frac{\partial}{\partial z} g(z, z; \kappa) = \begin{cases} -\dfrac{\lambda_1}{\lambda_1 + 2\kappa}\, e^{-2\kappa|z-a_1|} & \text{if} \quad z < a_1, \\ \\ +\dfrac{\lambda_1}{\lambda_1 + 2\kappa}\, e^{-2\kappa|z-a_1|} & \text{if} \quad z > a_1. \end{cases} \tag{3.7}$$

Note that $g(z, z; \kappa)$ is continuous at $z = a_1$ while its derivative has a jump discontinuity at $z = a_1$. Interpreting the value of a function at the point where it has a jump discontinuity to be the average of the jump lets us evaluate the quantity in curly brackets in the expression for the force in eq. (3.5), using eq. (3.7), to be zero. This leads to the expected result, that the force per area on a single plate is zero. Thus a single plate does not feel any force from the vacuum.

We next calculate the total energy per area for the case of a single plate using eq. (3.2). Using eq. (3.6) we evaluate

$$2\zeta^2 \int_{-\infty}^{\infty} dz\, g(z, z; \kappa) - \frac{\zeta^2}{\kappa^2} \int_{-\infty}^{\infty} \kappa\, dz = -\frac{\zeta^2}{\kappa^2} \frac{\lambda_1}{\lambda_1 + 2\kappa}, \tag{3.8}$$

which when substituted into the expression for energy in eq. (3.2) with the help of the integral in eq. (3.4) leads to

$$\frac{E_{\text{tot}}}{A} = \frac{E_{\text{bulk}}}{A} + \frac{E_1}{A}, \tag{3.9}$$

where E_{bulk} represents a divergent quantity

$$\frac{E_{\text{bulk}}}{A} = -\frac{1}{12\pi^2} \int_0^{\infty} \kappa^3 d\kappa \int_{-\infty}^{\infty} dz \tag{3.10}$$

which notably does not depend on the parameters associated with the potential. In

fact this part of the total energy would exist even in the absence of the potential. Further, this part does not contribute to the force because by definition the force on a plate can be interpreted as the change in energy due to a change in the position of the plate and since the above divergent part does not contribute to this change in energy we feel very safe in subtracting this from the total energy for all practical purposes except possibly for cosmology. The second term in the expression for total energy in eq. (3.9), which is also divergent, is given by the expression

$$\frac{E_1}{A} = \frac{1}{12\pi^2}\int_0^\infty \kappa^2 d\kappa \, \frac{\lambda_1}{\lambda_1 + 2\kappa} = \frac{1}{96\pi^2}\int_0^\infty \frac{dy}{y}\,\frac{y^3}{1+\frac{y}{\lambda_1}}. \tag{3.11}$$

We note that E_1/A, though divergent, depends on the coupling parameter λ_1. This signifies that this term relates to a single plate. Later, when we have more than one plate, terms associated with each plate will have a corresponding piece contributing to the total energy which would have made its contribution even in the absence of all other plates. We also note that the expression of energy in eq. (3.11) is independent of the position of the plate which is a consequence of the translational symmetry of the problem and there is no associated force.

3.2 Parallel semitransparent plates

We earlier mentioned that two semitransparent plates positioned parallel to each other at $z = a_{1,2}$, $a = a_2 - a_1 > 0$, is mathematically described using the potential presented in eq. (2.48). The total force per area on the complete Casimir apparatus consisting of the plates '1' and '2' is gotten by integrating over the complete z region in the expression for force in eq. (3.1). Thus, after integrating by parts in z in eq.

(3.1) and with the observation that the δ-functions in the potential contributes only at the position of the plates we can write

$$\frac{F_{1+2}}{A} = \frac{F_1}{A} + \frac{F_2}{A}, \tag{3.12}$$

where $F_{1,2}$ is the force on one of the plates

$$\frac{F_{1,2}}{A} = -\frac{\lambda_{1,2}}{2} \int_{-\infty}^{\infty} \frac{d\zeta}{2\pi} \int \frac{d^2k_\perp}{(2\pi)^2} \left\{ \frac{\partial}{\partial z} g(z, z; \kappa) \right\}_{z=z_{1,2}}. \tag{3.13}$$

We note that the force on one plate exactly equals and is opposite to the force acting on the other plate (using eq. (3.16)). Since the total force on the parallel plates is the sum of the two forces we learn that the total force on the Casimir apparatus is zero, which is expected.

For parallel plates we evaluated the solution to the reduced Green's function, $g(z, z; \kappa)$, in eq. (2.50). The force per area on the plate is given in terms of eq. (3.13) which is determined in terms of $g(z, z'; \kappa)$ when evaluated at $z = z'$, which is read off from the solution in eq. (2.50) to be

$$g(z, z; \kappa) = \begin{cases} \frac{1}{2\kappa} + A_{11}^{++}\, e^{2\kappa z} & \text{if} \quad z < a_1 < a_2, \\ \frac{1}{2\kappa} + A_{22}^{++}\, e^{2\kappa z} + A_{22}^{--}\, e^{-2\kappa z} + 2\, A_{22}^{+-} & \text{if} \quad a_1 < z < a_2, \\ \frac{1}{2\kappa} + A_{33}^{--}\, e^{-2\kappa z} & \text{if} \quad a_1 < a_2 < z. \end{cases} \tag{3.14}$$

It can be verified that $g(z, z; \kappa)$ is continuous at $z = a_1$ and $z = a_2$. The derivative

of $g(z,z;\kappa)$ is

$$\frac{\partial}{\partial z}g(z,z;\kappa) = \begin{cases} 2\kappa\, A_{11}^{++}\, e^{2\kappa z}, & \text{if} \quad z < a_1 < a_2, \\ 2\kappa\, A_{22}^{++}\, e^{2\kappa z} - 2\kappa\, A_{22}^{--}\, e^{-2\kappa z}, & \text{if} \quad a_1 < z < a_2, \\ -2\kappa\, A_{33}^{--}\, e^{-2\kappa z}, & \text{if} \quad a_1 < a_2 < z, \end{cases} \tag{3.15}$$

which has jump discontinuities at $z = a_1$ and $z = a_2$. Interpreting the value of the function at the point of discontinuity to be the average of the discontinuity lets us evaluate the derivative and write

$$\begin{aligned} \frac{\lambda_2}{2\kappa}\left\{\frac{\partial}{\partial z}g(z,z;\kappa)\right\}_{z=a_2} = -\frac{\lambda_1}{2\kappa}\left\{\frac{\partial}{\partial z}g(z,z;\kappa)\right\}_{z=a_1} &= \frac{1}{\Delta}\frac{\lambda_1}{2\kappa}\frac{\lambda_2}{2\kappa}\, e^{-2\kappa a} \\ &= \frac{1}{2\kappa}\frac{\partial}{\partial a}\ln\Delta, \end{aligned} \tag{3.16}$$

where we have made use of the fact that Δ, see eq. (2.52), has dependence on a_1 and a_2 only in the combination $a = a_2 - a_1$, which is the signature of translational invariance. Using eq. (3.16) in the expression for force in eq. (3.13), we can thus calculate the force per area on the plates to be, after using the integral in eq. (3.3),

$$\frac{F_2}{A} = -\frac{F_1}{A} = -\frac{1}{2\pi^2}\int_0^\infty \kappa^3\, d\kappa\, \frac{1}{2\kappa}\frac{\partial}{\partial a}\ln\Delta. \tag{3.17}$$

In the Dirichlet limit ($a\lambda_{1,2} \gg 1$) we have, after using the explicit expression for Δ in eq. (2.52) into eq. (3.16),

$$\frac{1}{2\kappa}\frac{\partial}{\partial a}\ln\Delta \to \frac{1}{e^{2\kappa a}-1} = \frac{1}{2\kappa}\frac{\partial}{\partial a}\ln\left(1 - e^{-2\kappa a}\right) \tag{3.18}$$

which leads to the result

$$\frac{F_{2,\mathrm{D}}}{A} = -\frac{F_{1,\mathrm{D}}}{A} = -\frac{1}{2\pi^2}\int_0^\infty \frac{d\kappa}{\kappa}\frac{\kappa^4}{e^{2\kappa a}-1} = -\frac{1}{32\pi^2\,a^4}\int_0^\infty \frac{dy}{y}\frac{y^4}{e^y-1}$$
$$= -\frac{\Gamma(4)\zeta(4)}{32\pi^2\,a^4} = -\frac{\pi^2}{480\,a^4}, \qquad (3.19)$$

where we have used $\Gamma(4) = 6$ and $\zeta(4) = \frac{\pi^4}{90}$. This result is exactly half of Casimir's result which was derived for the case of conducting plates. Since we started with the assumption $a_2 > a_1$, we have $a > 0$, we interpret the force on plate '2' to be negative, meaning it points towards '1', and vice versa. Thus the force between the plates is attractive.

We next calculate the total energy per area for the case of parallel plates. The total energy is evaluated using eq. (3.2) which requires integrating $g(z, z; \kappa)$ with respect to z. Using the expression for $g(z, z; \kappa)$ in eq. (3.14) we evaluate

$$2\zeta^2\int_{-\infty}^{\infty} dz\, g(z,z;\kappa) - \frac{\zeta^2}{\kappa^2}\int_{-\infty}^{\infty} dz$$
$$= -\frac{1}{\Delta}\frac{\zeta^2}{\kappa^2}\left[\frac{\lambda_a}{2\kappa} + \frac{\lambda_b}{2\kappa} + 2\frac{\lambda_a}{2\kappa}\frac{\lambda_b}{2\kappa}\left\{1 - e^{-2\kappa a}\right\} - 2\kappa a\,\frac{\lambda_a}{2\kappa}\frac{\lambda_b}{2\kappa}\,e^{-2\kappa a}\right], \qquad (3.20)$$

which when substituted into the expression for energy in eq. (3.2) with the help of the integral in eq. (3.4) and identifying the total bulk energy term using eq. (3.10) leads to

$$\frac{E_{\mathrm{tot}}}{A} - \frac{E_{\mathrm{bulk}}}{A}$$
$$= \frac{1}{12\pi^2}\int_0^\infty \kappa^2 d\kappa \frac{1}{\Delta}\left[\frac{\lambda_1}{2\kappa} + \frac{\lambda_2}{2\kappa} + 2\frac{\lambda_1}{2\kappa}\frac{\lambda_2}{2\kappa}\left\{1 - e^{-2\kappa a}\right\} - 2\kappa a\,\frac{\lambda_1}{2\kappa}\frac{\lambda_2}{2\kappa}\,e^{-2\kappa a}\right], \qquad (3.21)$$

which can be rewritten in the form

$$\frac{E_{\rm tot}}{A} - \frac{E_{\rm bulk}}{A} = \frac{E_1}{A} + \frac{E_2}{A} + \frac{E_{\rm Cas}}{A}, \tag{3.22}$$

where the first two terms are total energy per area due to single plates given in terms of eq. (3.11) and the third term is the Casimir energy per area given as

$$\frac{E_{\rm Cas}}{A} = -\frac{1}{12\pi^2}\int_0^\infty \kappa^2\, d\kappa \left[2\kappa a + \frac{1}{1+\frac{\lambda_1}{2\kappa}} + \frac{1}{1+\frac{\lambda_2}{2\kappa}}\right] \frac{1}{2\kappa}\frac{\partial}{\partial a}\ln\Delta. \tag{3.23}$$

In the Dirichlet limit the above expression using eq. (3.18) gives

$$\frac{E_{\rm Cas,D}}{A} = -\frac{1}{96\pi^2\, a^3}\int_0^\infty \frac{dy}{y}\,\frac{y^4}{e^y-1} = -\frac{\Gamma(4)\zeta(4)}{96\pi^2\, a^3} = -\frac{\pi^2}{1440\, a^3}. \tag{3.24}$$

As a consistency check we verify that the force and energy derived above are related by the relation

$$\frac{F_2}{A} = -\frac{\partial}{\partial a}\frac{E_{\rm tot}}{A}. \tag{3.25}$$

which is a consequence of the variation of the action with respect to the position of the plates. To this regard we observe the following relation

$$\left[2\kappa a + \frac{1}{1+\frac{\lambda_1}{2\kappa}} + \frac{1}{1+\frac{\lambda_2}{2\kappa}}\right] \frac{1}{2\kappa}\frac{\partial}{\partial a}\left\{\frac{1}{2\kappa}\frac{\partial}{\partial a}\ln\Delta\right\} = \kappa\frac{\partial}{\partial\kappa}\left\{\frac{1}{2\kappa}\frac{\partial}{\partial a}\ln\Delta\right\} \tag{3.26}$$

and using this in eq. (3.23) we evaluate

$$-\frac{\partial}{\partial a}\frac{E_{\rm tot}}{A} = \frac{F_2}{A} + \frac{1}{6\pi^2}\int_0^\infty d\kappa \frac{\partial}{\partial\kappa}\left[\kappa^4\frac{1}{2\kappa}\frac{\partial}{\partial a}\ln\Delta\right], \tag{3.27}$$

which immediately leads to eq. (3.25) after we observe that the surface term evaluates

to zero. Comparing the expression for force in eq. (3.25) and eq. (3.17) we also observe and conclude that

$$\frac{E_{\rm tot}}{A} = \frac{1}{4\pi^2}\int_0^\infty \kappa^2 d\kappa \, \ln\Delta + \text{constant}, \tag{3.28}$$

where the constant is a quantity independent of a. One can evaluate the constant term by comparing the above expression with eq. (3.22).

Chapter 4

How does Casimir energy fall?

In this chapter we demonstrate that quantum vacuum energy gravitates according to the equivalence principle. We consider parallel semitransparent plates, that is, δ-function potentials, acting on a massless scalar field, in a space-time defined by Rindler coordinates (τ, x, y, ξ). Fixed ξ in such a space-time represents uniform acceleration. We calculate the force on systems consisting of one or two such plates at fixed values of ξ. In the limit of large Rindler coordinate ξ (small acceleration), we recover (via the equivalence principle) the situation of weak gravity, and find that the gravitational force on the system is just Mg, where g is the gravitational acceleration and M is the total mass of the system, consisting of the mass of the plates renormalized by the Casimir energy of each plate separately, plus the energy of the Casimir interaction between the plates. This reproduces the result in [23] for the Dirichlet limit as the coupling to the δ-function potential approaches infinity.

We evaluated the quantum vacuum energy associated with semitransparent parallel plates in chapter 3. In particular we demonstrated that the total energy associated with the parallel plates consists of divergent parts associated with the single plates.

The subject of quantum vacuum energy, or of Casimir energy, has engendered a certain controversy from the beginning because of the presence of divergences, which make it difficult to extract self-energies for single bodies [24, 25, 26, 21, 27, 28]. Although these divergences can be consistently isolated when calculating the Casimir forces between distinct bodies, the issue of how divergent and finite Casimir energies couple to gravity remains unclear.

In the last few years there have been several calculations of the gravitational acceleration imparted to the Casimir energy associated with a pair of perfectly conducting plates [29, 30, 31, 32, 33]. The results were inconsistent, and there was no consensus that the gravitational force agreed with the equivalence principle. In a series of three papers [23, 34, 35] we have shown that indeed the gravitational force on a Casimir apparatus is exactly that required by the equivalence principle, that is, that the gravitational mass of the Casimir energy is just the Casimir energy itself. Other authors now agree with our conclusion [36]. The authors in [36] now also agree that there is no trace anomaly in their energy-momentum tensor [37].

We describe a uniformly accelerated system by Rindler coordinates [38], which naturally represent frames undergoing hyperbolic motion. We consider both a single plate, and two plates, both represented by δ-function potentials, which was discussed in chapters 2 and 3. In Minkowski space, the Casimir energies for such systems was discussed in chapter 3 and have been considered by many authors [18, 21, 22, 39, 40]. Saharian et al. [41] considered Dirichlet, Neumann, and perfectly conducting plates in Rindler coordinates, and showed for rigid acceleration of those plates, in the limit of large Rindler coordinate, which corresponds to the weak gravitational field limit, that the finite Casimir energy undergoes the normal acceleration. We carry out that calculation here for semitransparent plates (which reduce to Dirichlet plates in the

strong-coupling limit) and find that both for a single plate, and for two parallel plates (both orthogonal to the Rindler spatial coordinate) both the divergent and finite parts of the Casimir energy gravitate according to the equivalence principle, and that the divergent energies serve to renormalize the inertial and gravitational masses of each separate plate.

Acceleration of semitransparent plates has been considered by many authors in connection with quantum radiation [42, 43, 44, 45, 46]. Gravitational effects of surface energies in Rindler and de Sitter space-times are considered in Refs. [47, 48, 49].

In the following the superscript (0) will be used to signify that it is the zeroth order effect of gravity which would relate to the results in chapter 3.

4.1 Rindler Coordinates

We consider the situation when the plates are forced to move rigidly [50] in such a way that the proper distance between the plates is preserved. This is achieved if the two plates move with different but constant proper accelerations [38]. Let the position of the plates be specified by functions $z_a(t)$ and $z_b(t)$. Let the plates move with constant proper accelerations $\alpha_a = c^2\xi_a^{-1}$ and $\alpha_b = c^2\xi_b^{-1}$ $(c = 1)$ respectively. Further let us choose the position of the plates at time $t = 0$ to be $z_a(0) = \xi_a$ and $z_b(0) = \xi_b$ respectively. The equations of motion of the plates are

$$z_a(t)^2 - t^2 = \xi_a^2 \qquad \text{and} \qquad z_b(t)^2 - t^2 = \xi_b^2 \tag{4.1}$$

which represent hyperbolas. The relation between the Minkowski coordinates (z,t) and the Rindler coordinates (ξ,τ) for this setup are

$$z = \xi\cosh\tau \qquad \text{and} \qquad t = \xi\sinh\tau \tag{4.2}$$

and the corresponding metrics are related as

$$-ds^2 = -dt^2 + dz^2 + dx^2 + dy^2 = -\xi^2 d\tau^2 + d\xi^2 + dx^2 + dy^2. \tag{4.3}$$

It should be mentioned that $0 \leq \xi < \infty$ and $-\infty < \tau < +\infty$. Thus, Rindler coordinates maps only one quadrant of the light cone in the Minkowski space. Using this transformation we observe that the proper distance between the plates

$$(z_b - z_a)^2 - (t_b - t_a)^2 = (\xi_b - \xi_a)^2\left[\cosh^2\tau - \sinh^2\tau\right] = (\xi_b - \xi_a)^2 \tag{4.4}$$

is indeed preserved as required for it to move rigidly. We introduced subscripts to the time coordinate to emphasize that it depends on the position coordinate. Particularly for $\xi_a < \xi_b$, we have $t_a < t_b$.

Weak gravity will correspond to taking the limits $\xi \to \infty$ and $\tau \to 0$, such that the products, $\xi\tau$, and differences in ξ remain finite. Thus in weak gravity we will have $\Delta z = \Delta\xi$ and $t = \xi\tau$.

We shall now illustrate (for a single plate) how Rindler coordinates are used to separate the variables. We start with the action

$$W = \int d^4x \left[\frac{1}{2}\left(\frac{\partial\phi}{\partial t}\right)^2 - \frac{1}{2}\left(\frac{\partial\phi}{\partial z}\right)^2 - \frac{1}{2}\left(\boldsymbol{\nabla}_\perp\phi\right)^2 - \frac{1}{2}\lambda_a\,\delta\left(z^2 - z_a(t)^2\right)\phi^2\right] \tag{4.5}$$

which describes two plates, positioned at $z = \pm z_a(t)$, initially moving hyperbolically towards each other until they reach $z = \pm\xi_a$, and then moving hyperbolically away from each other. We next use eq. (4.2) to transform from (z,t) to (ξ,τ). The argument of the delta function, $z^2 - z_a(t)^2$, can be immediately transformed into $z^2 - t^2 - \xi_a^2 = \xi^2 - \xi_a^2$. We use the inverse transformation of eq. (4.2), $\xi^2 = z^2 - t^2$, and $\tau = \tanh^{-1}\frac{t}{z}$, to write the differential operators appearing in the action as

$$\frac{\partial}{\partial z} = \frac{\partial\xi}{\partial z}\frac{\partial}{\partial\xi} + \frac{\partial\tau}{\partial z}\frac{\partial}{\partial\tau} = +\cosh\tau\,\frac{\partial}{\partial\xi} - \sinh\tau\,\frac{1}{\xi}\frac{\partial}{\partial\tau}, \tag{4.6a}$$

$$\frac{\partial}{\partial t} = \frac{\partial\xi}{\partial t}\frac{\partial}{\partial\xi} + \frac{\partial\tau}{\partial t}\frac{\partial}{\partial\tau} = -\sinh\tau\,\frac{\partial}{\partial\xi} + \cosh\tau\,\frac{1}{\xi}\frac{\partial}{\partial\tau}, \tag{4.6b}$$

which helps us transform the differential operator in the action to

$$\frac{1}{2}\left(\frac{\partial\phi}{\partial t}\right)^2 - \frac{1}{2}\left(\frac{\partial\phi}{\partial z}\right)^2 = \frac{1}{2}\frac{1}{\xi^2}\left(\frac{\partial\phi}{\partial\tau}\right)^2 - \frac{1}{2}\left(\frac{\partial\phi}{\partial\xi}\right)^2. \tag{4.7}$$

We determine the Jacobian relating the differential elements to give $dz\,dt = \xi\,d\xi\,d\tau$. Finally, using the identity

$$\delta\left(\xi^2 - \xi_a^2\right) = \frac{1}{|2\xi_a|}\Big[\delta(\xi - \xi_a) + \delta(\xi + \xi_a)\Big] \tag{4.8}$$

and redefining $\lambda \to |2\xi_a|\lambda_a$, we rewrite the action in eq. (4.5) as

$$W = \int d^2x \int_0^\infty d\xi \int_{-\infty}^{+\infty} d\tau \times\frac{\xi}{2}\left[\frac{1}{\xi^2}\left(\frac{\partial\phi}{\partial\tau}\right)^2 - \left(\frac{\partial\phi}{\partial\xi}\right)^2 - (\boldsymbol{\nabla}_\perp\phi)^2 - \lambda_a\,\delta(\xi - \xi_a)\,\phi^2\right], \tag{4.9}$$

where we omitted one of the delta functions because it does not contribute in the

range of integration of ξ. We shall see that the equations corresponding to the action in the above form are separable.

4.2 Formalism for parallel plates falling in a constant gravitational field

In terms of the Rindler coordinates we can thus write the action describing the motion of parallel plates moving with constant proper accelerations ξ_a^{-1} and ξ_b^{-1} as

$$W = \int d^4x \sqrt{-g(x)} \mathcal{L}(\phi(x)), \tag{4.10}$$

where $x \equiv (\tau, x, y, \xi)$ represents the coordinates, $d^4x = d\tau\, d\xi\, dx\, dy$ is the coordinate volume element, $g(x) = \det g_{\mu\nu}(x)$ is the determinant of the metric, $g_{\mu\nu}(x) = \mathrm{diag}(-\xi^2, +1, +1, +1)$ defines the metric, and the Lagrangian density is

$$\mathcal{L}(\phi(x)) = -\frac{1}{2} g^{\mu\nu}(x) \partial_\mu \phi(x) \partial_\nu \phi(x) - \frac{1}{2} V(x) \phi(x)^2, \tag{4.11}$$

where

$$V(x) = \lambda_a \delta(\xi - \xi_a) + \lambda_b \delta(\xi - \xi_b). \tag{4.12}$$

Stationarity of the action under an arbitrary variation in the field leads to the equation of motion

$$\left[-\frac{1}{\xi^2} \frac{\partial^2}{\partial \tau^2} + \frac{1}{\xi} \frac{\partial}{\partial \xi} \xi \frac{\partial}{\partial \xi} + \boldsymbol{\nabla}_\perp^2 - V(x) \right] \phi(x) = 0 \tag{4.13}$$

and the corresponding stress tensor is

$$t_{\alpha\beta}(x) = \partial_\alpha\phi(x)\partial_\beta\phi(x) + g_{\alpha\beta}(x)\mathcal{L}(\phi(x)), \tag{4.14}$$

where we have chosen the conformal term to be zero. A couple of components relevant in the present calculation are

$$t_{33}(x) = +\frac{1}{2}\frac{1}{\xi^2}\left(\frac{\partial\phi}{\partial\tau}\right)^2 + \frac{1}{2}\left(\frac{\partial\phi}{\partial\xi}\right)^2 - \frac{1}{2}\left(\boldsymbol{\nabla}_\perp\phi\right)^2 - \frac{1}{2}V(x)\phi^2 \tag{4.15}$$

$$\frac{1}{\xi^2}\,t_{00}(x) = +\frac{1}{2}\frac{1}{\xi^2}\left(\frac{\partial\phi}{\partial\tau}\right)^2 + \frac{1}{2}\left(\frac{\partial\phi}{\partial\xi}\right)^2 + \frac{1}{2}\left(\boldsymbol{\nabla}_\perp\phi\right)^2 + \frac{1}{2}V(x)\phi^2. \tag{4.16}$$

The force density in a non-Minkowskian metric is given as the covariant derivative of the stress tensor and explicitly reads

$$f^\alpha(x) = t^{\alpha\beta}{}_{;\beta} = \frac{1}{\sqrt{-g(x)}}\,\partial_\beta\left\{\sqrt{-g(x)}\;t^{\alpha\beta}(x)\right\} + \Gamma^\alpha_{\mu\nu}(x)\,t^{\mu\nu}(x), \tag{4.17}$$

where $2\,\Gamma^\lambda_{\mu\nu}(x) = g^{\lambda\alpha}(x)\big[\partial_\mu g_{\nu\alpha}(x) + \partial_\nu g_{\mu\alpha}(x) - \partial_\alpha g_{\mu\nu}(x)\big]$, whose non zero components for the Rindler metric are obtained from $\Gamma^3_{00}(x) = \xi$ and $\Gamma^0_{03}(x) = \Gamma^0_{30}(x) = \xi^{-1}$. In this context it is worth pointing out that all the components of the Riemann tensor for the Rindler metric evaluate to zero which is the signature of a flat space time.

The above expression for the force density in eq. (4.17) should be contrasted with the expression for the force density in eq. (1.54). The expression with the negative sign in eq. (1.54) is interpreted to be the force on the potential. In chapter 3 the potentials described the plates and accordingly the expression for the force was interpreted to be on the plates. In the current chapter, and in the next chapter, the potentials describe suitable gravitational fields and thus the force on the Casimir apparatus due

to the gravitational field is interpreted to be the negative of that in eq. (1.54), after generalizing it to the non-Monkowskian case. In the same spirit the expression for the force in this chapter differs from the corresponding expressions in [34] by an overall sign.

Using the non zero components of $\Gamma^{\lambda}_{\mu\nu}(x)$ in the expression for the force density in eq. (4.17) gives the component for the force density in the ξ-direction as

$$f^3(\xi) = \frac{1}{\xi}\frac{\partial}{\partial\xi}\left[\xi\, t^{33}(x)\right] + \xi\, t^{00}(x). \tag{4.18}$$

We also note that $t^{33}(x) = t_{33}(x)$ and $t_{00}(x) = \xi^4 t^{00}(x)$. Thus the force density reads

$$f^3(\xi) = -\frac{1}{2}\phi(x)^2\frac{\partial}{\partial\xi}V(\xi) + \frac{1}{\xi^2}\frac{\partial}{\partial\tau}\left[\frac{\partial\phi}{\partial\tau}\frac{\partial\phi}{\partial\xi}\right] - \boldsymbol{\nabla}_\perp\cdot\left[(\boldsymbol{\nabla}_\perp\phi)\frac{\partial\phi}{\partial\xi}\right]. \tag{4.19}$$

The force density at the one loop level can be written in terms of the Green's function using the correspondence in eq. (1.47), which Green's function in this case satisfies the differential equation

$$-\left[-\frac{1}{\xi^2}\frac{\partial^2}{\partial\tau^2} + \frac{1}{\xi}\frac{\partial}{\partial\xi}\xi\frac{\partial}{\partial\xi} + \boldsymbol{\nabla}_\perp^2 - V(x)\right]G(x,x') = \frac{\delta(\xi-\xi')}{\xi}\delta(\tau-\tau')\delta(\mathbf{x}_\perp - \mathbf{x}'_\perp). \tag{4.20}$$

Since in our case $V(x)$ has only ξ dependence we can write

$$G(x,x') = \int_{-\infty}^{+\infty}\frac{d\omega}{2\pi}\int\frac{d^2k_\perp}{(2\pi)^2}e^{-i\omega(\tau-\tau')}e^{i\mathbf{k}_\perp\cdot(\mathbf{x}_\perp-\mathbf{x}'_\perp)}g(\xi,\xi'), \tag{4.21}$$

where $g(\xi,\xi')$ satisfies

$$-\left[\frac{1}{\xi}\frac{\partial}{\partial\xi}\xi\frac{\partial}{\partial\xi}+\frac{\omega^2}{\xi^2}-k_\perp^2-V(x)\right]g(\xi,\xi')=\frac{\delta(\xi-\xi')}{\xi}. \tag{4.22}$$

In terms of the Green's function the force density takes the form

$$f^3(\xi)=-\frac{1}{2i}G(\xi,\xi)\frac{\partial}{\partial\xi}V(\xi)+\frac{1}{i}\frac{1}{\xi^2}\frac{\partial}{\partial\tau}\left\{\frac{\partial}{\partial\tau}\frac{\partial}{\partial\xi'}G(x,x')\right\}_{x=x'} \\ -\frac{1}{i}\boldsymbol{\nabla}_\perp\cdot\left\{\boldsymbol{\nabla}_\perp\frac{\partial}{\partial\xi'}G(x,x')\right\}_{x=x'}, \tag{4.23}$$

in which the last two terms evaluate to zero because after evaluation of the bracketed terms at $x=x'$ they are independent of τ and $\mathbf{x}$. Thus we have after using eq. (4.21) and $\omega\to i\zeta$

$$f^3(\xi)=-\frac{1}{2}\int_{-\infty}^{+\infty}\frac{d\zeta}{2\pi}\int\frac{d^2k_\perp}{(2\pi)^2}g(\xi,\xi)\frac{\partial}{\partial\xi}V(\xi) \tag{4.24}$$

just as expected from eq. (1.58)

The force density integrated over the complete Rindler space time gives us the total change in momentum which for our case reads

$$\Delta P^3=\int d^4x\sqrt{-g(x)}f^3(\xi)=-\frac{1}{2}\int_{-\infty}^{+\infty}\frac{d\zeta}{2\pi}\int\frac{d^2k_\perp}{(2\pi)^2}\int d^4x\,\xi\,g(\xi,\xi)\frac{\partial}{\partial\xi}V(\xi), \tag{4.25}$$

in terms of which we have

$$\frac{E^3}{A}=\frac{\Delta P^3}{A\int d\tau}=-\frac{1}{2}\int_{-\infty}^{+\infty}\frac{d\zeta}{2\pi}\int\frac{d^2k_\perp}{(2\pi)^2}\int_0^\infty d\xi\,\xi\,g(\xi,\xi)\frac{\partial}{\partial\xi}V(\xi), \tag{4.26}$$

where at this point E^3 is introduced to be the coordinate force defined as the change in momentum per unit coordinate time τ. The coordinate force is intentionally, with

foresight, denoted as E^3 (for energy, which will be demonstrated in the next sections). The physical force on a body situated at the coordinate ξ_0 as measured by an observer while at the coordinate ξ_0 is expected and presumed to be

$$F^3 = \frac{E^3}{\xi_0}. \tag{4.27}$$

If we identify the proper acceleration due to a constant gravitational field as $g = c^2\xi_0^{-1}$ we can write

$$F^3 = \frac{E^3}{c^2}\, g \tag{4.28}$$

which naturally suggests that we interpret the coordinate force as the energy.

A more convincing definition for the force will be derived in the next chapter.

4.2.1 Single plate falling in a constant gravitational field

A single plate moving with acceleration $\xi^{-1} = \xi_a^{-1}$ is described by the potential

$$V(\xi) = \lambda_a\, \delta(\xi - \xi_a). \tag{4.29}$$

Using the above potential in eq. (4.26), integrating by parts, and observing that due to the delta function nature of the potential the coordinate force per unit area gets contributions only at the point $\xi = \xi_a$, the total coordinate force per unit area on the field is

$$\frac{E^3}{A} = \frac{\lambda_a}{2} \int_{-\infty}^{+\infty} \frac{d\zeta}{2\pi} \int \frac{d^2k_\perp}{(2\pi)^2} \left\{ \frac{\partial}{\partial\xi} \Big[\xi\, g(\xi,\xi) \Big] \right\}_{\xi=\xi_a}. \tag{4.30}$$

For the potential in eq. (4.29) the differential equation in eq. (4.22) has the

following solution in terms of the modified Bessel functions (see eq. (2.57), $m \to \zeta$)

$$g(\xi,\xi') = \begin{cases} I_\zeta(k_\perp\xi_<)K_\zeta(k_\perp\xi_>) - \dfrac{\lambda_a\xi_a K_a^2}{1+\lambda_a\xi_a I_a K_a}\, I_\zeta(k_\perp\xi)I_\zeta(k_\perp\xi') & \text{if } \{\xi,\xi'\} < \xi_a, \\ I_\zeta(k_\perp\xi_<)K_\zeta(k_\perp\xi_>) - \dfrac{\lambda_a\xi_a I_a^2}{1+\lambda_a\xi_a I_a K_a}\, K_\zeta(k_\perp\xi)K_\zeta(k_\perp\xi') & \text{if } \xi_a < \{\xi,\xi'\}. \end{cases}$$

Again, $g(\xi,\xi)$ is continuous at $\xi = \xi_a$ and at this point evaluates to

$$g(\xi_a,\xi_a) = \frac{I_a K_a}{1+\lambda_a\xi_a I_a K_a}. \tag{4.31}$$

The first derivative of $g(\xi,\xi)$ has a jump discontinuity at $\xi = \xi_a$. Interpreting the value of a function at the point where it has jump discontinuity to be the average of the jump leads us to evaluate

$$\left\{\xi\frac{\partial}{\partial\xi}g(\xi,\xi)\right\}_{\xi=\xi_a} = \frac{1}{1+\lambda_a\xi_a I_a K_a}\,\xi_a\frac{\partial}{\partial\xi_a}\Big\{I_a K_a\Big\} \tag{4.32}$$

and make the observation

$$\lambda_a\left\{\frac{\partial}{\partial\xi}\Big[\xi\, g(\xi,\xi)\Big]\right\}_{\xi=\xi_a} = \frac{\partial}{\partial\xi_a}\ln(1+\lambda_a\xi_a I_a K_a). \tag{4.33}$$

Using the above in eq. (4.30) lets us write the coordinate force per unit area (which is the energy per unit area) as

$$\frac{E^3}{A} = \frac{1}{2}\int_{-\infty}^{+\infty}\frac{d\zeta}{2\pi}\int\frac{d^2k_\perp}{(2\pi)^2}\frac{\partial}{\partial\xi_a}\ln(1+\lambda_a\xi_a I_a K_a). \tag{4.34}$$

4.2.2 Parallel plates falling in a constant gravitational field

Two plates moving with accelerations $\xi = \xi_a$ and $\xi = \xi_b$, along the hyperbolas in eq. (4.2), are described by the potential

$$V(\xi) = \lambda_a\, \delta(\xi - \xi_a) + \lambda_b\, \delta(\xi - \xi_b) \tag{4.35}$$

Using the above potential in eq. (4.26), integrating by parts, and observing that due to the delta function nature of the potential the coordinate force per unit area gets contributions only at the points $\xi = \xi_a$ and $\xi = \xi_b$, the total coordinate force per unit area on the field is

$$\frac{E^3}{A} = \frac{E^3_{\rm a}}{A} + \frac{E^3_{\rm b}}{A} \tag{4.36}$$

where

$$\frac{E^3_{\rm a,b}}{A} = \frac{\lambda_{a,b}}{2} \int_{-\infty}^{+\infty} \frac{d\zeta}{2\pi} \int \frac{d^2k_\perp}{(2\pi)^2} \left\{ \frac{\partial}{\partial\xi} \Big[\xi\, g(\xi,\xi) \Big] \right\}_{\xi=\xi_{a,b}} . \tag{4.37}$$

For the potential in eq. (4.35) the differential equation in eq. (4.22) has the following solution in terms of the modified Bessel functions (see eq. (2.63), $m \to \zeta$)

$$g(\xi,\xi') = \begin{cases} I_\zeta(k_\perp\xi_<)K_\zeta(k_\perp\xi_>) - \dfrac{\Delta_1}{\Delta}\, I_\zeta(k_\perp\xi)I_\zeta(k_\perp\xi') & \text{if } \{\xi,\xi'\} < \xi_a < \xi_b, \\ I_\zeta(k_\perp\xi_<)K_\zeta(k_\perp\xi_>) - \dfrac{\Delta_{ij}}{\Delta}\, I^i_\zeta(k_\perp\xi)I^j_\zeta(k_\perp\xi') & \text{if } \xi_a < \{\xi,\xi'\} < \xi_b, \\ I_\zeta(k_\perp\xi_<)K_\zeta(k_\perp\xi_>) - \dfrac{\Delta_2}{\Delta}\, K_\zeta(k_\perp\xi)K_\zeta(k_\perp\xi') & \text{if } \xi_a < \xi_b < \{\xi,\xi'\}, \end{cases} \tag{4.38}$$

where we have used summation convention in the indices i, j, and temporarily, only in this equation, attached superscript indices for the modified Bessel functions with

the notation $I_\zeta^1(k_\perp\xi) = I_\zeta(k_\perp\xi)$ and $I_\zeta^2(k_\perp\xi) = K_\zeta(k_\perp\xi)$. We have also introduced

$$\Delta = 1 + \lambda_a\xi_a I_a K_a + \lambda_b\xi_b I_b K_b + \lambda_a\xi_a\lambda_b\xi_b\left[(I_aK_a)(I_bK_b) - (I_aK_b)^2\right], \quad (4.39)$$

$$\Delta_{11} = \lambda_b\xi_b K_b^2(1 + \lambda_a\xi_a I_a K_a), \quad (4.40)$$

$$\Delta_1 = \lambda_a\xi_a K_a^2 + \lambda_b\xi_b K_b^2 - \lambda_a\xi_a\lambda_b\xi_b K_a K_b[I_aK_b - I_bK_a], \quad (4.41)$$

$$\Delta_{22} = \lambda_a\xi_a I_a^2(1 + \lambda_b\xi_b I_b K_b), \quad (4.42)$$

$$\Delta_2 = \lambda_a\xi_a I_a^2 + \lambda_b\xi_b I_b^2 - \lambda_a\xi_a\lambda_b\xi_b I_a I_b[I_aK_b - I_bK_a], \quad (4.43)$$

$$\Delta_{12} = \Delta_{21} = -\lambda_a\xi_a\lambda_b\xi_b I_a^2 K_b^2, \quad (4.44)$$

where the typographical abbreviations correspond to $I_{a,b} = I_\zeta(k_\perp\xi_{a,b})$ and $K_{a,b} = K_\zeta(k_\perp\xi_{a,b})$. It can be verified that $g(\xi,\xi)$ is continuous at $\xi = \xi_a$ and $\xi = \xi_b$ and at these points evaluates to

$$g(\xi_a,\xi_a) = \frac{1}{\Delta}\Big\{I_aK_a + \lambda_b\xi_b\left[(I_aK_a)(I_bK_b) - (I_aK_b)^2\right]\Big\} \quad (4.45)$$

$$g(\xi_b,\xi_b) = \frac{1}{\Delta}\Big\{I_bK_b + \lambda_a\xi_a\left[(I_aK_a)(I_bK_b) - (I_aK_b)^2\right]\Big\}. \quad (4.46)$$

The first derivative of $g(\xi,\xi)$ has jump discontinuities at $\xi = \xi_a$ and $\xi = \xi_b$. Interpreting the value of a function at the point where it has a jump discontinuity to be the average of the jump leads us to evaluate, analogous to the single plate case,

$$\left\{\xi\frac{\partial}{\partial\xi}g(\xi,\xi)\right\}_{\xi=\xi_a} = \frac{1}{\Delta}\,\xi_a\frac{\partial}{\partial\xi_a}\Big\{I_aK_a + \lambda_b\xi_b\left[(I_aK_a)(I_bK_b) - (I_aK_b)^2\right]\Big\} \quad (4.47)$$

$$\left\{\xi\frac{\partial}{\partial\xi}g(\xi,\xi)\right\}_{\xi=\xi_b} = \frac{1}{\Delta}\,\xi_b\frac{\partial}{\partial\xi_b}\Big\{I_bK_b + \lambda_a\xi_a\left[(I_aK_a)(I_bK_b) - (I_aK_b)^2\right]\Big\} \quad (4.48)$$

and make the observations

$$\lambda_{a,b}\left\{\frac{\partial}{\partial\xi}\Big[\xi\, g(\xi,\xi)\Big]\right\}_{\xi=\xi_{a,b}} = \frac{\partial}{\partial\xi_{a,b}}\ln\Delta. \tag{4.49}$$

Using the above in eq. (4.37) lets us write the two contributions to the coordinate force per unit area on the field, in eq. (4.36), as

$$\frac{E^3_{\mathrm{a,b}}}{A} = \frac{1}{2}\int_{-\infty}^{+\infty}\frac{d\zeta}{2\pi}\int\frac{d^2k_\perp}{(2\pi)^2}\frac{\partial}{\partial\xi_{a,b}}\ln\Delta. \tag{4.50}$$

4.3 Weak gravity approximation

In the weak gravity approximation we can proceed further than we could in section 4.2. At the beginning of section 4.1 we mentioned the appropriate limits corresponding to weak gravity. In terms of the Fourier variable ζ corresponding to τ these limits are $\xi\to\infty$ and $\zeta\to\infty$, such that constructions $\frac{\xi}{\zeta}$ and differences in ξ remain finite. These limits are compatible with the uniform asymptotic expansions of the modified Bessel function for large orders, for example see [19], which in terms of our variables read

$$I_\zeta(k_\perp\xi) \sim \sqrt{\frac{t}{2\pi\zeta}}\, e^{\zeta\eta(\xi)}\sum_{n=0}^{\infty}\frac{1}{\zeta^n}u_n(t), \tag{4.51}$$

$$K_\zeta(k_\perp\xi) \sim \sqrt{\frac{\pi t}{2\zeta}}\, e^{-\zeta\eta(\xi)}\sum_{n=0}^{\infty}\frac{(-1)^n}{\zeta^n}u_n(t), \tag{4.52}$$

where

$$t = \frac{1}{\sqrt{1+\frac{k_\perp^2\xi^2}{\zeta^2}}} \qquad \text{and} \qquad \eta(\xi) = \sqrt{1+\frac{k_\perp^2\xi^2}{\zeta^2}} + \ln\left[\frac{\frac{k_\perp\xi}{\zeta}}{1+\sqrt{1+\frac{k_\perp^2\xi^2}{\zeta^2}}}\right] \tag{4.53}$$

and $u_k(t)$ are polynomials in t. Expanding the above expressions around ξ_0, chosen such that the differences $\xi_a - \xi_0$ and $\xi_b - \xi_0$ are finite, we can evaluate

$$\sqrt{\xi_a\xi_b}\, I_a K_b \sim \frac{1}{2\kappa_0}\, e^{-\kappa_0(\xi_b-\xi_a)} \times \left[1 + \frac{1}{\xi_0}\, t_0^2 \left\{1+\kappa_0(\xi_b-\xi_a)\right\}\left\{\frac{\xi_a+\xi_b}{2} - \xi_0\right\} + \mathcal{O}\left(\frac{1}{\xi_0}\right)^2\right], \tag{4.54}$$

where $\kappa_0^2 = k_\perp^2 + \frac{\zeta^2}{\xi_0^2}$, and $t_0 = \frac{\zeta}{\kappa_0\xi_0}$.

Let us first consider a single plate falling in a weak gravitational field. Using eq. (4.54) we can write

$$\frac{\partial}{\partial\xi_a}\ln(1+\lambda_a\xi_a I_a K_a) = t_0^2\,\frac{1}{\xi_0}\,\frac{\lambda_a}{\lambda_a+2\kappa_0} + \mathcal{O}\left(\frac{1}{\xi_0}\right)^2 \tag{4.55}$$

which when used in eq. (4.34) lets us write

$$\frac{E^3}{A} = \frac{1}{2}\int_{-\infty}^{+\infty}\frac{d\zeta}{2\pi}\frac{1}{\xi_0}\int\frac{d^2k_\perp}{(2\pi)^2}\,\frac{\zeta^2}{\kappa_0^2}\frac{1}{\xi_0^2}\,\frac{\lambda_a}{\lambda_a+2\kappa_0} + \mathcal{O}\left(\frac{1}{\xi_0}\right). \tag{4.56}$$

Making the identifications, $\frac{\zeta}{\xi_0} \to \zeta$, and $\kappa_0 \to \kappa$, which are appropriate and consistent with the uniform asymptotic expansions, then using eq. (3.4), and comparing the resultant equation with eq. (3.11), lets us notice

$$\frac{E^3}{A} = \frac{E_{\rm a}^{(0)}}{A} + \mathcal{O}\left(\frac{1}{\xi_0}\right), \tag{4.57}$$

which states that the coordinate force per unit area in a weak gravitational field exactly equals to the energy per unit area for a single plate in zero gravity. Using eq. (4.28) we immediately have

$$F^3 = E_{\rm a}^{(0)} g + \mathcal{O}(g)^2. \tag{4.58}$$

Let us next consider parallel plates falling in a weak gravitational field. Using eq. (4.54) we can write

$$\Delta(\xi_a, \xi_b) = \Delta^{(0)}(\xi_b - \xi_a) + \frac{1}{\xi_0}\Delta^{(1)}(\xi_a, \xi_b) + \mathcal{O}\left(\frac{1}{\xi_0}\right)^2 \tag{4.59}$$

where $\Delta^{(0)}(\xi_b - \xi_a)$ is given by eq. (2.52) if we make the identifications $\xi_b - \xi_a \to z_b - z_a = a$, $\frac{\zeta}{\xi_0} \to \zeta$, and $\kappa_0 \to \kappa$, which are appropriate and consistent with the uniform asymptotic expansions. The first order term in eq. (4.59) is

$$\Delta^{(1)}(\xi_a, \xi_b) = t_0^2 \left\{\frac{\xi_a + \xi_b}{2} - \xi_0\right\}\left[\frac{\lambda_a}{2\kappa_0} + \frac{\lambda_b}{2\kappa_0} + 2\frac{\lambda_a}{2\kappa_0}\frac{\lambda_a}{2\kappa_0}\left\{1 - e^{-2\kappa_0(\xi_b - \xi_a)}\right\}\right.$$
$$\left. -\kappa_0(\xi_b - \xi_a)\frac{\lambda_a}{2\kappa_0}\frac{\lambda_a}{2\kappa_0}\, e^{-2\kappa_0(\xi_b - \xi_a)}\right]. \tag{4.60}$$

We can thus evaluate the terms contributing to the coordinate force on the plates in eq. (4.36) using eq. (4.50) to the first order to be

$$\left\{\frac{\partial}{\partial \xi_a} + \frac{\partial}{\partial \xi_b}\right\} \ln \Delta(\xi_a, \xi_b) = \frac{1}{\Delta^{(0)}(\xi_b - \xi_a)}\left\{\frac{\partial}{\partial \xi_a} + \frac{\partial}{\partial \xi_b}\right\}\Delta^{(1)}(\xi_a, \xi_b) + \mathcal{O}\left(\frac{1}{\xi_0}\right) \tag{4.61}$$

which using eq. (4.60) evaluates to

$$\frac{1}{\Delta^{(0)}(\xi_b-\xi_a)}\,t_0^2\left[\frac{\lambda_a}{2\kappa_0}+\frac{\lambda_b}{2\kappa_0}+2\frac{\lambda_a}{2\kappa_0}\frac{\lambda_a}{2\kappa_0}\Big\{1-e^{-2\kappa_0(\xi_b-\xi_a)}\Big\}\right.$$
$$\left.-2\kappa_0(\xi_b-\xi_a)\frac{\lambda_a}{2\kappa_0}\frac{\lambda_a}{2\kappa_0}\,e^{-2\kappa_0(\xi_b-\xi_a)}\right] \tag{4.62}$$

which is exactly the right hand side of eq. (3.20) if we make the identifications we listed after eq. (4.59). Thus going through the exact same evaluations after eq. (3.20) until eq. (3.22) we can evaluate the total coordinate force per unit area given by eq. (4.36) to be

$$\frac{E^3}{A}=\frac{E_{\rm a}^{(0)}}{A}+\frac{E_{\rm b}^{(0)}}{A}+\frac{E_{\rm cas}^{(0)}}{A}+\mathcal{O}\left(\frac{1}{\xi_0}\right) \tag{4.63}$$

which states that the coordinate force per unit area on the field when the gravity is weak exactly equals to the total energy per unit area (modulo the bulk energy term) for parallel plates in zero gravity. Using eq. (4.28) we immediately have

$$F^3=\left[E_{\rm a}^{(0)}+E_{\rm b}^{(0)}+E_{\rm cas}^{(0)}\right]\,g+\mathcal{O}(g)^2. \tag{4.64}$$

4.4 Interpretations and conclusions

A single particle with mass m_a is described by the action

$$W=-m_a\int_{-\infty}^{+\infty}ds_a, \tag{4.65}$$

where ds_a is the proper time of the particle. $-(ds)^2 = g_{\mu\nu}(x)dx^\mu dx^\nu$. After introducing a delta function, we can write the action in eq. (4.65) in the form

$$W = -m_a \int d^4x \int_{-\infty}^{+\infty} ds\, \delta^{(4)}\left(x - x_a(s)\right), \tag{4.66}$$

which we shall find suitable for variation with respect to $g_{\mu\nu}(x)$.

Let us next determine the energy-momentum tensor for a single particle described by eq. (4.66). The energy-momentum tensor corresponding to an action is identified by writing the variation of the action with respect to $g^{\mu\nu}(x)$, or $g_{\mu\nu}(x)$, in the form

$$\delta W = -\frac{1}{2}\int d^4x \sqrt{-g(x)}\; \delta g^{\mu\nu}(x)\, t_{\mu\nu}(x) = \frac{1}{2}\int d^4x \sqrt{-g(x)}\; \delta g_{\mu\nu}(x)\, t^{\mu\nu}(x) \tag{4.67}$$

where we have used $g_{\mu\lambda}(x)\delta g^{\lambda\nu}(x) = -[\delta g_{\mu\lambda}(x)]g^{\lambda\nu}(x)$. This equation was used as the starting point in [23]. As a check we go through the identification of $t_{\mu\nu}(x)$ explicitly for

$$W = \int d^4x \sqrt{-g(x)}\, \mathcal{L}. \tag{4.68}$$

Variation with respect to $g^{\mu\nu}(x)$ leads to

$$\begin{aligned} \delta W &= \int d^4x \sqrt{-g(x)} \left[\frac{\delta\sqrt{-g}}{\sqrt{-g}}\,\mathcal{L} + \delta\mathcal{L}\right] \\ &= -\frac{1}{2}\int d^4x \sqrt{-g(x)}\; \delta g^{\mu\nu}(x) \left[g_{\mu\nu}(x)\mathcal{L} - 2\,\frac{\delta\mathcal{L}}{\delta g^{\mu\nu}(x)}\right], \end{aligned} \tag{4.69}$$

which lets us identify the quantity in the square brackets as the stress tensor. The above evaluation required the variation of determinant of the metric, $\delta g(x)$, which is

determined as

$$\frac{\delta\sqrt{-g}}{\sqrt{-g}} = \frac{1}{2}\,\delta\ln(-g) = \frac{1}{2}\,g^{\mu\nu}(x)\delta g_{\mu\nu}(x) = -\frac{1}{2}\,g_{\mu\nu}(x)\delta g^{\mu\nu}(x). \tag{4.70}$$

As a simple check for the correctness of the sign we verified it for the case of diagonal $g_{\mu\nu}(x)$. The stress tensor thus identified when evaluated for the Lagrangian density in eq. (1.1) indeed reproduces the stress tensor in eq. (1.37), thus verifying our sign convention in eq. (4.67). Varying the action for a single particle given by eq. (4.66), with respect to $g_{\mu\nu}(x)$ gives

$$\delta W = \frac{1}{2}\,m_a \int d^4x\,\delta g_{\mu\nu}(x) \int_{-\infty}^{+\infty} ds\,\delta^{(4)}\left(x - x_a(s)\right)\,\frac{dx^\mu}{ds}\frac{dx^\nu}{ds}, \tag{4.71}$$

which lets us identify the stress tensor for a single particle to be, using eq. (4.67),

$$t^{\mu\nu}(x) = m_a \frac{1}{\sqrt{-g(x)}} \int_{-\infty}^{+\infty} ds\,\delta^{(4)}\left(x - x_a(s)\right)\,\frac{dx^\mu}{ds}\frac{dx^\nu}{ds}. \tag{4.72}$$

4.4.1 Gravitational force on a single particle

We next proceed to evaluate the coordinate force, as prescribed by the first equality in eq. (4.26), for a single particle as described by the action in eq. (4.66). This will help us identify the gravitational force. We start by evaluating $f^3(\xi)$ as given in eq. (4.18) (or (4.17)) and use this in the first equality in eq. (4.25) to arrive at

$$\Delta P^3 = m_a \int d^4x\,\Gamma^3_{00}(x) \int_{-\infty}^{+\infty} ds\,\delta^{(4)}\left(x - x_a(s)\right)\,\frac{dx^0}{ds}\frac{dx^0}{ds} \tag{4.73}$$

where we have used the fact that the first term in eq. (4.17) is a surface term and thus does not contribute after integration and noticed that only the 00 component of

the stress tensor contributes because all other relevant components of Γ evaluate to zero. Using $\Gamma^3_{00} = \xi$ and evaluating the space time integral leads to

$$\Delta P^3 = m_a \int_{-\infty}^{+\infty} ds\, \xi_a \frac{d\tau_a}{ds}\frac{d\tau_a}{ds} = m_a \int_{-\infty}^{+\infty} d\tau \tag{4.74}$$

after identifying $dx^0_a = d\tau_a$ and interpreting $-ds^2 = -\xi^2 d\tau^2$ which lets us use $ds = \xi\, d\tau$. Thus we evaluate the coordinate force, as defined in eq. (4.26), to be

$$E^3 = \frac{\Delta P^3}{\int d\tau} = m_a. \tag{4.75}$$

The corresponding physical force got using eq. (4.28) is

$$F = m_a g \tag{4.76}$$

which we identify as the gravitational force. The above analysis can be easily generalized for a plate.

4.4.2 Renormalization

Eq. (4.58) and eq. (4.64), in the light of eq. (4.76), states that the vacuum energy, including the divergent contributions, falls under a weak gravitational field exactly like conventional mass or energy. Thus we can identify the gravitational force on the Casimir apparatus consisting of two plates to be

$$F = \left[m_a + m_b + E^{(0)}_a + E^{(0)}_b + E^{(0)}_{\text{cas}}\right] g + \mathcal{O}(g)^2. \tag{4.77}$$

We identify $m_{a,b}$ as the bare mass of the plates, and interpret the divergent Casimir energy contribution from each plate as renormalizing the bare mass. Thus we renormalize the masses by the prescription

$$m_{a,b} + E^{(0)}_{a,b} \to M_{a,b} \tag{4.78}$$

and define $M_{a,b}$ to be the renormalized mass of the plates. Thus we have

$$F = \left[M_a + M_b + E^{(0)}_{\text{cas}}\right] g + \mathcal{O}(g)^2. \tag{4.79}$$

Note here that the Casimir interaction energy $E^{(0)}_{\text{cas}}$ is negative, so it reduces the gravitational attraction of the system.

Chapter 5

Inertial forces on vacuum energy

In chapter 4 we have demonstrated that Casimir energy due to parallel plates, including its divergent parts, falls like conventional mass in a weak gravitational field. The divergent parts were suitably interpreted as renormalizing the bare masses of the plates. In this chapter we corroborate our result regarding the inertial nature of Casimir energy by calculating the centripetal force on a Casimir apparatus rotating with constant angular speed. We show that the centripetal force is independent of the orientation of the Casimir apparatus in a frame whose origin is at the center of inertia of the apparatus.

In Fall I [23] we demonstrated, using variational principles, that the gravitational force on Casimir energy is the same as that on a conventional mass. In Fall II [34], which was described in chapter 4, we considered the motion of a Casimir apparatus undergoing a constant acceleration. The Casimir apparatus consisted of semi-transparent parallel plates, realized by background fields consisting of delta function potentials, which induced boundary conditions on a massless scalar field. The motion of the apparatus was studied in the accelerated frame of reference, described by

Rindler coordinates, in which it experiences a pseudo-force. This fictitious force is equated to the gravitational force by the principle of equivalence. We concluded that Casimir energy, including the divergent contributions, falls under gravity like conventional mass. We made the remarkable observation that the divergent contributions to Casimir energy could be suitably interpreted as renormalizing the bare masses of the individual Casimir plates. Saharian et al. [41], using the zeta function technique for regularization, earlier reached at a similar conclusion for the finite part of the Casimir energy. Thus, in Fall I and II, which has been summarized in [51], we have convincingly demonstrated that Casimir energy falls like conventional mass in a weak gravitational field.

To further verify our conclusion we here study the centripetal force acting on a rotating Casimir apparatus. Firstly, we use this opportunity to refine our definition of the force on the energy associated with the field. Next, we consider a Casimir apparatus rotating with constant angular speed such that the surfaces of the plates remain parallel to the tangent to the circle of rotation. We use appropriate curvilinear coordinates to transform into the accelerated frame of reference. We demonstrate that, exactly as in the case of Rindler acceleration, the Casimir energy, including its divergent parts, experiences a centripetal force exactly like a conventional mass. We express the centripetal acceleration in terms of the center of inertia of the apparatus. Finally, we consider a rotating Casimir apparatus such that the plates make an arbitrary angle with respect to the tangent to the circle. We demonstrate that the centripetal force is independent of the orientation of the Casimir apparatus in a frame in which the center of inertia is at the origin.

5.1 Force in the local Lorentz coordinates

Consider the curvilinear coordinates $x^\mu \equiv (t, x, y, z)$ with the associated metric $g_{\mu\nu}(x)$. A particular set of coordinates $\bar{x}^a \equiv (\bar{t}, \bar{x}, \bar{y}, \bar{z})$ with metric $\eta_{ab} = (-1, +1, +1, +1)$ is called the local Lorentz coordinate system. Let us consider a transformation $\bar{x}^a = \bar{x}^a(x)$ which can always be defined in a local neighbourhood. Any spatial point $\mathbf{x}$ in the curvilinear coordinates is called a point of reference [52]. As a warm-up, and to acquaint ourselves with the notations, let us define the velocity of the point of reference $\mathbf{x}$ as measured in the local Lorentz coordinates at time $\bar{t}$. To this regard we can write

$$\Delta\bar{\mathbf{x}} = \Delta x^i \frac{\partial\bar{\mathbf{x}}}{\partial x^i} + \Delta t \frac{\partial\bar{\mathbf{x}}}{\partial t}, \tag{5.1}$$

$$\Delta\bar{t} = \Delta x^i \frac{\partial\bar{t}}{\partial x^i} + \Delta t \frac{\partial\bar{t}}{\partial t}, \tag{5.2}$$

in terms of which the velocity of the point of reference $\mathbf{x}$ as measured in the local Lorentz coordinates at time $\bar{t}$ will be

$$\mathbf{v}(\bar{\mathbf{x}}, \bar{t}) = \left.\frac{\Delta\bar{\mathbf{x}}}{\Delta\bar{t}}\right|_{\mathbf{x}} = \left[\frac{\partial\bar{t}(x)}{\partial t}\right]^{-1} \frac{\partial\bar{\mathbf{x}}(x)}{\partial t}, \tag{5.3}$$

because $\Delta x^i = 0$ for the point of reference.

A specific field, which is an analog of a fluid, is described by the corresponding energy-momentum tensor $t_{\mu\nu}(x)$. The momentum of a small volume containing the field at a point of reference $\mathbf{x}$ as measured in the local Lorentz coordinates at time $\bar{t}$ is

$$\bar{P}^a(\bar{x}) = d\Sigma_b(\bar{x})\, t^{ab}(\bar{x}) = d\Sigma_\nu(x)\, t^{\mu\nu}(x)\, \frac{\partial\bar{x}^a(x)}{\partial x^\mu} = P^\mu(x) \frac{\partial\bar{x}^a(x)}{\partial x^\mu}, \tag{5.4}$$

where we have used tensor transformation properties. The spatial volume elements are constructed as the antisymmetric product of three space like vectors, $d\Sigma_a(\bar{x}) = \epsilon_{abcd}\,\delta_1\bar{x}^b\,\delta_2\bar{x}^c\,\delta_3\bar{x}^d$, and $d\Sigma_\mu(x) = \sqrt{-g(x)}\,\epsilon_{\mu\nu\alpha\beta}\,\delta_1 x^\nu\,\delta_2 x^\alpha\,\delta_3 x^\beta$, where $g(x) = \det g_{\mu\nu}(x)$. The change in momentum when the coordinates are displaced will be

$$\Delta\bar{P}^a(\bar{x}) = \Delta\bar{x}^i\frac{\partial}{\partial\bar{x}^i}\bar{P}^a(\bar{x}) + \Delta\bar{t}\frac{\partial}{\partial\bar{t}}\bar{P}^a(\bar{x}) \tag{5.5}$$

and the force density as measured in the local Lorentz coordinates at time $\bar{t}$ is

$$\begin{aligned}\bar{F}^a(\bar{x}) = \left.\frac{\Delta\bar{P}^a}{\Delta\bar{t}}\right|_{\mathbf{x}} &= \left.\frac{\Delta\bar{x}^i}{\Delta\bar{t}}\right|_{\mathbf{x}}\left.\frac{\partial}{\partial\bar{x}^i}\bar{P}^a(\bar{x})\right|_{\mathbf{x}} + \left.\frac{\partial}{\partial\bar{t}}\bar{P}^a(\bar{x})\right|_{\mathbf{x}} \\ &= \left[\frac{\partial\bar{t}(x)}{\partial t}\right]^{-1}\left[\frac{\partial}{\partial t}\bar{P}^a(\bar{x})\right]_{\mathbf{x}} \\ &= \left[\frac{\partial\bar{t}(x)}{\partial t}\right]^{-1}\frac{\partial}{\partial t}\left[P^\mu(x)\frac{\partial\bar{x}^a(x)}{\partial x^\mu}\right],\end{aligned} \tag{5.6}$$

where we used (5.3) in going from first line to the second line.

The total force on the energy associated with the field as measured in the local Lorentz coordinates at time $\bar{t}$ is obtained by integrating the force density over a surface S described by constant $\bar{t}$. Thus

$$\begin{aligned}\bar{F}^a(\bar{t}) &= \int_S\left[\frac{\partial\bar{t}(x)}{\partial t}\right]^{-1}\frac{\partial}{\partial t}\left[P^\mu(x)\frac{\partial\bar{x}^a(x)}{\partial x^\mu}\right] \\ &= \int d^3x\left[\frac{\partial\bar{t}(x)}{\partial t}\right]^{-1}\frac{\partial}{\partial t}\left[\sqrt{-g(x)}\,t^{\mu 0}(x)\,\frac{\partial\bar{x}^a(x)}{\partial x^\mu}\right].\end{aligned} \tag{5.7}$$

This probably is rigorously true only for situations when the field under consideration is sufficiently localized and thus requires scrutiny. In the special case when both the metric tensor and the energy momentum tensor are independent of the coordinate

time t the above expression takes the simpler form

$$\bar{F}^a(\bar{t}) = \int d^3x \sqrt{-g(x)}\, t^{\mu 0}(x) \left[\frac{\partial}{\partial t}\frac{\partial \bar{x}^a(x)}{\partial x^\mu}\right]\left[\frac{\partial \bar{t}(x)}{\partial t}\right]^{-1}. \tag{5.8}$$

5.1.1 Rindler metric

As an illustrative example let us reconsider the situation in chapter 4 using the above definition. The local Lorentz coordinates $\bar{x}^a$ are related to the Rindler coordinates $x^\mu \equiv (\tau, x, y, \xi)$ by the transformations: $\bar{t} = \xi \sinh\tau,\ \bar{x} = x,\ \bar{y} = y,\ \bar{z} = \xi\cosh\tau$. The Rindler metric is $g_{\mu\nu}(x) = (-\xi^2, +1, +1, +1)$ which returns $g(x) = -\xi^2$. Further for the Casimir apparatus considered in chapter 4 we have only the diagonal components of $t_{\mu\nu}(x)$ to be nonzero which are independent of τ. Using these in (5.8) we determine the force on the vacuum energy associated with the Casimir apparatus to be

$$\frac{F^3}{A} = \int_0^\infty \frac{d\xi}{\xi}\,\xi^2\, t^{00}(\xi) = \int_0^\infty \frac{d\xi}{\xi}\,\frac{1}{\xi^2}\, t_{00}(\xi) = -\int_0^\infty \frac{d\xi}{\xi}\, t^0{}_0(\xi), \tag{5.9}$$

which leads to the result in chapter 4, see eq. (4.64),

$$F^3 = \left[E^{(0)}_{\rm a} + E^{(0)}_{\rm b} + E^{(0)}_{\rm cas}\right] g, \tag{5.10}$$

where the first two terms are the divergent energies associated with the individual plates and $E^{(0)}_{\rm cas}$ is the Casimir energy. Further, using the stress tensor for a conventional mass,

$$t^{\mu\nu}(x) = m_{\rm a}\frac{1}{\sqrt{-g(x)}}\int_{-\infty}^{+\infty} ds\,\delta^{(4)}(x - x_{\rm a}(s))\frac{dx^\mu}{ds}\frac{dx^\nu}{ds}, \tag{5.11}$$

in (5.9) we have the force on the plates to be

$$F^3 = [m_{\rm a} + m_{\rm b}]\, g. \tag{5.12}$$

Thus, the total force on the Casimir apparatus, including the sum of the force on the vacuum energy, and the plates, is

$$F^3 = \left[m_{\rm a} + m_{\rm b} + E^{(0)}_{\rm a} + E^{(0)}_{\rm b} + E^{(0)}_{\rm cas}\right] g. \tag{5.13}$$

Interpreting $m_{\rm a,b}$ to be the bare masses of the plates and renormalizing $m_{\rm a,b} + E^{(0)}_{\rm a,b} \to M_{\rm a,b}$ we thus conclude

$$F^3 = \left[M_{\rm a} + M_{\rm b} + E^{(0)}_{\rm cas}\right] g, \tag{5.14}$$

where $M_{a,b}$ are the renormalized masses of the plates.

5.2 Rotating Casimir apparatus

A scalar field $\bar{\phi}(\bar{x})$ in the presence of a background $\bar{V}(\bar{x})$ is described by the action

$$W = \int d^4\bar{x} \left[-\frac{1}{2}\eta^{ab}\bar{\partial}_a\bar{\phi}(\bar{x})\bar{\partial}_b\bar{\phi}(\bar{x}) - \frac{1}{2}\bar{V}(\bar{x})\bar{\phi}(\bar{x})^2\right]. \tag{5.15}$$

A Casimir apparatus, built out of so-called semi-transparent plates, rotating with constant angular speed ω about the $\bar{x}$ axis, as illustrated in 5.1, will be described by the potential

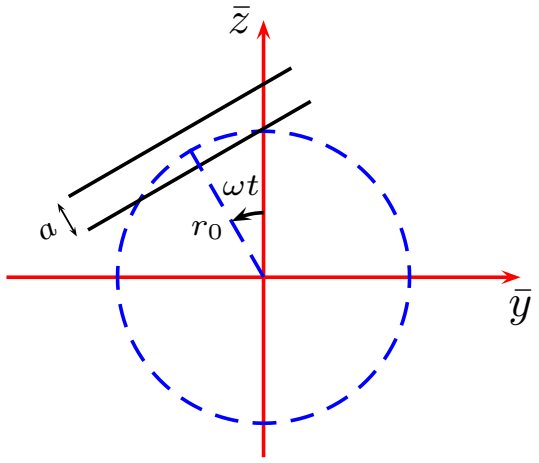

Figure 5.1: Casimir apparatus rotating with constant angular speed ω about the $\bar{x}$ axis. The plane of the plates are chosen to be perpendicular to the radial direction. We have $r_a = r_0 - \frac{a}{2}$, and $r_b = r_0 + \frac{a}{2}$.

$$\begin{aligned}\bar{V}(\bar{x}) &= \lambda_a\,\delta(\bar{z}\cos\omega\bar{t} - \bar{y}\sin\omega\bar{t} - r_a) + \lambda_b\,\delta(\bar{z}\cos\omega\bar{t} - \bar{y}\sin\omega\bar{t} - r_b) \\ &= \lambda_a\,\delta\left(\bar{z}\cos\omega\bar{t} - \bar{y}\sin\omega\bar{t} - r_0 + \frac{a}{2}\right) \\ &\qquad +\lambda_b\,\delta\left(\bar{z}\cos\omega\bar{t} - \bar{y}\sin\omega\bar{t} - r_0 - \frac{a}{2}\right). \end{aligned} \tag{5.16}$$

If we make the following transformations

$$y = +\bar{y}\cos\omega\bar{t} + \bar{z}\sin\omega\bar{t}, \qquad x = \bar{x}, \tag{5.17a}$$

$$z = -\bar{y}\sin\omega\bar{t} + \bar{z}\cos\omega\bar{t} - r_0, \qquad t = \bar{t}, \tag{5.17b}$$

which has the following inverse transformations

$$\bar{y} = y\cos\omega t - (z + r_0)\sin\omega t, \qquad \bar{x} = x, \tag{5.18a}$$

$$\bar{z} = y\sin\omega t + (z + r_0)\cos\omega t, \qquad \bar{t} = t, \tag{5.18b}$$

the action in (5.15) takes the form

$$W = \int d^4x \sqrt{-g(x)}\, \mathcal{L}(\phi(x)), \tag{5.19}$$

where

$$\mathcal{L}(\phi(x)) = -\frac{1}{2} g^{\mu\nu}(x) \partial_\mu \phi(x) \partial_\nu \phi(x) - \frac{1}{2} V(x) \phi(x)^2, \tag{5.20}$$

in which the background potential,

$$V(x) = \lambda_a\, \delta\left(z + \frac{a}{2}\right) + \lambda_b\, \delta\left(z - \frac{a}{2}\right), \tag{5.21}$$

is now independent of t. The metric is

$$g_{\mu\nu}(x) = \begin{bmatrix} -(1-\omega^2 r^2) & 0 & -\omega(z+r_0) & \omega y \\ 0 & 1 & 0 & 0 \\ -\omega(z+r_0) & 0 & 1 & 0 \\ \omega y & 0 & 0 & 1 \end{bmatrix}, \tag{5.22}$$

and its inverse is

$$g^{\mu\nu}(x) = \begin{bmatrix} -1 & 0 & -\omega(z+r_0) & \omega y \\ 0 & 1 & 0 & 0 \\ -\omega(z+r_0) & 0 & \{1-\omega^2(z+r_0)^2\} & \omega^2 y(z+r_0) \\ \omega y & 0 & \omega^2 y(z+r_0) & (1-\omega^2 y^2) \end{bmatrix}, \tag{5.23}$$

where $r^2 = y^2 + (z+r_0)^2$, and $g(x) = \det g_{\mu\nu}(x) = -1$. For the sake of bookkeeping we note the corresponding nonzero components of the connection symbols: $\Gamma^2_{00} = -\omega^2 y, \Gamma^3_{00} = -\omega^2 z$, and $\Gamma^3_{02} = -\Gamma^2_{03} = \omega$. The energy-momentum tensor, or the stress

tensor, in the curvilinear coordinates is

$$t_{\alpha\beta}(x) = \partial_\alpha\phi(x)\partial_\beta\phi(x) + g_{\alpha\beta}(x)\mathcal{L}(\phi(x)). \tag{5.24}$$

At the one-loop level the Green's function $G(x, x')$ is related to the fields by the correspondence $\langle T\phi(x)\phi(x')\rangle = -i\, G(x, x')$.

5.2.1 Centripetal force

In terms of the curvilinear coordinates the potential (5.21) is independent of time t which renders the energy-momentum tensor independent of time. Using this in (5.8) we calculate the force on the vacuum energy associated with the Casimir apparatus to be

$$\bar{F}^a(\bar{t}) = \int d^3x\, t^{\mu 0}(x)\, \frac{\partial}{\partial t}\frac{\partial \bar{x}^a(x)}{\partial x^\mu}. \tag{5.25}$$

We shall be interested in the leading order contributions to the force in the parameter ωr_0. To this end we observe that only the zeroth order term in the energy-momentum tensor contributes, which is diagonal and a function of z alone. Using this in (5.25) we can write the centripetal force on the vacuum energy to be

$$\bar{\mathbf{F}}(\bar{t}) = -\omega^2\, \hat{\bar{\mathbf{r}}}(\omega\bar{t})\, r_0 \int d^3x\, t_{00}^{(0)}(z) - \omega^2\, \hat{\bar{\mathbf{r}}}(\omega\bar{t}) \int d^3x\, z\, t_{00}^{(0)}(z) + \omega^2\mathcal{O}(\omega r_0), \tag{5.26}$$

where the unit vector is $\hat{\bar{\mathbf{r}}}(\theta) = \cos\theta\, \hat{\bar{\mathbf{z}}} - \sin\theta\, \hat{\bar{\mathbf{y}}}$. We define the total energy associated with the field and the center of inertia (energy) as measured in the curvilinear coordinates as

$$E_{\rm tot}^{(0)} = \int d^3x\, t_{00}^{(0)}(x) \qquad \text{and} \qquad z_{\rm cm} = \frac{1}{E_{\rm tot}^{(0)}} \int d^3x\, z\, t_{00}^{(0)}(x) \tag{5.27}$$

respectively, in terms of which the centripetal force in (5.26) can be written in the form

$$\bar{\mathbf{F}}(\bar{t}) = -\omega^2\ [r_0 + z_{\rm cm}]\ \hat{\bar{\mathbf{r}}}(\omega\bar{t})\, E^{(0)}_{\rm tot} = -\omega^2\, \bar{r}_{\rm cm}\, \hat{\bar{\mathbf{r}}}(\omega\bar{t})\, E^{(0)}_{\rm tot}, \tag{5.28}$$

where $\bar{r}_{\rm cm} = r_0 + z_{\rm cm}$, is the center of inertia in the local Lorentz coordinates, and $z_{\rm cm}$ is the center of inertia relative to $r_0\hat{\bar{\mathbf{r}}}$. $t^{(0)}_{00}(z)$ is the energy density of the plates when the acceleration is switched off. In particular we recall, see eq. (1.48),

$$t^{(0)}_{00}(x) = \frac{1}{2i}\left\{\left(\frac{\partial}{\partial t}\frac{\partial}{\partial t'} - \frac{\partial^2}{\partial t^2}\right) G^{(0)}(x,x')\right\}_{x=x'} + \frac{1}{4i}\,\nabla^2 G^{(0)}(x,x), \tag{5.29}$$

where the Green's function is of the form, see eq. (2.40),

$$G^{(0)}(x,x') = \int_{-\infty}^{+\infty}\frac{d\omega}{2\pi}\int\frac{d^2k_\perp}{(2\pi)^2}\, e^{-i\omega(t-t')}e^{i\mathbf{k}_\perp\cdot(\mathbf{x}_\perp-\mathbf{x}'_\perp)}g^{(0)}(z,z';\kappa), \tag{5.30}$$

with $\kappa^2 = \mathbf{k}^2_\perp - \omega^2$, and $g^{(0)}(z,z';\kappa)$ satisfies

$$-\left[\frac{\partial^2}{\partial z^2} - \kappa^2 - V^{(0)}(z)\right] g^{(0)}(z,z';\kappa) = \delta(z-z'). \tag{5.31}$$

Using these relations the total energy per unit area in (5.27) takes the form, see eq. (1.53),

$$\frac{E^{(0)}_{\rm tot}}{A} = -\frac{1}{2}\int_{-\infty}^{+\infty}\frac{d\zeta}{2\pi}\int\frac{d^2k_\perp}{(2\pi)^2}\,2\zeta^2\int_{-\infty}^{+\infty}dz\, g^{(0)}(z,z;\kappa), \tag{5.32}$$

where we have switched to imaginary frequencies, $\omega \to i\zeta$, thus $\kappa^2 = \mathbf{k}^2_\perp + \zeta^2$. The center of inertia in (5.27) can be similarly expressed in terms of the first moment of $g^{(0)}(z,z;\kappa)$.

5.2.2 Centripetal force on a single plate

A single plate rotating with constant angular speed is described by a single delta function in the potential in (5.21) (letting $a = 0$, $r_0 = r_a$, and $\lambda_b = 0$),

$$V(z) = \lambda_a \, \delta(z), \tag{5.33}$$

and the corresponding solution to eq. (5.31) evaluated at $z = z'$ is, (refer to eq. (2.47) with $a_1 = 0$ and $\lambda_1 \to \lambda_a$ there),

$$g^{(0)}(z, z; \kappa) = \frac{1}{2\kappa} - \frac{\lambda_a}{\lambda_a + 2\kappa} \frac{1}{2\kappa} \, e^{-2\kappa|z|} \tag{5.34}$$

in terms of which the force in (5.28) evaluates to

$$\bar{\mathbf{F}}(\bar{t}) = -\hat{\bar{\mathbf{r}}}(\omega\bar{t}) \, \omega^2 \bar{r}_{\rm cm} \, E_a^{(0)}, \tag{5.35}$$

where $\bar{r}_{\rm cm} = r_0 = r_a$, and

$$\frac{E_a^{(0)}}{A} = \frac{1}{12\pi^2} \int_0^\infty \kappa^2 d\kappa \, \frac{\lambda_a}{\lambda_a + 2\kappa} = \frac{1}{96\pi^2} \int_0^\infty \frac{dy}{y} \, \frac{y^3}{1 + \frac{y}{\lambda_a}}, \tag{5.36}$$

a divergent quantity, is the energy per unit area associated with a single plate. The center of inertia relative to r_0, $z_{\rm cm}$, in (5.27) evaluates to zero for a single plate.

5.2.3 Parallel plates

Two parallel plates separated by a distance a and rotating with constant angular speed ω is described by the potential in (5.21). The reduced Green's function, $g^{(0)}(z, z'; \kappa)$, which is solution to (5.31), evaluated at $z = z'$, (refer to eq. (2.50) with $a_1 \to -a/2$,

$a_2 \to a/2$, and $\lambda_{1,2} \to \lambda_{a,b}$ there), in the region $z < -\frac{a}{2}$ is,

$$\frac{1}{2\kappa} - \frac{1}{2\kappa}\frac{e^{2\kappa z}}{\Delta}\left[\frac{\lambda_a}{2\kappa}\left(1+\frac{\lambda_b}{2\kappa}\right)e^{\kappa a} + \frac{\lambda_b}{2\kappa}\left(1-\frac{\lambda_a}{2\kappa}\right)e^{-\kappa a}\right], \tag{5.37}$$

in the region $-\frac{a}{2} < z < \frac{a}{2}$ is

$$\frac{1}{2\kappa} - \frac{1}{2\kappa}\frac{e^{-\kappa a}}{\Delta}\left[\frac{\lambda_a}{2\kappa}\left(1+\frac{\lambda_b}{2\kappa}\right)e^{-2\kappa z} + \frac{\lambda_b}{2\kappa}\left(1+\frac{\lambda_a}{2\kappa}\right)e^{2\kappa z} - 2\frac{\lambda_a}{2\kappa}\frac{\lambda_b}{2\kappa}e^{-\kappa a}\right], \tag{5.38}$$

and in the region $\frac{a}{2} < z$ is

$$\frac{1}{2\kappa} - \frac{1}{2\kappa}\frac{e^{-2\kappa z}}{\Delta}\left[\frac{\lambda_a}{2\kappa}\left(1-\frac{\lambda_b}{2\kappa}\right)e^{-\kappa a} + \frac{\lambda_b}{2\kappa}\left(1+\frac{\lambda_a}{2\kappa}\right)e^{\kappa a}\right], \tag{5.39}$$

where

$$\Delta = \left(1+\frac{\lambda_a}{2\kappa}\right)\left(1+\frac{\lambda_b}{2\kappa}\right) - \frac{\lambda_a}{2\kappa}\frac{\lambda_b}{2\kappa}e^{-2\kappa a}. \tag{5.40}$$

Using the above expressions for $g^{(0)}(z,z;\kappa)$ in the appropriate regions of the z integral in (5.32) the centripetal force in (5.28) evaluates to

$$\bar{\mathbf{F}}(\bar{t}) = -\hat{\bar{\mathbf{r}}}(\omega\bar{t})\,\omega^2\bar{r}_{\rm cm}\left[E^{(0)}_{\rm a} + E^{(0)}_{\rm b} + E^{(0)}_{\rm cas}\right], \tag{5.41}$$

where $E^{(0)}_{\rm a,b}$ are the total energies due to single plates given in terms of (5.36), $E^{(0)}_{\rm cas}$ is the Casimir energy given as, see eq. (3.23),

$$\frac{E^{(0)}_{\rm cas}}{A} = -\frac{1}{12\pi^2}\int_0^\infty \kappa^2\,d\kappa\left[2\kappa a + \frac{1}{1+\frac{\lambda_a}{2\kappa}} + \frac{1}{1+\frac{\lambda_b}{2\kappa}}\right]\frac{1}{2\kappa}\frac{\partial}{\partial a}\ln\Delta, \tag{5.42}$$

and $\bar{r}_{\rm cm} = r_0 + z_{\rm cm}$, where the center of inertia relative to r_0 in the curvilinear coordinates, $z_{\rm cm}$, for parallel plates evaluates to

$$z_{\rm cm}\, E^{(0)}_{\rm tot} = -\frac{a}{24\pi^2}\int_0^\infty \kappa^2 d\kappa \frac{1}{\Delta}\left[\frac{\lambda_b}{2\kappa} - \frac{\lambda_a}{2\kappa}\right], \tag{5.43}$$

which is in general not zero because of the asymmetry in the couplings, but evaluates to zero when $\lambda_a = \lambda_b$, or in the Dirichlet limit.

5.3 Orientation independence of centripetal force

A Casimir apparatus making an arbitrary angle α with respect to the tangent while rotating with constant angular speed ω, as illustrated in 5.2, is described by the potential, (displaying the potential only for one plate to save typographic space)

$$\bar{V}(\bar{x}) = \lambda_a\, \delta(\bar{z}\cos(\alpha+\omega\bar{t}) - \bar{y}\sin(\alpha+\omega\bar{t}) - r_a\cos\alpha) \tag{5.44a}$$

$$= \lambda_a\, \delta\left(\bar{z}\cos(\alpha+\omega\bar{t}) - \bar{y}\sin(\alpha+\omega\bar{t}) - r_0\cos\alpha + \frac{a}{2}\right). \tag{5.44b}$$

We make the transformations

$$y = +\bar{y}\cos(\alpha+\omega\bar{t}) + \bar{z}\sin(\alpha+\omega\bar{t}) - r_0\sin\alpha, \qquad x = \bar{x}, \tag{5.45a}$$

$$z = -\bar{y}\sin(\alpha+\omega\bar{t}) + \bar{z}\cos(\alpha+\omega\bar{t}) - r_0\cos\alpha, \qquad t = \bar{t}, \tag{5.45b}$$

which has the inverse transformations

$$\bar{y} = (y + r_0\sin\alpha)\cos(\alpha+\omega\bar{t}) - (z + r_0\cos\alpha)\sin(\alpha+\omega\bar{t}), \qquad \bar{x} = x, \tag{5.46a}$$

$$\bar{z} = (y + r_0\sin\alpha)\sin(\alpha+\omega\bar{t}) + (z + r_0\cos\alpha)\cos(\alpha+\omega\bar{t}), \qquad \bar{t} = t, \tag{5.46b}$$

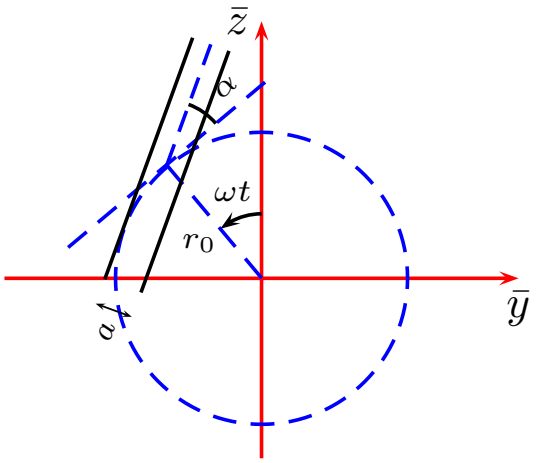

Figure 5.2: A Casimir apparatus oriented at an angle α with respect to the tangent to the circle of radius r_0 and rotating with constant angular speed ω about the $\bar{x}$ axis. We have $r_a \cos\alpha = r_0 \cos\alpha - \frac{a}{2}$, $r_b \cos\alpha = r_0 \cos\alpha + \frac{a}{2}$, $r_0 = (r_a + r_b)/2$, and $a = (r_b - r_a)\cos\alpha$.

which reduces to the transformations in (5.17a) and (5.17b) for $\alpha = 0$. The metric corresponding to this transformation evaluates to be

$$g_{\mu\nu}(x) = \begin{bmatrix} -(1-\omega^2 r^2) & 0 & -\omega(z + r_0\cos\alpha) & \omega(y + r_0\sin\alpha) \\ 0 & 1 & 0 & 0 \\ -\omega(z + r_0\cos\alpha) & 0 & 1 & 0 \\ +\omega(y + r_0\sin\alpha) & 0 & 0 & 1 \end{bmatrix}, \tag{5.47}$$

where $r^2 = (y + r_0\sin\alpha)^2 + (z + r_0\cos\alpha)^2$, and reduces to the metric in (5.22) for $\alpha = 0$. Carrying on by repeating the steps in section 5.2, we evaluate the centripetal force to be

$$\bar{\mathbf{F}}(\bar{t}) = -\omega^2\, \bar{\mathbf{r}}_{\rm cm}(\omega\bar{t}) \left[E^{(0)}_{\rm a} + E^{(0)}_{\rm b} + E^{(0)}_{\rm cas}\right], \tag{5.48}$$

where the center of inertia in the local Lorentz coordinates is

$$\bar{\mathbf{r}}_{\rm cm}(\omega\bar{t}) = r_0\hat{\bar{\mathbf{r}}}(\omega\bar{t}) + z_{\rm cm}\hat{\bar{\mathbf{r}}}(\alpha + \omega\bar{t}), \tag{5.49}$$

in which the center of inertia in the curvilinear coordinates, $z_{\rm cm}$, is again given using (5.43). We observe that if the origin of the curvilinear coordinates is chosen such that $z_{\rm cm} = 0$ then the centripetal force is independent of the orientation of the Casimir apparatus. We shall end by pointing to the discussion on frame dependence of center of mass in page 176 of reference [52] and to the original work cited in it.

Chapter 6

Lateral Casimir force

In the earlier chapters we confined ourselves to flat plates for which the Casimir force solely acts in a direction normal to the surface of the plates. In this chapter we calculate the lateral Casimir force between corrugated parallel plates, described by δ-function potentials, interacting through a scalar field, using the multiple scattering formalism. The contributions to the Casimir energy due to uncorrugated parallel plates are treated as a background from the outset. We derive the leading—and next-to-leading—order contribution to the lateral Casimir force for the case when the corrugation amplitudes are small in comparison to corrugation wavelengths. We present explicit results in terms of finite integrals for the case of the Dirichlet limit, and exact results for the weak-coupling limit, for the leading—and next-to-leading—orders. The correction due to the next-to-leading contribution is significant. In the weak coupling limit we calculate the lateral Casimir force nonperturbatively in terms of a single integral which we evaluate numerically. These exact nonperturbative results for the case of the weak limit allows us to estimate the error in the perturbative results. We show that the error in the lateral Casimir force, in the weak coupling limit, when

the next-to-leading order contribution is included is remarkably low when the corrugation amplitudes are small in comparison to corrugation wavelengths. We expect similar conclusions to hold for the Dirichlet case. The analogous calculation for the electromagnetic case should reduce the theoretical error sufficiently for comparison with the experiments. Very recently the authors in [53] have reported that they have been able to numerically calculate the Casimir force between dielectric parallel plates with rectangular gratings exactly which match the experimental results in [54] with an accuracy of 0.1%.

We earlier mentioned that the Casimir force, as exhibited between neutral metallic parallel plates, was discovered theoretically in 1948 [1]. This was described for the case of semitransparent parallel plates for the scalar case in chapter 3. The Casimir torque between asymmetric materials was first studied in 1973 [55]. Recently, theoretical study of the lateral Casimir force between corrugated parallel plates was pioneered and developed by the MIT group in [56, 57, 58, 59, 60]. In particular, in [59], the authors evaluated analytic expressions for the lateral Casimir force, to the leading order, between two corrugated parallel plates perturbatively. Experimentally, the Casimir interaction between corrugated surfaces was explored during the same period of time by Roy and Mohideen in [61]. This experiment measured the lateral Casimir force between a plate, with small sinusoidal corrugations, and a large sphere with identical corrugations. The motivation was to study the nontrivial boundary dependence in the Casimir force. The experimental parameters in our notation are (see figure 6.1): $h = 60$ nm, $d = 1.1$ μm, and $a = 0.1 - 0.9$ μm, where h is the height of the corrugations, d is the wavelength of the corrugations, and a is the mean distance between the plates. The corresponding dimensionless quantities are: $k_0 a = 0.6 - 5.1$, $\frac{h}{a} = 0.07 - 0.6$, and $k_0 h = 0.3$, where k_0 is the wavenumber related to the spatial

wavelength of the corrugations.

Experimental data was analyzed based on the theoretical results obtained from the proximity force approximation (PFA), and has been presented in [62, 63]. The validity of the PFA in the above analysis has been the topic of a recent debate and controversy, see [64, 65, 66]. Theoretical results based on perturbative approximations as done in [58] do not settle the issue because the error keeping only the leading order may be high. It is generally believed that the next-to-leading-order calculation will be able to throw light on the issue. We carried out this calculation for the case of scalar fields in [67]. The analogous calculation for the electromagnetic case should now be straightforward.

This chapter is an offshoot of [68] where we have dealt with corrugated cylinders to study non-contact gears. While evaluating the leading order for the case of corrugated cylinders it was noticed that it would be possible to extend the calculation to the next-to-leading order. This led to the study in the present chapter.

6.1 Statement of the problem

We consider two semitransparent, corrugated plates, parallel to the $x-y$ plane, described by the potentials,

$$V_i(z,y) = \lambda_i\,\delta(z - a_i - h_i(y)), \tag{6.1}$$

where $i = 1, 2$, are labels that identify the individual plates, and we define $a = a_2 - a_1 > 0$. The functions $h_i(y)$ are designed to describe the corrugations associated

with the individual plates. Let us define the function

$$a(y) = a + h_2(y) - h_1(y) \tag{6.2}$$

which measures the relative corrugations between the two plates. We shall define the corrugations $h_i(y)$ so that the mean of the relative corrugations is a. In general we require $a(y) > 0$, which is a restriction on the corrugations. Translational invariance is assumed in the x direction.

The change in energy due to the change in the mean distance between the plates, a, leads to the conventional Casimir force which points in the direction perpendicular to the mean surface of the plates, and is expressed as

$$F_{\text{Cas}} = -\frac{\partial E}{\partial a}, \tag{6.3}$$

where E is the total Casimir energy associated with the corrugated plates including the divergent contributions, associated with the single plates. The divergent contributions being independent of a, do not contribute to the Casimir force. When the plates have corrugations on them we expect to have a change in the total energy due to a shift of one of the plates parallel (lateral) to the other plate. The force corresponding to the change in the total energy due to this shift acts in the lateral direction and is called the lateral Casimir force. The shift is mathematically described by a translation in the y-coordinate, $h_1(y + y_0)$, which corresponds to a lateral shift of one plate with respect to the other. The lateral force is expressed as

$$F_{\text{Lat}} = -\frac{\partial E}{\partial y_0}, \tag{6.4}$$

where y_0 is the measure of the translational shift.

We note that there will be no lateral force between the plates if the corrugations are switched off by setting $h_i(y) = 0$, $i = 1$ and 2. The physical quantities associated with this configuration will thus act as a background, and a reference, and we shall find it convenient to denote them by the superscript (0) to mean zeroth order. The potential for the background will thus be described by

$$V_i^{(0)}(z) = \lambda_i \, \delta(z - a_i), \tag{6.5}$$

which has no y dependence. The total Casimir energy associated with the background, due to the two uncorrugated plates, will be denoted as $E^{(0)}$, which will include the divergent contributions associated with the single plates. This background energy will be independent of the displacement y_0 due to the y independence of this configuration. Thus, we can conclude that

$$F_{\rm Lat}^{(0)} = -\frac{\partial E^{(0)}}{\partial y_0} = 0. \tag{6.6}$$

We further note that there will be no lateral force between the plates if either one of the plates have their corrugations switched off by setting $h_i(y) = 0$, $i = 1$ or 2. The Casimir energy associated with this configuration can be written as

$$E_i = E - E^{(0)} \tag{6.7}$$

where E_i is the additional contribution to the energy with respect to the background energy due to the presence of the corrugations on one of the plates. Throughout this article we shall use Δ to mean the deviation from the background. For example, we will have $\Delta V_i(z, y) = V_i(z, y) - V_i^{(0)}(z)$. Using the argument of y independence, or

translational symmetry, we can again conclude that

$$(F_{\rm Lat})_i = -\frac{\partial E_i}{\partial y_0} = 0. \tag{6.8}$$

In light of the above observations we are led to write the total Casimir energy, for the case when both the plates have their corrugations switched on, in the form

$$\Delta E = E - E^{(0)}(a) = E_1(a, h_1) + E_2(a, h_2) + E_{12}(a, h_1, h_2, y_0), \tag{6.9}$$

where E_{12} is the contribution to the total energy due to the interaction between the corrugations in the plates. Only this part of the total energy contributes to the lateral Casimir force. Thus, we conclude that

$$F_{\rm Lat} = -\frac{\partial}{\partial y_0}\Delta E = -\frac{\partial E_{12}}{\partial y_0}. \tag{6.10}$$

Our central problem will be to evaluate E_{12} using eq. (1.24).

6.1.1 Casimir energy contributing to the lateral force

Using the central formula derived in the multiple scattering formalism in eq. (1.24) to evaluate eq. (6.9) we have

$$\Delta E = E - E^{(0)} = \frac{i}{2\tau}\,\mathrm{Tr}\ln GG_0^{-1} - \frac{i}{2\tau}\,\mathrm{Tr}\ln G^{(0)}G_0^{-1} = \frac{i}{2\tau}\,\mathrm{Tr}\ln GG^{(0)^{-1}}, \tag{6.11}$$

where G_0 is the free Green's function introduced in eq. (1.15). Note that G_0 cancels in the above expression and the reference is now with respect to the uncorrugated plates. The Green's function G satisfies eq. (1.12) with potentials described by eq. (6.1),

which in symbolic notation reads

$$\Big[-\partial^2 + V_1 + V_2 \Big] G = 1, \tag{6.12}$$

and the corresponding Green's function associated with the background satisfies the differential equation,

$$\Big[-\partial^2 + V_1^{(0)} + V_2^{(0)} \Big] G^{(0)} = 1. \tag{6.13}$$

The above two equations can be used to deduce

$$G {G^{(0)}}^{-1} = \left[1 + G^{(0)} \Delta V_1 + G^{(0)} \Delta V_2 \right]^{-1}. \tag{6.14}$$

Next, one makes the observation that the above expression can be rewritten in the form

$$G {G^{(0)}}^{-1} = G_2 {G^{(0)}}^{-1} \Big[1 - G_1 \Delta V_1 G_2 \Delta V_2 \Big]^{-1} G_1 {G^{(0)}}^{-1}, \tag{6.15}$$

where G_i $(i = 1, 2)$ are the Green's functions for the parallel plates when only one of the plates has corrugations on it. The differential equations for G_i's are

$$\Big[-\partial^2 + V_1^{(0)} + V_2^{(0)} + \Delta V_i \Big] \, G_i = 1, \tag{6.16}$$

which together with eq. (6.13) can be used to deduce

$$\begin{aligned} G_i {G^{(0)}}^{-1} = (1 + G^{(0)} \Delta V_i)^{-1} &= 1 - G^{(0)} \Delta V_i (1 + G^{(0)} \Delta V_i)^{-1} \\ &= 1 - (1 + G^{(0)} \Delta V_i)^{-1} G^{(0)} \Delta V_i. \end{aligned} \tag{6.17}$$

Using eq. (6.15) in eq. (6.11) we we immediately obtain eq. (6.9). The last term in eq. (6.9), E_{12}, which is the only term that contributes to the lateral force between the two corrugated plates, can be read out from eq. (6.15) to be given by the expression

$$E_{12} = -\frac{i}{2\tau}\,\mathrm{Tr}\ln\Big[1 - G_1\Delta V_1 G_2 \Delta V_2\Big]. \tag{6.18}$$

We could have written this down immediately, but we hope it was instructive to go through the steps because it clarifies our notation, which would anyhow have required us to write many of the above equations, and also to emphasize that the configuration due to parallel plates is treated as a background from the outset.

6.1.2 Formal series expansion

Formally expanding the logarithm in the above expression and using eq. (6.17) to expand $G_i\Delta V_i$ in terms of $G^{(0)}\Delta V_i$ we can write

$$E_{12} = \frac{i}{2\tau}\,\mathrm{Tr}\sum_{m=1}^{\infty}\frac{1}{m}\left[\sum_{n_1=1}^{\infty}\sum_{n_1=1}^{\infty}(-1)^{n_1}(-1)^{n_2}\left\{G^{(0)}\Delta V_1\right\}^{n_1}\left\{G^{(0)}\Delta V_2\right\}^{n_2}\right]^m. \tag{6.19}$$

Our potentials in eq. (6.1) can be formally expanded in powers of h_i in the form

$$\begin{aligned}\Delta V_i(z,y) = \sum_{n=1}^{\infty} V_i^{(n)}(z,y) &= \sum_{n=1}^{\infty}\frac{[-h_i(y)]^n}{n!}\frac{\partial^n}{\partial z^n}V_i^{(0)}(z)\\ &= \lambda_i\Big[e^{-h_i(y)\frac{\partial}{\partial z}} - 1\Big]\delta(z-a_i).\end{aligned} \tag{6.20}$$

6.2 Leading order contribution

In this section we shall derive the leading order contribution to the Casimir energy when the corrugation amplitude is small in comparison to the corrugation wavelength. This has been evaluated for the Dirichlet scalar case and the electromagnetic case in [58, 59]. We obtain the result for scalar δ-function potentials as a warm up exercise in preparation for the calculation for the next-to-leading order. In this section we shall illustrate our methodology which will be further used in the higher order calculation.

6.2.1 Second order perturbation in Casimir energy due to corrugations

For the particular case when the corrugations can be treated as small perturbations we can approximate the potentials by keeping a few terms in the expansion in eq. (6.19) where we use the superscripts (n) to represent the n-th order perturbation in a quantity. Thus, to the leading order the interaction energy of the corrugations in eq. (6.19) takes the form

$$E_{12}^{(2)} = \frac{i}{2\tau}\,\mathrm{Tr}\Big[G^{(0)}\Delta V_1^{(1)} G^{(0)}\Delta V_2^{(1)}\Big]. \tag{6.21}$$

We observe that the potentials in the n-th order are given by derivatives acting on δ-functions in eq. (6.20) which can be transferred over to the Green's functions after integration by parts. The background Green's function, which is a solution to eq. (6.13), can be written as, also see eq. (2.40),

$$G^{(0)}(\mathbf{x},t,\mathbf{x}',t') = \int \frac{d\omega}{2\pi}\, e^{-i\omega(t-t')} \int \frac{dk_x}{2\pi}\, e^{ik_x(x-x')} \int \frac{dk_y}{2\pi}\, e^{ik_y(y-y')}\, g^{(0)}(z,z';\kappa), \tag{6.22}$$

where $\kappa^2 = \bar{\kappa}^2 + k_y^2$, with $\bar{\kappa}^2 = k_x^2 - \omega^2$, where $k_{x,y}$ and ω are the Fourier variables corresponding to the space-time coordinates x, y and t respectively. The reduced Green's function, $g^{(0)}(z, z'; \kappa)$, satisfies the equation, also see eq. (2.49),

$$-\left[\frac{\partial^2}{\partial z^2} - \kappa^2 - \lambda_1\delta(z - a_1) - \lambda_2\delta(z - a_2)\right] g^{(0)}(z, z'; \kappa) = \delta(z - z'). \tag{6.23}$$

In terms of the reduced Green's function defined above we can write eq. (6.21) as

$$\frac{E_{12}^{(2)}}{L_x} = \int_{-\infty}^{\infty} \frac{dk_1}{2\pi} \int_{-\infty}^{\infty} \frac{dk_2}{2\pi}\, \tilde{h}_1(k_1 - k_2)\, \tilde{h}_2(k_2 - k_1)\, L^{(2)}(k_1, k_2), \tag{6.24}$$

where L_x is a large length in the x direction and where $\tilde{h}_i(k)$ are the Fourier transforms of the functions $h_i(y)$, which describe the corrugations on the parallel plates,

$$\tilde{h}_i(k) = \int_{-\infty}^{\infty} dy\, e^{-iky}\, h_i(y). \tag{6.25}$$

The kernel $L^{(2)}(k_1, k_2)$ in eq. (6.24) is suitably expressed in the form

$$L^{(2)}(k_1, k_2) = -\frac{1}{4\pi} \int_0^{\infty} \bar{\kappa}\, d\bar{\kappa}\; I^{(2)}(\kappa_1, \kappa_2), \tag{6.26}$$

where we have switched to imaginary frequencies by a Euclidean rotation, $\omega \to i\zeta$, and defined

$$I^{(2)}(\kappa_1, \kappa_2) = \lambda_1\lambda_2 \frac{\partial}{\partial z} \frac{\partial}{\partial \bar{z}} \Big[\, g^{(0)}(z, \bar{z}; \kappa_1)\, g^{(0)}(\bar{z}, z; \kappa_2)\Big]\Big|_{\bar{z}=a_1, z=a_2}, \tag{6.27}$$

where $\kappa_i^2 = \bar{\kappa}^2 + k_i^2$. Using the reciprocal symmetry in the Green's function in

eq. (6.27) we deduce that

$$I^{(2)}(\kappa_1, \kappa_2) = I^{(2)}(\kappa_2, \kappa_1). \tag{6.28}$$

We evaluate the derivatives in the expression for $I^{(2)}(\kappa_1, \kappa_2)$, using the prescription described in section 2.4, as

$$\begin{aligned} I^{(2)}(\kappa_1, \kappa_2) = & -\frac{\lambda_1}{2\kappa_1}\frac{\lambda_2}{2\kappa_2}\frac{e^{-a(\kappa_1+\kappa_2)}}{\Delta_1\Delta_2} \\ & \times \Bigg[\kappa_1^2\Big(1+\frac{\lambda_1}{2\kappa_1}\Big)\Big(1+\frac{\lambda_2}{2\kappa_1}\Big) + \kappa_1\kappa_2\Big(1+\frac{\lambda_1}{2\kappa_1}\Big)\Big(1+\frac{\lambda_2}{2\kappa_2}\Big) \\ & +\kappa_1\kappa_2\Big(1+\frac{\lambda_1}{2\kappa_2}\Big)\Big(1+\frac{\lambda_2}{2\kappa_1}\Big) + \kappa_2^2\Big(1+\frac{\lambda_1}{2\kappa_2}\Big)\Big(1+\frac{\lambda_2}{2\kappa_2}\Big)\Bigg], \end{aligned} \tag{6.29}$$

where Δ_i's are given by eq. (2.52) after replacing $\kappa \to \kappa_i$.

Dirichlet limit

For the case of the Dirichlet limit ($a\lambda_{1,2} \gg 1$) the expression for $I^{(2)}(\kappa_1, \kappa_2)$ in eq. (6.29) takes on the relatively simple form

$$I_D^{(2)}(\kappa_1, \kappa_2) = -\frac{\kappa_1}{\sinh \kappa_1 a}\frac{\kappa_2}{\sinh \kappa_2 a}, \tag{6.30}$$

where the subscript D stands for Dirichlet limit. Using the above expression in eq. (6.26) we have

$$L_D^{(2)}(k_1, k_2) = \frac{1}{4\pi}\int_0^\infty \bar{\kappa}\, d\bar{\kappa}\frac{\kappa_1}{\sinh \kappa_1 a}\frac{\kappa_2}{\sinh \kappa_2 a}. \tag{6.31}$$

We describe the correspondence of the expression for the interaction energy, in eq. (6.24), in the Dirichlet limit, to the result in [59] in section 6.2.2.

We shall digress a little to answer how the above result is related to the Dirichlet Green's function. We start by recalling the reduced Green's function corresponding to the Dirichlet problem associated with eq. (6.23), which can be derived by taking the $\lambda_{1,2} \to \infty$ limit in $g_{22}^{(0)}(z, z'; \kappa)$ in eq. (2.50b) defined in region 2 ($a_1 < z, z' < a_2$) in figure 2.2,

$$g_D^{(0)}(z, z'; \kappa) = \frac{\sinh \kappa(z_< - a_1) \sinh \kappa(a_2 - z_>)}{\kappa \sinh \kappa a}, \tag{6.32}$$

where $z_<$ and $z_>$ stand for $\mathrm{Min}(z, z')$ and $\mathrm{Max}(z, z')$ respectively. It is trivially verified that the above function satisfies the Dirichlet boundary conditions, $g_D^{(0)}(a_i, z'; \kappa) = 0$ and $g_D^{(0)}(z, a_i; \kappa) = 0$. Using eq. (6.32) we can evaluate

$$\left[\frac{d}{dz_<}\frac{d}{dz_>} g_D^{(0)}(z, z'; \kappa)\right]_{z_<=a_1, z_>=a_2} = -\frac{\kappa}{\sinh \kappa a}. \tag{6.33}$$

Using the above result eq. (6.30) can be expressed as the product of derivatives of two Dirichlet Green's functions. It is also worth mentioning that the result in eq. (6.30) can also be derived by exclusively using $g_{22}^{(0)}(z, z'; \kappa)$ in eq. (6.27) after taking the limit $\lambda_{1,2} \to \infty$. This is expected because the result in the Dirichlet limit should depend only on the quantities between the plates. Thus, all the results related to the Dirichlet limit can be derived without relying on the averaging prescription for taking derivatives described in section 2.4. However, for the more general case being considered here, we require the averaging prescription to derive eq. (6.29).

Weak coupling limit

For the weak coupling limit ($a\lambda_{1,2} \ll 1$) the expression for $I^{(2)}(\kappa_1, \kappa_2)$ in eq. (6.29) takes the very simple form

$$I_W^{(2)}(\kappa_1, \kappa_2) = -\frac{\lambda_1}{2\kappa_1}\frac{\lambda_2}{2\kappa_2}(\kappa_1 + \kappa_2)^2\, e^{-a(\kappa_1+\kappa_2)}, \tag{6.34}$$

where the subscript W stands for the weak limit. We point out that in the case of weak coupling the averaging prescription for the evaluation of the I-kernels was also not necessary because only the free Green's functions come in. Using the above expression in eq. (6.26) we can evaluate the corresponding L-kernel as

$$\begin{aligned} L_W^{(2)}(k_1, k_2) &= \frac{\lambda_1\lambda_2}{16\pi}\int_0^\infty \bar{\kappa}\, d\bar{\kappa}\, \frac{(\kappa_1+\kappa_2)^2}{\kappa_1\kappa_2}\, e^{-a(\kappa_1+\kappa_2)} \\ &= -\frac{\lambda_1\lambda_2}{16\pi}\frac{\partial}{\partial a}\left[\frac{1}{a}e^{-a(|k_1|+|k_2|)}\right], \end{aligned} \tag{6.35}$$

where in the evaluation of the integral we used the change of variables $\kappa_1 + \kappa_2 = x$, and the corresponding relation $\bar{\kappa}\, d\bar{\kappa}\, (\kappa_1 + \kappa_2) = \kappa_1\kappa_2\, dx$.

6.2.2 Comparison of our leading order result with earlier results in the literature

Here we wish to explicitly compare our results—in the leading order—with those in [59]. In particular we show how the Dirichlet limit of our expression for the interaction energy in the leading order, [eq. (6.24) with eq. (6.31) inserted] match with the results in [59] [in eq. (11) with eqs. (13) and (17) there]. To this end we begin from eq. (6.21)

and write the interaction energy in the form

$$E_{12}^{(2)} = -\int d(t-t') \int\int dx\, dy \int\int dx' dy'\, h_1(y) Q(|\mathbf{y}-\mathbf{y}'|) h_2(y'), \tag{6.36}$$

where we have used the notation introduced in [59]: $\mathbf{y} \equiv (t, x, y)$, $|\mathbf{y}-\mathbf{y}'|^2 = (t-t')^2 + (x-x')^2 + (y-y')^2$, and switched to Euclidean time by replacing $t, t', \tau \to -it, -it', -i\tau$. The Q-kernel introduced above, following [59], is given as

$$Q(|\mathbf{y}-\mathbf{y}'|) = \frac{\lambda_1 \lambda_2}{2} \frac{\partial}{\partial z} \frac{\partial}{\partial z'} \Big[G_E^{(0)}(\mathbf{x}, t, \mathbf{x}', t')\, G_E^{(0)}(\mathbf{x}', t', \mathbf{x}, t) \Big] \Big|_{z'=a_1, z=a_2}, \tag{6.37}$$

where $\mathbf{x} \equiv (x, y, z)$ and $G_E^{(0)}(\mathbf{x}, t, \mathbf{x}', t')$ is given in terms of eq. (2.40) after switching to Euclidean time as

$$G_E^{(0)}(\mathbf{x}, t, \mathbf{x}', t') = \frac{1}{i} G^{(0)}(\mathbf{x}, t, \mathbf{x}', t') = \int \frac{d^3\kappa}{(2\pi)^3}\, e^{i\boldsymbol{\kappa}\cdot(\mathbf{y}-\mathbf{y}')}\, g^{(0)}(z, z'; \kappa), \tag{6.38}$$

where $\boldsymbol{\kappa} \equiv (\zeta, k_x, k_y)$.

Dirichlet Limit

In the Dirichlet limit the above expression should correspond to the Q-kernel introduced in [59] [in eq. (13) there]. Note that in [59] the interaction energy is not isolated from the outset unlike in our eq. (6.18). This is achieved in [59] by identifying and subtracting the contributions to the energy from the single plates. We identify the presence of our I-kernel [see eq. (6.27)] in eq. (6.37) which lets us express the Dirichlet limit of the Q-kernel, using eq. (6.30), in the form

$$Q_D(|\mathbf{y}-\mathbf{y}'|) = \frac{1}{2} \Big[\int \frac{d^3\kappa}{(2\pi)^3}\, e^{i\boldsymbol{\kappa}\cdot(\mathbf{y}-\mathbf{y}')}\, \frac{\kappa}{\sinh \kappa a} \Big]^2 = \frac{1}{2} \Big[\frac{1}{a^4} P\Big(\frac{|\mathbf{y}-\mathbf{y}'|}{a} \Big) \Big]^2 \tag{6.39}$$

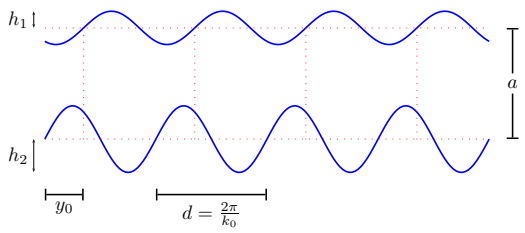

Figure 6.1: Parallel plates with sinusoidal corrugations.

in terms of the integral

$$P(x) = \frac{1}{2\pi^2}\frac{1}{x}\int_0^\infty t^2\, dt\, \frac{\sin(tx)}{\sinh t} = \frac{\pi}{8}\frac{1}{x}\frac{\sinh(\pi x/2)}{\cosh^3(\pi x/2)}. \tag{6.40}$$

This exact form for the Q-kernel in the Dirichlet limit reproduces the result in [59].

This exact form for the Q-kernel in the Dirichlet limit suggests that we can consider a class of corrugations for which exact results, in the perturbative approximation, might be achievable. Like the exact results achieved in [69, 70] for the weak coupling limit, we should be able to explore geometries in the Dirichlet limit in the perturbative approximation starting from eq. (6.36). Further, it should also be possible to extend these explorations to the next-to-leading orders. And, for very special geometries it might just be possible to transcend the perturbative approximation and get exact results in the Dirichlet limit alone. We hope to be able to address some of these explorations in our forthcoming publications.

6.2.3 Sinusoidal corrugations: Leading order

For the particular case of sinusoidal corrugations, as described in figure 6.1, we will have

$$h_1(y) = h_1 \sin[k_0(y + y_0)], \tag{6.41a}$$

$$h_2(y) = h_2 \sin[k_0 y], \tag{6.41b}$$

where $k_0 = 2\pi/d$ is the wavenumber corresponding to the corrugation wavelength d. We get nonzero contributions, to the leading order, only for the case when both plates have the same corrugation wavelength. The Fourier transforms $\tilde{h}_i(k)$ for sinusoidal corrugations get contributions in the form of delta functions

$$\tilde{h}_1(k) = h_1 \frac{2\pi}{2i} \Big[e^{ik_0 y_0} \delta(k - k_0) - e^{-ik_0 y_0} \delta(k + k_0) \Big]. \tag{6.42}$$

Using the above expression in eq. (6.24), and after interpreting $2\pi\delta(0) = L_y$ to be the infinite length in the y direction, we write

$$\begin{aligned} \frac{E_{12}^{(2)}}{L_x L_y} &= \cos k_0 y_0 \, \frac{h_1 h_2}{4\pi} \int_{-\infty}^{\infty} dk \, L^{(2)}(k, k_+) \\ &= -\cos k_0 y_0 \, \frac{h_1 h_2}{16\pi^2} \int_{-\infty}^{\infty} dk \int_0^{\infty} \bar{\kappa} \, d\bar{\kappa} \, I^{(2)}(\kappa, \kappa_+), \end{aligned} \tag{6.43}$$

where we have used the symmetry property in the $I^{(2)}$-kernel, noted in eq. (6.28), and performed a suitable shift in the integration variables. We have used the notations $k_\pm = k \pm k_0$, and $\kappa_\pm^2 = \bar{\kappa}^2 + k_\pm^2$. The $I^{(2)}$-kernel in the above expression is provided by eq. (6.29).

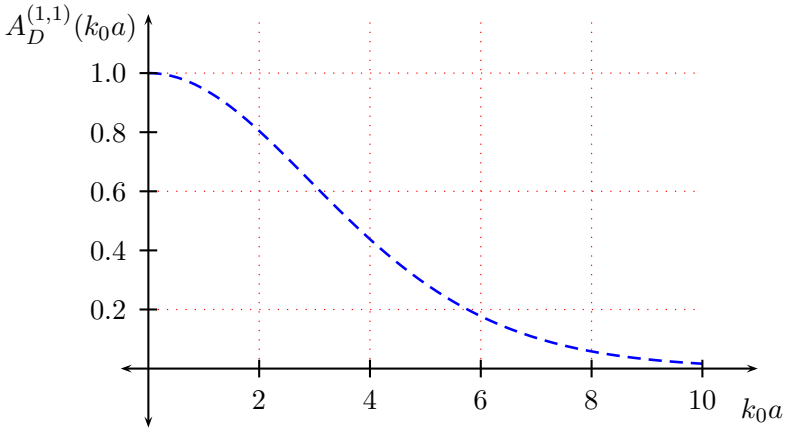

Figure 6.2: Dirichlet limit: Plot of $A_D^{(1,1)}(k_0a)$ versus k_0a.

Dirichlet limit

In the Dirichlet limit, where the $I^{(2)}$-kernel is given by eq. (6.30), the interaction energy in eq. (6.43) can be expressed in the form

$$\frac{E_{12}^{(2)}}{L_xL_y} = \cos(k_0y_0)\,\frac{\pi^2}{240\,a^3}\,\frac{h_1}{a}\frac{h_2}{a}\,A_D^{(1,1)}(k_0a), \tag{6.44}$$

where the function $A_D^{(1,1)}(k_0a)$ is normalized such that $A_D^{(1,1)}(0) = 1$, which becomes a convenience when we compare the results with those obtained by the proximity force approximation. The expression for $A_D^{(1,1)}(k_0a)$ is

$$\begin{aligned} A_D^{(1,1)}(k_0a) &= \frac{60\,a^5}{\pi^3}\int_{-\infty}^{\infty} dk L_D^{(2)}(k,k_+) \\ &= -\frac{1}{4\pi}\frac{60\,a^5}{\pi^3}\int_{-\infty}^{\infty} dk \int_0^{\infty} \bar{\kappa}\,d\bar{\kappa}\,I_D^{(2)}(\kappa,\kappa_+), \end{aligned} \tag{6.45}$$

where the $I_D^{(2)}$-kernel, and the corresponding $L_D^{(2)}$-kernel, in the Dirichlet limit were given in eq. (6.30) and eq. (6.31) respectively. Using the notations, $s^2 = \bar{s}^2 + t^2$, $s_\pm^2 = \bar{s}^2 + (t \pm t_0)^2$, and $t_0 = k_0 a$, we can write

$$A_D^{(1,1)}(t_0) = \frac{15}{\pi^4} \int_0^\infty \bar{s}\, d\bar{s} \int_{-\infty}^\infty dt \frac{s}{\sinh s} \frac{s_+}{\sinh s_+}. \tag{6.46}$$

This expression can be numerically evaluated and has been plotted in figure 6.2. The value of the function at $t_0 = 0$ can be evaluated exactly by rewriting the integral in terms of spherical polar coordinates to yield

$$A_D^{(1,1)}(0) = \frac{30}{\pi^4} \int_0^\infty s^2\, ds \left[\frac{s}{\sinh s}\right]^2 = 1. \tag{6.47}$$

It should be mentioned that the result corresponding to eq. (6.46) for the electromagnetic case and the scalar Dirichlet case have been evaluated exactly in [59] and as shown above exactly agree with our results.

The lateral Casimir force can be evaluated using eq. (6.44) in the definition of lateral force in eq. (6.10) which yields

$$F_{\text{Lat,D}}^{(2)} = 2\, k_0 a\, \sin(k_0 y_0) \left| F_{\text{Cas,D}}^{(0)} \right| \frac{h_1}{a} \frac{h_2}{a} A_D^{(1,1)}(k_0 a), \tag{6.48}$$

where $|F_{\text{Cas,D}}^{(0)}|$ is the magnitude of the normal scalar Casimir force between two uncorrugated parallel Dirichlet plates given as

$$\frac{F_{\text{Cas,D}}^{(0)}}{L_x L_y} = -\frac{\pi^2}{480} \frac{1}{a^4}, \tag{6.49}$$

which was derived in eq. (3.19).

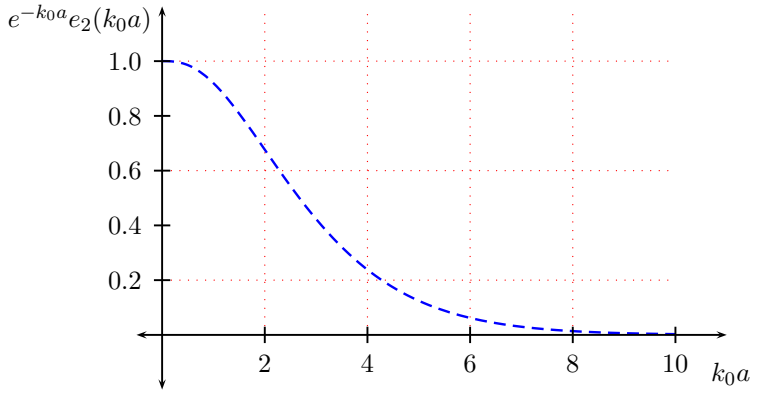

Figure 6.3: Weak coupling limit: Plot of $A_W^{(2)}(k_0 a) = e^{-k_0 a} e_2(k_0 a)$ versus $k_0 a$.

Weak coupling limit

Let us start by recalling the expression for the Casimir energy and Casimir force between uncorrugated parallel plates in the weak limit:

$$\frac{E^{(0)}_{\mathrm{Cas,W}}}{L_x L_y} = -\frac{\lambda_1 \lambda_2}{32\,\pi^2}\frac{1}{a} \qquad \text{and} \qquad \frac{F^{(0)}_{\mathrm{Cas,W}}}{L_x L_y} = -\frac{\lambda_1 \lambda_2}{32\,\pi^2}\frac{1}{a^2}. \tag{6.50}$$

In the weak limit we have seen that it is possible to evaluate the L-kernel in eq. (6.35) without any effort. Using this in eq. (6.43) we have

$$\frac{E^{(2)}_{12,W}}{L_x L_y} = -\cos(k_0 y_0)\,\frac{\lambda_1 \lambda_2}{16\,\pi}\,\frac{h_1 h_2}{4\,\pi}\,\frac{\partial}{\partial a}\left[\frac{1}{a}\int_{-\infty}^{\infty} dk\, e^{-a(|k|+|k+k_0|)}\right], \tag{6.51}$$

which after performing the integral can be written in the form

$$E^{(2)}_{12,\mathrm{W}} = \cos(k_0 y_0)\,\left|E^{(0)}_{\mathrm{Cas,W}}\right|\,\frac{h_1}{a}\frac{h_2}{a}\,A^{(2)}_W(k_0 a), \tag{6.52}$$

where we have introduced the function

$$A_W^{(2)}(t_0) = \frac{t_0^3}{2}\frac{\partial^2}{\partial t_0^2}\left[\frac{1}{t_0}\,e^{-t_0}\right] = e^{-t_0}\sum_{m=0}^{2}\frac{t_0^m}{m!} = \frac{e_2(t_0)}{e^{t_0}}, \tag{6.53}$$

where $e_n(x) = \sum_{m=0}^{n}\frac{x^m}{m!}$ is the the truncated exponential function which approximates to unity for $x \ll n$. $A_W^{(2)}(t_0)$ has been plotted in figure 6.3. Using eq. (6.10) we evaluate the lateral Casimir force in this perturbation order as

$$F_{\mathrm{Lat,W}}^{(2)} = k_0 a\,\sin(k_0 y_0)\,\left|F_{\mathrm{Cas,W}}^{(0)}\right|\,\frac{h_1}{a}\frac{h_2}{a}\,A_W^{(2)}(k_0 a). \tag{6.54}$$

6.3 Next-to-leading-order contribution

We start by collecting the terms in eq. (6.19) in the form

$$E_{12} = E_{12}^{(2)} + E_{12}^{(3)} + E_{12}^{(4)} + \mathcal{O}(h/a)^5. \tag{6.55}$$

To economize typographical space and for bookkeeping purposes we introduce the notation

$$[G^{(0)}\Delta V]_{(i_1,i_2,\ldots,i_N)}^{(m_1,m_2,\ldots,m_N)} = \mathrm{Tr}\Big[G^{(0)}\Delta V_{i_1}^{(m_1)}G^{(0)}\Delta V_{i_2}^{(m_2)}\cdots G^{(0)}\Delta V_{i_N}^{(m_N)}\Big], \tag{6.56}$$

where the superscripts m_n denote the m_n-th order contribution in the power series expansion of the potential as defined in eq. (6.20). The subscripts i_n identifies the potential that is contributing. In the case under consideration we have only two

potentials coupling and thus $i_n = 1, 2$ for any n. As an illustrative example we have

$$[G^{(0)}\Delta V]^{(2,1,1)}_{(1,1,2)} = \mathrm{Tr}\Big[G^{(0)}\Delta V_1^{(2)} G^{(0)}\Delta V_1^{(1)} G^{(0)}\Delta V_2^{(1)}\Big]. \tag{6.57}$$

Using the above notation we can write

$$E_{12}^{(3)} = \frac{i}{2\tau}\Big\{[G^{(0)}\Delta V]^{(2,1)}_{(1,2)} + [G^{(0)}\Delta V]^{(1,2)}_{(1,2)} - [G^{(0)}\Delta V]^{(1,1,1)}_{(1,1,2)} - [G^{(0)}\Delta V]^{(1,1,1)}_{(1,2,2)}\Big\}. \tag{6.58}$$

We argue that for the case of sinusoidal corrugations of the same wavelength on both plates the third order perturbation does not contribute. (Contributions from third order are nonzero if the wavelength of the corrugations of one plate is double that of the other plate.) Since the plates under consideration are infinite in extent, the interaction energy is independent of translations in the y direction. Let us now make a translation of the amount $k_0 y = \pi$ in the potentials in eq. (6.41). This amounts to replacing $h_i \to -h_i$. Thus invariance under translation requires that the total power of h_i's in the result should be even. This rules out the third order perturbation from contributing.

6.3.1 Fourth order perturbation in Casimir energy due to corrugations

Starting from eq. (6.19) and keeping terms contributing to the fourth order we have

$$E_{12}^{(4)} = E_{12}^{(2,2)} + E_{12}^{(3,1)} + E_{12}^{(1,3)}, \tag{6.59}$$

where the superscripts represent the powers of h_i's. For example, the superscript $(3,1)$ represents terms involving $h_1^3 h_2$. All terms except one gets contributions from $m = 1$ in the logarithm expansion in eq. (6.19). Since the $m = 2$ term is distinct in structure we further separate it out by defining

$$E_{12}^{(2,2)} = E_{12}^{(2,2)A} + E_{12}^{(2,2)B}, \tag{6.60}$$

where the term involving the superscript A is the contribution from $m = 2$ in (6.19). Using the notation in eq. (6.56) we can thus collect the terms contributing to eq. (6.59) and eq. (6.60) as

$$E_{12}^{(2,2)A} = \frac{i}{2\tau}\Big\{\frac{1}{2}\,[G^{(0)}\Delta V]^{(1,1,1,1)}_{(1,2,1,2)}\Big\}, \tag{6.61a}$$

$$E_{12}^{(2,2)B} = \frac{i}{2\tau}\Big\{[G^{(0)}\Delta V]^{(1,1,1,1)}_{(1,1,2,2)} - [G^{(0)}\Delta V]^{(1,1,2)}_{(1,1,2)} - [G^{(0)}\Delta V]^{(2,1,1)}_{(1,2,2)} + [G^{(0)}\Delta V]^{(2,2)}_{(1,2)}\Big\}, \tag{6.61b}$$

$$E_{12}^{(3,1)} = \frac{i}{2\tau}\Big\{[G^{(0)}\Delta V]^{(1,1,1,1)}_{(1,1,1,2)} - [G^{(0)}\Delta V]^{(1,2,1)}_{(1,1,2)} - [G^{(0)}\Delta V]^{(2,1,1)}_{(1,1,2)} + [G^{(0)}\Delta V]^{(3,1)}_{(1,2)}\Big\}, \tag{6.61c}$$

$$E_{12}^{(1,3)} = \frac{i}{2\tau}\Big\{[G^{(0)}\Delta V]^{(1,1,1,1)}_{(1,2,2,2)} - [G^{(0)}\Delta V]^{(1,2,1)}_{(1,2,2)} - [G^{(0)}\Delta V]^{(1,1,2)}_{(1,2,2)} + [G^{(0)}\Delta V]^{(1,3)}_{(1,2)}\Big\}. \tag{6.61d}$$

In terms of the reduced Green's function defined in eq. (6.22) and eq. (6.23), and the Fourier transform of the corrugations in eq. (6.25), we can write each of the terms in eq. (6.61) in terms of a corresponding L-kernel. In terms of the notation introduced

in eq. (6.56) these will read as

$$(-1)^N \frac{i}{2\tau} [G^{(0)} \Delta V]^{(m_1,\ldots,m_N)}_{(i_1,\ldots,i_N)}$$
$$= L_x \int \frac{dk_1}{2\pi} \cdots \frac{dk_N}{2\pi} \, \tilde{h}^{m_1}_{i_1}(k_1 - k_2) \cdots \tilde{h}^{m_N}_{i_N}(k_N - k_1) \, L^{(m_1,\ldots,m_N)}_{(i_1,\ldots,i_N)}(k_1, \ldots, k_N), \quad (6.62)$$

where implicitly we have interpreted the powers of the Fourier transformed corrugations as

$$\tilde{h}^{m_1}_{i_1}(k_1 - k_2) = \int \frac{dq_1}{2\pi} \cdots \frac{dq_{m_1-1}}{2\pi} \, \tilde{h}_{i_1}(k_1 - q_1) \tilde{h}_{i_1}(q_1 - q_2) \cdots \tilde{h}_{i_1}(q_{m_1-1} - k_2). \quad (6.63)$$

Observe that each term contributing to the M-th order ($M = m_1 + m_2 + \ldots + m_N$) has exactly M h's. Also, the total number of variables inside the L-kernel is N which is in general less than or equal to M. It might be appropriate to call them N-point kernels. Proceeding further, in the spirit of the second order calculation in eq. (6.26), we introduce the corresponding I-kernels for the L-kernels as

$$L^{(m_1,\ldots,m_N)}_{(i_1,\ldots,i_N)}(k_1, \ldots, k_N) = -\frac{1}{4\pi} \int_0^\infty \bar{\kappa} \, d\bar{\kappa} \; I^{(m_1,\ldots,m_N)}_{(i_1,\ldots,i_N)}(\kappa_1, \ldots, \kappa_N), \quad (6.64)$$

where the I-kernels are expressed in terms of derivatives operating on the reduced Green's function defined in eq. (6.23) as

$$I^{(m_1,\ldots,m_N)}_{(i_1,\ldots,i_N)}(\kappa_1, \ldots, \kappa_N) = (-1)^N \, \frac{\lambda_{i_1}}{m_1!} \cdots \frac{\lambda_{i_N}}{m_N!}$$
$$\times \frac{\partial^{m_1}}{\partial z_1^{m_1}} \cdots \frac{\partial^{m_N}}{\partial z_N^{m_N}} \Big[g^{(0)}(z_N, z_1; \kappa_1) \cdots g^{(0)}(z_{N-1}, z_N; \kappa_N) \Big] \Big|_{z_n = a_{i_n}}. \quad (6.65)$$

For clarification we evaluate a particular term which should also serve as an illustration of the notation. The term we consider is

$$
\begin{aligned}
&-\frac{i}{2\tau}\,[G^{(0)}\Delta V]^{(1,2,1)}_{(1,1,2)} \\
&\qquad = L_x \int \frac{dk_1}{2\pi}\frac{dk_2}{2\pi}\frac{dk_3}{2\pi}\,\tilde{h}_1(k_1-k_2)\tilde{h}_1^2(k_2-k_3)\tilde{h}_2(k_3-k_1)\,L^{(1,2,1)}_{(1,1,2)}(k_1,k_2,k_3) \\
&\qquad = L_x \int \frac{dk_1}{2\pi}\frac{dk_2}{2\pi}\frac{dk_3}{2\pi}\frac{dk_4}{2\pi}\,\tilde{h}_1(k_1-k_2) \\
&\qquad\qquad\qquad \times \tilde{h}_1(k_2-k_3)\tilde{h}_1(k_3-k_4)\,\tilde{h}_2(k_4-k_1)\,L^{(1,2,1)}_{(1,1,2)}(k_1,k_2,k_4). \qquad (6.66)
\end{aligned}
$$

Notice how the particular k dependence in the L-kernel is unambiguously specified. The corresponding I-kernel according to eq. (6.64) and eq. (6.65) is given as

$$
\begin{aligned}
&I^{(1,2,1)}_{(1,1,2)}(\kappa_1,\kappa_2,\kappa_4) \\
&= -\frac{\lambda_1^2\lambda_2}{2}\frac{\partial}{\partial z_1}\frac{\partial^2}{\partial z_2^2}\frac{\partial}{\partial z_3}\Big[g^{(0)}(z_3,z_1;\kappa_1)g^{(0)}(z_1,z_2;\kappa_2)g^{(0)}(z_2,z_3;\kappa_4)\Big]\Big|_{z_{1,2}=a_1,z_3=a_2}. \qquad (6.67)
\end{aligned}
$$

Using the reciprocal symmetry in the Green's functions we can learn the following symmetries in the I-kernels associated with the terms in eq. (6.61):

$$I^{(1,1,1,1)}_{(1,2,1,2)}(\kappa_1,\kappa_2,\kappa_3,\kappa_4) = I^{(1,1,1,1)}_{(1,2,1,2)}(\kappa_2,\kappa_1,\kappa_4,\kappa_3), \tag{6.68a}$$

$$I^{(1,1,1,1)}_{(1,1,2,2)}(\kappa_1,\kappa_2,\kappa_3,\kappa_4) = I^{(1,1,1,1)}_{(1,1,2,2)}(\kappa_3,\kappa_2,\kappa_1,\kappa_4), \tag{6.68b}$$

$$I^{(1,1,1,1)}_{(1,2,2,2)}(\kappa_1,\kappa_2,\kappa_3,\kappa_4) = I^{(1,1,1,1)}_{(1,2,2,2)}(\kappa_2,\kappa_1,\kappa_4,\kappa_3), \tag{6.68c}$$

$$I^{(1,1,1,1)}_{(1,1,1,2)}(\kappa_1,\kappa_2,\kappa_3,\kappa_4) = I^{(1,1,1,1)}_{(1,1,1,2)}(\kappa_4,\kappa_3,\kappa_2,\kappa_1), \tag{6.68d}$$

$$I^{(1,1,2)}_{(1,1,2)}(\kappa_1,\kappa_2,\kappa_3) = I^{(1,1,2)}_{(1,1,2)}(\kappa_3,\kappa_2,\kappa_1), \tag{6.68e}$$

$$I^{(2,1,1)}_{(1,2,2)}(\kappa_1,\kappa_2,\kappa_3) = I^{(2,1,1)}_{(1,2,2)}(\kappa_2,\kappa_1,\kappa_3), \tag{6.68f}$$

$$I^{(1,2,1)}_{(1,2,2)}(\kappa_1,\kappa_2,\kappa_3) = I^{(1,1,2)}_{(1,2,2)}(\kappa_2,\kappa_1,\kappa_3), \tag{6.68g}$$

$$I^{(1,2,1)}_{(1,1,2)}(\kappa_1,\kappa_2,\kappa_3) = I^{(2,1,1)}_{(1,1,2)}(\kappa_3,\kappa_2,\kappa_1). \tag{6.68h}$$

We have not listed the 2-point I-kernels in the above list because they have the symmetry of the kind in eq. (6.28). In fact any 2-point kernel will have the following symmetry:

$$I^{(m_1,m_2)}_{(1,2)}(\kappa_1,\kappa_2) = I^{(m_1,m_2)}_{(1,2)}(\kappa_2,\kappa_1). \tag{6.69}$$

In the above discussion involving very general notations we have in principle expressed each term in eq. (6.61). Specific evaluation of each term involves the evaluation of the corresponding I-kernels which are given in terms of the derivatives of the Green's functions. The derivatives are evaluated using the prescription described in section 2.4. We can thus collect the terms in eq. (6.61) into four distinct L-kernels in

the form

$$\frac{E_{12}^{(2,2)A}}{L_x} = \frac{1}{2}\int \frac{dk_1}{2\pi}\frac{dk_2}{2\pi}\frac{dk_3}{2\pi}\frac{dk_4}{2\pi}\,\tilde{h}_1(k_1-k_2) \times\tilde{h}_2(k_2-k_3)\tilde{h}_1(k_3-k_4)\tilde{h}_2(k_4-k_1)\,L^{(2,2)A}(k_1,k_2,k_3,k_4), \quad (6.70a)$$

$$\frac{E_{12}^{(2,2)B}}{L_x} = \int \frac{dk_1}{2\pi}\frac{dk_2}{2\pi}\frac{dk_3}{2\pi}\frac{dk_4}{2\pi}\,\tilde{h}_1(k_1-k_2) \times\tilde{h}_1(k_2-k_3)\tilde{h}_2(k_3-k_4)\tilde{h}_2(k_4-k_1)\,L^{(2,2)B}(k_1,k_2,k_3,k_4), \quad (6.70b)$$

$$\frac{E_{12}^{(3,1)}}{L_x} = \int \frac{dk_1}{2\pi}\frac{dk_2}{2\pi}\frac{dk_3}{2\pi}\frac{dk_4}{2\pi}\,\tilde{h}_1(k_1-k_2) \times\tilde{h}_1(k_2-k_3)\tilde{h}_1(k_3-k_4)\tilde{h}_2(k_4-k_1)\,L^{(3,1)}(k_1,k_2,k_3,k_4), \quad (6.70c)$$

$$\frac{E_{12}^{(1,3)}}{L_x} = \int \frac{dk_1}{2\pi}\frac{dk_2}{2\pi}\frac{dk_3}{2\pi}\frac{dk_4}{2\pi}\,\tilde{h}_1(k_1-k_2) \times\tilde{h}_2(k_2-k_3)\tilde{h}_2(k_3-k_4)\tilde{h}_2(k_4-k_1)\,L^{(1,3)}(k_1,k_2,k_3,k_4), \quad (6.70d)$$

where it should be noted that different L's combine with specific combination of h's. The factor of one-half in eq. (6.70a) can be traced back to the coefficient of the second term in the expansion of logarithm in eq. (6.19). The respective kernels $L^{(m,n)}$ above are related to their corresponding $I^{(m,n)}$ by eq. (6.64), which are given by

$$I^{(2,2)A}(\kappa_1,\kappa_2,\kappa_3,\kappa_4) = I^{(1,1,1,1)}_{(1,2,1,2)}(\kappa_1,\kappa_2,\kappa_3,\kappa_4), \quad (6.71a)$$

$$I^{(2,2)B}(\kappa_1,\kappa_2,\kappa_3,\kappa_4) = I^{(1,1,1,1)}_{(1,1,2,2)}(\kappa_1,\kappa_2,\kappa_3,\kappa_4) + I^{(1,1,2)}_{(1,1,2)}(\kappa_1,\kappa_2,\kappa_3) + I^{(2,1,1)}_{(1,2,2)}(\kappa_1,\kappa_3,\kappa_4) + I^{(2,2)}_{(1,2)}(\kappa_1,\kappa_3), \quad (6.71b)$$

$$I^{(3,1)}(\kappa_1,\kappa_2,\kappa_3,\kappa_4) = I^{(1,1,1,1)}_{(1,1,1,2)}(\kappa_1,\kappa_2,\kappa_3,\kappa_4) + I^{(1,2,1)}_{(1,1,2)}(\kappa_1,\kappa_2,\kappa_4) + I^{(2,1,1)}_{(1,1,2)}(\kappa_1,\kappa_3,\kappa_4) + I^{(3,1)}_{(1,2)}(\kappa_1,\kappa_4), \quad (6.71c)$$

$$I^{(1,3)}(\kappa_1,\kappa_2,\kappa_3,\kappa_4) = I^{(1,1,1,1)}_{(1,2,2,2)}(\kappa_1,\kappa_2,\kappa_3,\kappa_4) + I^{(1,2,1)}_{(1,2,2)}(\kappa_1,\kappa_2,\kappa_4) + I^{(1,1,2)}_{(1,2,2)}(\kappa_1,\kappa_2,\kappa_3) + I^{(1,3)}_{(1,2)}(\kappa_1,\kappa_2). \quad (6.71d)$$

Proceeding in the spirit of section 6.2 has brought us to the point of evaluation of the thirteen I-kernels on the right hand side of eq. (6.71). Using the prescription described in the section 2.4 we have evaluated all the thirteen kernels and explicit expressions analogous to eq. (6.29) have been derived. This would have involved a lot more labor and bookkeeping if not for the facilitation achieved by the use of Mathematica. We shall not display the explicit expressions here because they are too long. But, as in section 6.2, these expressions simplify considerably in the Dirichlet limit and the weak coupling limit.

Dirichlet limit

Observe that the reduced Green's function defined by eq. (6.23) has a well defined Dirichlet limit. In the light of this observation in conjunction with the expression for the I-kernels in eq. (6.65) taken at face value suggests that these kernels might not have a well-defined finite Dirichlet limit. However, we evaluated the second order contribution in eq. (6.30). In fact it can be verified that all 2-point kernels have a well-defined finite Dirichlet limit. Further, $I^{(1,1,1,1)}_{(1,2,1,2)}$ also has a well-defined finite Dirichlet limit. The rest of the nine I-kernels on the right hand side of eq. (6.71) do not have a finite Dirichlet limit. But, the sums of the I-kernels listed in eq. (6.71) have finite Dirichlet limits. The higher powers in $\lambda_{1,2}$ in the numerator of each of these sums cancel identically to give a well-defined limit as $\lambda_{1,2} \to \infty$. This seems to be a generic phenomena. Here we list the I-kernels in eq. (6.71) evaluated in the

Dirichlet limit:

$$I_D^{(2,2)A}(\kappa_1,\kappa_2,\kappa_3,\kappa_4) = \frac{\kappa_1}{\sinh\kappa_1 a}\frac{\kappa_2}{\sinh\kappa_2 a}\frac{\kappa_3}{\sinh\kappa_3 a}\frac{\kappa_4}{\sinh\kappa_4 a}, \tag{6.72a}$$

$$I_D^{(2,2)B}(\kappa_1,\kappa_2,\kappa_3,\kappa_4) = \frac{\kappa_1}{\sinh\kappa_1 a}\frac{\kappa_2}{\tanh\kappa_2 a}\frac{\kappa_3}{\sinh\kappa_3 a}\frac{\kappa_4}{\tanh\kappa_4 a}, \tag{6.72b}$$

$$\begin{aligned} I_D^{(3,1)}(\kappa_1,\kappa_2,\kappa_3,\kappa_4) &= -\frac{\kappa_1}{\sinh\kappa_1 a}\frac{\kappa_4}{\sinh\kappa_4 a} \\ &\quad\times\frac{1}{4}\left[4\frac{\kappa_2}{\tanh\kappa_2 a}\frac{\kappa_3}{\tanh\kappa_3 a}+\frac{\kappa_1^2+\kappa_4^2}{3}-\kappa_2^2-\kappa_3^2\right], \end{aligned} \tag{6.72c}$$

$$\begin{aligned} I_D^{(1,3)}(\kappa_1,\kappa_2,\kappa_3,\kappa_4) &= -\frac{\kappa_1}{\sinh\kappa_1 a}\frac{\kappa_2}{\sinh\kappa_2 a} \\ &\quad\times\frac{1}{4}\left[4\frac{\kappa_3}{\tanh\kappa_3 a}\frac{\kappa_4}{\tanh\kappa_4 a}+\frac{\kappa_1^2+\kappa_2^2}{3}-\kappa_3^2-\kappa_4^2\right]. \end{aligned} \tag{6.72d}$$

Weak coupling limit

We can similarly evaluate the I-kernels in the weak limit by keeping terms to order $\lambda_1\lambda_2$ in the general expressions for the I-kernels. But, we find it instructive, and simpler, to start over from eq. (6.61). We observe that only the 2-point kernels contribute in the weak limit. We further notice that only the contributions from the free Green's function (which is obtained by switching off the couplings $\lambda_{1,2}$ in eq. (6.23)) contribute in the evaluation of the weak limit. These observations allows us to write the 2-point kernels in the weak limit as

$$\begin{aligned} I_{(1,2),W}^{(m_1,m_2)}(\kappa_1,\kappa_2) &= \frac{\lambda_1}{m_1!}\frac{\lambda_2}{m_2!}\left[\frac{\partial^{m_1}}{\partial z_1^{m_1}}\frac{\partial^{m_2}}{\partial z_2^{m_2}}\frac{e^{-\kappa_1|z_2-z_1|}}{2\kappa_1}\frac{e^{-\kappa_2|z_1-z_2|}}{2\kappa_2}\right]_{z_1=a_1,z_2=a_2} \\ &= \frac{(-1)^{m_1}}{m_1!\,m_2!}\frac{\lambda_1\lambda_2}{2\kappa_1 2\kappa_2}\left(\kappa_1+\kappa_2\right)^M e^{-a(\kappa_1+\kappa_2)}, \end{aligned} \tag{6.73}$$

where $M = m_1 + m_2$. Note that the derivatives in the above expressions are well defined because they are evaluated at a point where $z_2 > z_1$. In particular using these in eq. (6.71) with the observation that only the 2-point kernels contribute in the weak limit we get $I_W^{(2,2)A}(\kappa_1, \kappa_2, \kappa_3, \kappa_4) = 0$ and

$$I_W^{(2,2)B}(\kappa_1, \kappa_2, \kappa_3, \kappa_4) = I_{(1,2),W}^{(2,2)}(\kappa_1, \kappa_3) = \frac{1}{2!\,2!}\,\frac{\lambda_1\lambda_2}{2\kappa_1 2\kappa_3}\,(\kappa_1+\kappa_3)^4\,e^{-a(\kappa_1+\kappa_3)}, \quad (6.74a)$$

$$I_W^{(3,1)}(\kappa_1, \kappa_2, \kappa_3, \kappa_4) = I_{(1,2),W}^{(3,1)}(\kappa_1, \kappa_4) = \frac{1}{3!\,1!}\,\frac{\lambda_1\lambda_2}{2\kappa_1 2\kappa_4}\,(\kappa_1+\kappa_4)^4\,e^{-a(\kappa_1+\kappa_4)}, \quad (6.74b)$$

$$I_W^{(1,3)}(\kappa_1, \kappa_2, \kappa_3, \kappa_4) = I_{(1,2),W}^{(1,3)}(\kappa_1, \kappa_2) = \frac{1}{1!\,3!}\,\frac{\lambda_1\lambda_2}{2\kappa_1 2\kappa_2}\,(\kappa_1+\kappa_2)^4\,e^{-a(\kappa_1+\kappa_2)}, \quad (6.74c)$$

where notice how they differ in the particular dependence on the variables. We again (see comments after eq. (6.34)) point out that the averaging prescription for the evaluation of the I-kernels was not necessary to arrive at the above expressions.

Using the change of variables introduced in evaluating eq. (6.35) we can similarly evaluate the L-kernels using eq. (6.64) in the weak limit as

$$L_{(1,2),W}^{(m_1,m_2)}(k_1, k_2) = \frac{(-1)^{m_2}}{m_1!\,m_2!}\,\frac{\lambda_1\lambda_2}{16\,\pi}\,\left(\frac{\partial}{\partial a}\right)^{M-1}\left[\frac{1}{a}\,e^{-a(|k_1|+|k_2|)}\right], \quad (6.75)$$

which reproduces the result in eq. (6.35) for $M = 2$.

6.3.2 Sinusoidal corrugations: Next-to-leading order

We shall now specialize to the particular case of sinusoidal corrugations described by eq. (6.41). Using the Fourier transforms in eq. (6.42) all but one of the k integrals in eq. (6.70) can be immediately performed. The symmetries listed in eq. (6.68) lead to simplifications in the expressions. As in section 6.2 the expressions boil down to two

integrals in variables k and $\bar{\kappa}$. In particular eq. (6.70) takes the form

$$\frac{E_{12}^{(2,2)}}{L_x L_y} = -\cos(2k_0 y_0)\,\frac{h_1^2 h_2^2}{64\pi^2}\int_{-\infty}^{\infty} dk \int_0^{\infty} \bar{\kappa}\, d\bar{\kappa}\Big[\,\frac{1}{2}\, I^{(2,2)A}(\kappa,\kappa_+,\kappa,\kappa_+) + I^{(2,2)B}(\kappa_-,\kappa,\kappa_+,\kappa)\Big], \tag{6.76a}$$

$$\frac{E_{12}^{(3,1)}}{L_x L_y} = -\cos(k_0 y_0)\,\frac{h_1^3 h_2}{64\pi^2}\int_{-\infty}^{\infty} dk \int_0^{\infty} \bar{\kappa}\, d\bar{\kappa}\Big[I^{(3,1)}(\kappa,\kappa_+,\kappa,\kappa_+) + I^{(3,1)}(\kappa,\kappa_+,\kappa,\kappa_-) + I^{(3,1)}(\kappa,\kappa_-,\kappa,\kappa_+)\Big], \tag{6.76b}$$

$$\frac{E_{12}^{(1,3)}}{L_x L_y} = -\cos(k_0 y_0)\,\frac{h_1 h_2^3}{64\pi^2}\int_{-\infty}^{\infty} dk \int_0^{\infty} \bar{\kappa}\, d\bar{\kappa}\Big[I^{(1,3)}(\kappa,\kappa_+,\kappa,\kappa_+) + I^{(1,3)}(\kappa,\kappa_+,\kappa,\kappa_-) + I^{(1,3)}(\kappa,\kappa_-,\kappa,\kappa_+)\Big], \tag{6.76c}$$

where the I-kernels are given from eq. (6.71). We use the notations $k_\pm$ and $\kappa_\pm$ introduced after eq. (6.43). We note the factor of 2 in the argument of cosine function of the first term above is a mark of the fourth order in perturbation theory. It should be mentioned here that in the above expressions we have omitted finite terms not having any dependence in the lateral shift variable y_0. These terms do not contribute to the lateral force.

Dirichlet limit

We presented the expressions for the I-kernels in the Dirichlet limit in eq. (6.72). Using these in eq. (6.76) and then adding the contributions from the three terms in eq. (6.59) we can write the total contribution to the interaction energy due to the

presence of corrugations as

$$\frac{E_{12}^{(4)}}{L_x L_y} = \frac{\pi^2}{240\,a^3}\frac{h_1}{a}\frac{h_2}{a}\frac{15}{4}\left[\cos(k_0 y_0)\left\{\frac{h_1^2}{a^2}\,A_D^{(3,1)}(k_0 a) + \frac{h_2^2}{a^2}\,A_D^{(1,3)}(k_0 a)\right\}\right.$$
$$\left. - \cos(2k_0 y_0)\,\frac{1}{2}\frac{h_1}{a}\frac{h_2}{a}\,A_D^{(2,2)}(k_0 a)\right], \qquad (6.77)$$

where we have introduced the functions

$$A_D^{(3,1)}(t_0) = A_D^{(1,3)}(t_0)$$
$$= \frac{1}{2\pi^4}\int_0^\infty \bar{s}\,d\bar{s}\int_{-\infty}^\infty dt \frac{s}{\sinh s}\frac{s_+}{\sinh s_+}$$
$$\times\left[4\frac{s}{\tanh s}\frac{s_-}{\tanh s_-} + 2\frac{s}{\tanh s}\frac{s_+}{\tanh s_+} - s^2 - s_-^2\right], \qquad (6.78a)$$
$$A_D^{(2,2)}(t_0) = \frac{1}{\pi^4}\int_0^\infty \bar{s}\,d\bar{s}\int_{-\infty}^\infty dt\left[\frac{s^2}{\sinh^2 s}\frac{s_-^2}{\sinh^2 s_-} + 2\frac{s^2}{\tanh^2 s}\frac{s_+}{\sinh s_+}\frac{s_-}{\sinh s_-}\right]. \qquad (6.78b)$$

These functions are plotted in figure 6.4. As in section 6.2 the above functions are suitably normalized such that they evaluate to unity when evaluated at $t_0 = 0$. Verification of this statement involves the following integrals:

$$A_D^{(3,1)}(0) = \frac{2}{\pi^4}\int_0^\infty s^2\,ds\frac{s^2}{\sinh^2 s}\left[3\frac{s^2}{\tanh^2 s} - s^2\right]$$
$$= \left(1 + \frac{\pi^2}{21}\right) - \frac{\pi^2}{21} = 1, \qquad (6.79a)$$
$$A_D^{(2,2)}(0) = \frac{2}{\pi^4}\int_0^\infty s^2\,ds\left[\frac{s^4}{\sinh^4 s} + 2\frac{s^2}{\tanh^2 s}\frac{s^2}{\sinh^2 s}\right]$$
$$= \left(\frac{1}{3} + \frac{2\,\pi^2}{63}\right) + \left(\frac{2}{3} - \frac{2\,\pi^2}{63}\right) = 1. \qquad (6.79b)$$

Therefore, the next-to-leading-order contribution to the lateral Casimir force in

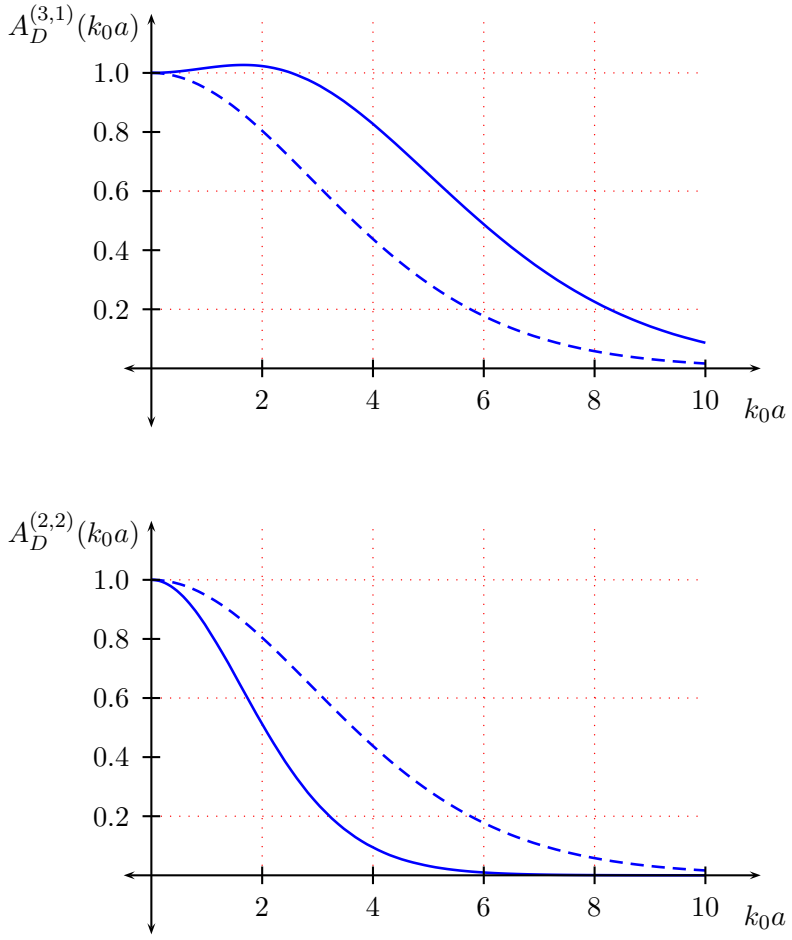

Figure 6.4: Dirichlet limit: Plot of $A_D^{(3,1)}(k_0a)$ and $A_D^{(2,2)}(k_0a)$ versus k_0a. The dashed curve represents $A_D^{(1,1)}(k_0a)$ which is plotted here for reference.

the Dirichlet limit reads

$$F^{(4)}_{\rm Lat,D} = 2\,k_0 a\,\sin(k_0 y_0)\,\left|F^{(0)}_{\rm Cas,D}\right|\,\frac{h_1}{a}\frac{h_2}{a}\,\frac{15}{4}\left[\left(\frac{h_1^2}{a^2}+\frac{h_2^2}{a^2}\right)A_D^{(3,1)}(k_0 a)\right.$$
$$\left.-2\cos(k_0 y_0)\,\frac{h_1}{a}\frac{h_2}{a}\,A_D^{(2,2)}(k_0 a)\right]. \quad (6.80)$$

Weak coupling limit

We have already evaluated the L-kernel for the weak coupling case in eq (6.75), so we can immediately evaluate the interaction energy. Alternatively, we can use the expressions for the I-kernels in the weak coupling limit (see eq. (6.74)) into eq. (6.76) to evaluate the integrals exactly in the spirit of section 6.2 and the answer can be expressed as derivatives. Using these in (6.59) we can write the total contribution to the interaction energy in the presence of corrugations in the weak limit to be

$$E^{(4)}_{12,W} = \left|E^{(0)}_{\rm Cas,W}\right|\,\frac{h_1}{a}\frac{h_2}{a}\frac{3}{2}\left[\cos(k_0 y_0)\left(\frac{h_1^2}{a^2}+\frac{h_2^2}{a^2}\right)A_W^{(4)}(k_0 a)\right.$$
$$\left.-\cos(2k_0 y_0)\frac{1}{2}\frac{h_1}{a}\frac{h_2}{a}A_W^{(4)}(2k_0 a)\right], \quad (6.81)$$

where in contrast to the result in the Dirichlet limit we observe the appearance of the same function, though with different arguments, as coefficients. This function has been suitably defined as

$$A_W^{(4)}(t_0) = \frac{t_0^5}{4!}\frac{\partial^4}{\partial t_0^4}\left[\frac{1}{t_0}\,e^{-t_0}\right] = e^{-t_0}\sum_{m=0}^{4}\frac{t_0^m}{m!} = \frac{e_4(t_0)}{e^{t_0}}, \quad (6.82)$$

so that it equals unity at $t_0 = 0$. These are plotted in figure 6.5. Using eq. (6.81) in eq. (6.10) we find that the fourth order contribution to the lateral Casimir force in

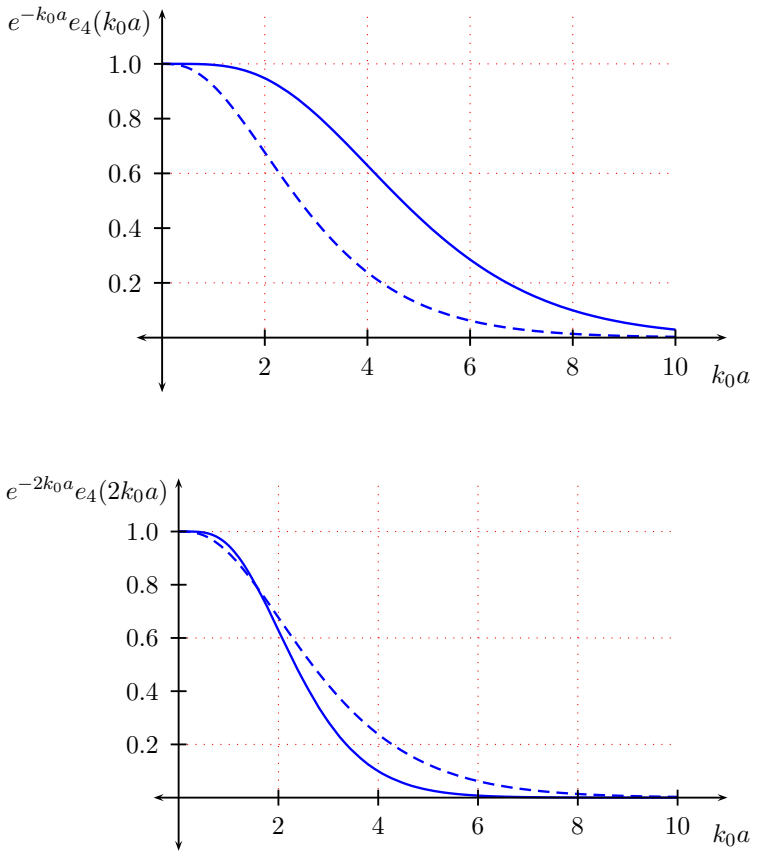

Figure 6.5: Weak coupling limit: Plot of $A_W^{(4)}(k_0 a)$ and $A_W^{(4)}(2k_0 a)$ versus $k_0 a$. The dashed curve represents $A_W^{(2)}(k_0 a)$ which is plotted here for reference.

the weak coupling limit equals

$$F^{(4)}_{\mathrm{Lat,W}} = k_0 a \, \sin(k_0 y_0) \left| F^{(0)}_{\mathrm{Cas,W}} \right| \, \frac{h_1}{a} \frac{h_2}{a} \, \frac{3}{2} \left[\left(\frac{h_1^2}{a^2} + \frac{h_2^2}{a^2} \right) A^{(4)}_W(k_0 a) \right.$$
$$\left. -2 \cos(k_0 y_0) \, \frac{h_1}{a} \frac{h_2}{a} \, A^{(4)}_W(2 k_0 a) \right] . \quad (6.83)$$

An exact functional form for the lateral force in the weak coupling limit in the second and fourth order in the perturbative expansion, see eq. (6.54) and eq. (6.83), allows us to investigate the approximation involved in the perturbative analysis more closely. We observe that in each perturbative order the leading powers of $k_0 a$ in the A-function cancels the a dependence in the prefactors associated with h_i. Thus we conclude that the perturbation analysis is valid for $k_0 h \ll 1$. The formal expansions performed in the intermediate steps further restricts our analysis to be valid for $h_1 + h_2 < a$ for arbitrary offset.

6.4 Proximity force approximation

As a preliminary check for the results calculated for the lateral force we shall verify that in the proximity force limit ($k_0 a \to 0$, keeping h_i/a fixed) our results in eqs. (6.48), (6.54), (6.80), and (6.83) reproduce the standard PFA result approximated to appropriate orders in h_i/a. For this purpose let us evaluate the lateral Casimir force in the proximity force approximation for the sinusoidal corrugations described by eq. (6.41). We begin by writing the distance between the corrugated plates as

$$a(y) = a + h_2 \sin[k_0 y] - h_1 \sin[k_0 (y + y_0)]. \quad (6.84)$$

For sufficiently small a (in comparison to $d = 2\pi\, k_0^{-1}$) we can treat the plates to be built out of small sections of length dy for which the energy is approximately that of the parallel plate geometry.

Dirichlet limit

Using the expression for the Casimir force between parallel plates in the Dirichlet limit we can thus write

$$dE_D^{\rm PFA}(a(y)) = -L_x\, dy\, \frac{\pi^2}{1440}\frac{1}{a(y)^3}, \tag{6.85}$$

where we interpret $L_x\, dy$ to be the area of the small section under consideration. Thus the total Casimir energy in this approximation, after interpreting $L_y = \lim_{N\to\infty} Nd$, will be

$$\begin{aligned}\frac{E_D^{\rm PFA}}{L_x L_y} &= -\frac{\pi^2}{1440}\,\frac{1}{a^3}\,\frac{1}{2\pi}\int_{-\pi}^{\pi} d\theta \frac{1}{\left[1+\frac{h_2}{a}\sin\theta - \frac{h_1}{a}\sin(\theta + k_0 y_0)\right]^3} \\ &= -\frac{\pi^2}{1440}\,\frac{1}{a^3}\,\frac{1}{2\pi}\int_{-\pi}^{\pi} d\theta \frac{1}{\left[1-\frac{r}{a}\cos\theta\right]^3},\end{aligned} \tag{6.86}$$

where we have used the substitutions: $r\sin\alpha = h_2 - h_1\cos k_0 y_0$, $r\cos\alpha = h_1 \sin k_0 y_0$, and used the periodicity property of the function to eliminate α. We note that $r^2 = h_1^2 + h_2^2 - 2h_1 h_2 \cos(k_0 y_0)$.

As was emphasized in the calculations in the earlier sections we have been subtracting the energies that do not contribute to the lateral force by treating them as a background. This has not been achieved in the above expression in eq. (6.86) and thus should not be naively compared with our earlier results. But, evaluation of the lateral force will let us compare the expressions. Thus, we calculate the lateral

Casimir force in the proximity force approximation, using eq. (6.86) in eq. (6.10), to be

$$F^{\rm PFA}_{\rm Lat,D} = 2\,k_0 a\,\sin(k_0 y_0)\,\left|F^{(0)}_{\rm Cas,D}\right|\,\frac{h_1}{a}\frac{h_2}{a}\,\frac{1}{4}\left[\frac{5}{(1-\frac{r^2}{a^2})^{\frac{7}{2}}} - \frac{1}{(1-\frac{r^2}{a^2})^{\frac{5}{2}}}\right], \tag{6.87}$$

for $|h_1| + |h_2| < a$. The basic integral involved in evaluating the above expression is

$$\frac{1}{2\pi}\int_{-\pi}^{\pi} d\theta\,\frac{1}{(a - r\cos\theta)} = \frac{1}{\sqrt{a^2 - r^2}}, \quad \text{for} \quad r < a, \tag{6.88}$$

which, after the substitution $z = \exp(i\theta)$, leads to a contour integral on the unit circle in the complex plane. Thus, using Cauchy's theorem only those roots of the denominator that are within the unit circle contribute to the integral.

The PFA result in the leading order for the perturbation parameter is obtained by setting $r = 0$ in eq. (6.87). This matches exactly with eq. (6.48) to the leading order in $k_0 a$. This verifies the proximity force limit of the leading order perturbative result. The proximity force limit of the next-to-leading-order result in eq. (6.80) is similarly verified by matching it with eq. (6.87) after evaluating eq. (6.87) to the fourth order in the perturbation parameter r/a.

Weak coupling limit

In the weak coupling limit and in the proximity approximation the equation corresponding to eq. (6.85) is

$$dE^{\rm PFA}_W(a(y)) = -L_x\,dy\,\frac{\lambda_1\lambda_2}{32\,\pi^2}\frac{1}{a(y)} \tag{6.89}$$

and leads to, after extracting L_y, and proceeding in the same manner as in eq. (6.86),

$$\frac{E_W^{\rm PFA}}{L_x L_y} = -\frac{\lambda_1\lambda_2}{32\,\pi^2}\,\frac{1}{a}\,\frac{1}{2\pi}\int_{-\pi}^{\pi} d\theta \frac{1}{(1+\frac{r}{a}\cos\theta)} = -\frac{\lambda_1\lambda_2}{32\,\pi^2}\,\frac{1}{a}\frac{1}{(1-\frac{r^2}{a^2})^{\frac{1}{2}}}, \qquad (6.90)$$

for $|h_1| + |h_2| < a$. We calculate the lateral Casimir force in the weak coupling limit in the proximity force approximation, using eq. (6.10), to be

$$F_{\rm Lat,W}^{\rm PFA} = k_0 a\,\sin(k_0 y_0)\,\left|F_{\rm Cas,W}^{(0)}\right|\,\frac{h_1}{a}\frac{h_2}{a}\,\frac{1}{(1-\frac{r^2}{a^2})^{\frac{3}{2}}}, \quad \text{for} \quad |h_1| + |h_2| < a. \qquad (6.91)$$

The proximity force limit of the leading- and next-to-leading-order results in the weak coupling limit, eq. (6.54) and eq. (6.83), can be verified by keeping the appropriate terms in eq. (6.91).

6.5 Analysis and discussion

In this section we shall exclusively deal either in the Dirichlet limit or in the weak coupling limit. We shall further confine ourselves to the case $h_1 = h_2 = h$. Also, we shall find it convenient to define the following dimensionless quantities

$$\mathcal{F}_D\left(k_0 a, \frac{h}{a}, k_0 y_0\right) = \frac{F_{\rm Lat,D}\left(k_0 a, \frac{h}{a}, k_0 y_0\right)}{2\,\left|F_{\rm Cas,D}^{(0)}\right|\,\frac{h^2}{a^2}\,k_0 a\,\sin(k_0 y_0)}, \qquad (6.92a)$$

$$\mathcal{F}_W\left(k_0 a, \frac{h}{a}, k_0 y_0\right) = \frac{F_{\rm Lat,W}\left(k_0 a, \frac{h}{a}, k_0 y_0\right)}{\left|F_{\rm Cas,W}^{(0)}\right|\,\frac{h^2}{a^2}\,k_0 a\,\sin(k_0 y_0)}. \qquad (6.92b)$$

We shall use superscripts $[m, n]$ on these dimensionless quantities to denote the order in the power series expansion to which the lateral force (not $\mathcal{F}$) have been calculated. In particular m will signify the order in the parameter $k_0 a$, and n will denote the

order in h/a. The result in the proximity force approximation should be valid to the first order in $k_0 a$. Thus $\mathcal{F}^{[1,\infty]}$ will represent the PFA result in our notation. The perturbative results are complete in the $k_0 a$ dependence and thus will be denoted by $\mathcal{F}^{[\infty,n]}$. We use square brackets to avoid the confusion it might lead to with the already introduced notation to denote the powers in h_i's in the superscripts of the A-functions. This notation is being introduced purely for convenience and the analyticity in the variables needs scrutiny. In these notations our results can be summarized as (see eqs. (6.48), (6.54), (6.80), (6.83), (6.87), and (6.91))

$$\mathcal{F}_D^{[\infty,4]} = A_D^{(1,1)}(k_0 a) + \frac{15}{2}\frac{h^2}{a^2}\Big[A_D^{(3,1)}(k_0 a) - \cos(k_0 y_0)\, A_D^{(2,2)}(k_0 a)\Big], \tag{6.93a}$$

$$\mathcal{F}_W^{[\infty,4]} = \frac{e_2(k_0 a)}{e^{k_0 a}} + 3\frac{h^2}{a^2}\left[\frac{e_4(k_0 a)}{e^{k_0 a}} - \cos(k_0 y_0)\,\frac{e_4(2k_0 a)}{e^{2k_0 a}}\right], \tag{6.93b}$$

$$\mathcal{F}_D^{[1,\infty]} = \frac{1}{4}\left[\frac{5}{(1-\frac{r^2}{a^2})^{\frac{7}{2}}} - \frac{1}{(1-\frac{r^2}{a^2})^{\frac{5}{2}}}\right], \tag{6.93c}$$

$$\mathcal{F}_W^{[1,\infty]} = \frac{1}{(1-\frac{r^2}{a^2})^{\frac{3}{2}}}, \tag{6.93d}$$

where we recall the definition of r after eq. (6.86). As we mentioned earlier these expressions match to the order $[1,4]$ both in the Dirichlet and weak limit. Recall, as justified after eq. (6.83), that $k_0 h$ is the perturbative parameter. Thus, we shall find it convenient to keep $k_0 h$ fixed while discussing the perturbative results. This should be contrasted with the case of proximity force approximation where it is more convenient to keep the parameter h/a fixed. All of the results in eq. (6.93) are valid for $2h < a$.

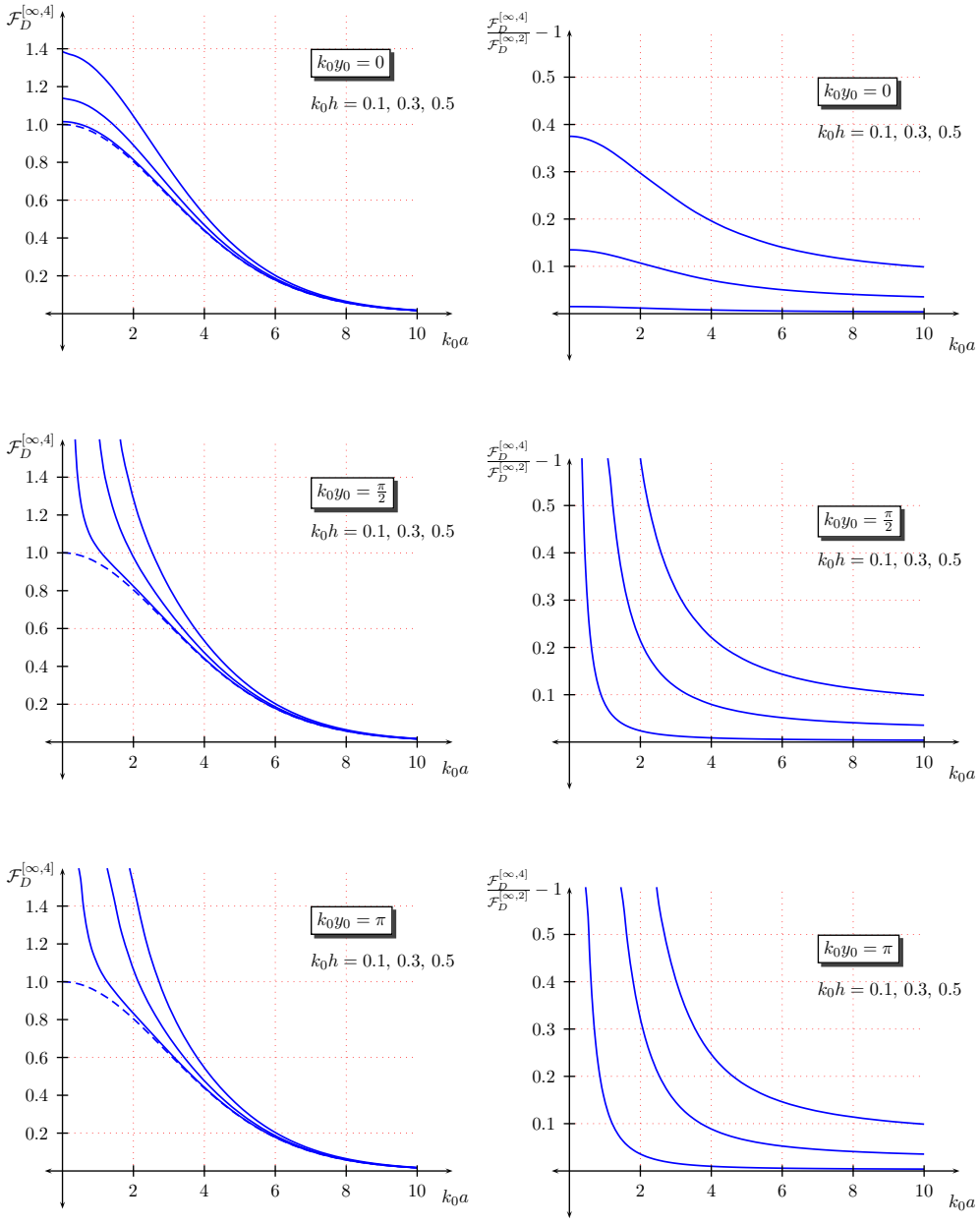

Figure 6.6: Dirichlet limit: The plots on the left show $\mathcal{F}_D^{[\infty,4]}$ versus k_0a for various values of k_0y_0. The dashed curve represents $\mathcal{F}_D^{[\infty,2]}$ which is plotted here for reference. In each plot the higher values of k_0h deviate more from the reference. The plots on the right show the fractional correction in the next-to-leading order contribution. In each plot the higher values of k_0h have larger corrections.

Dirichlet limit

We plot the lateral force for the Dirichlet limit, $\mathcal{F}_D^{[\infty,4]}$, with the fractional corrections due to the next-to-leading contribution, in figure 6.6. The plots diverge as $k_0 a \to 2k_0 h$ because the perturbation series breaks down beyond that point. The plots for $k_0 y_0 = 0$ do not diverge, see eq. (6.93). We observe that, while keeping $k_0 y_0$ fixed, the fractional corrections due to the next-to-leading order are small for $k_0 h \ll 1$.

In the absence of an exact answer, for the Dirichlet case, to compare with it is not possible to extract the precise error in the perturbative results. In the next section we shall evaluate the corresponding result in the weak coupling limit and evaluate the lateral Casimir force non-perturbatively. We show that the error in the lateral force, for the weak coupling limit, after the next-to-leading order has been included is small for $k_0 h \ll 1$. Presuming that the same would hold for the Dirichlet case, we can expect the error to be sufficiently small for comparison with experimental data. (Comparison with experiments requires the corresponding evaluation for the electromagnetic case, which will be taken up in a later publication.)

Weak coupling limit - Non-perturbative results

The plots for the lateral force in the weak coupling limit, $\mathcal{F}_W^{[\infty,4]}$, which have not been displayed here, have the same qualitative content as the Dirichlet case shown in figure 6.6. To estimate the error in the perturbative results we shall now attempt a non-perturbative evaluation of the lateral Casimir force in the weak coupling limit.

We begin by pointing out the remarkable observation in [6] that exact results for the Casimir force, in the weak coupling limit, can be achieved for specific geometries. This is being extended for a class of geometries, for the scalar case, in [69], and

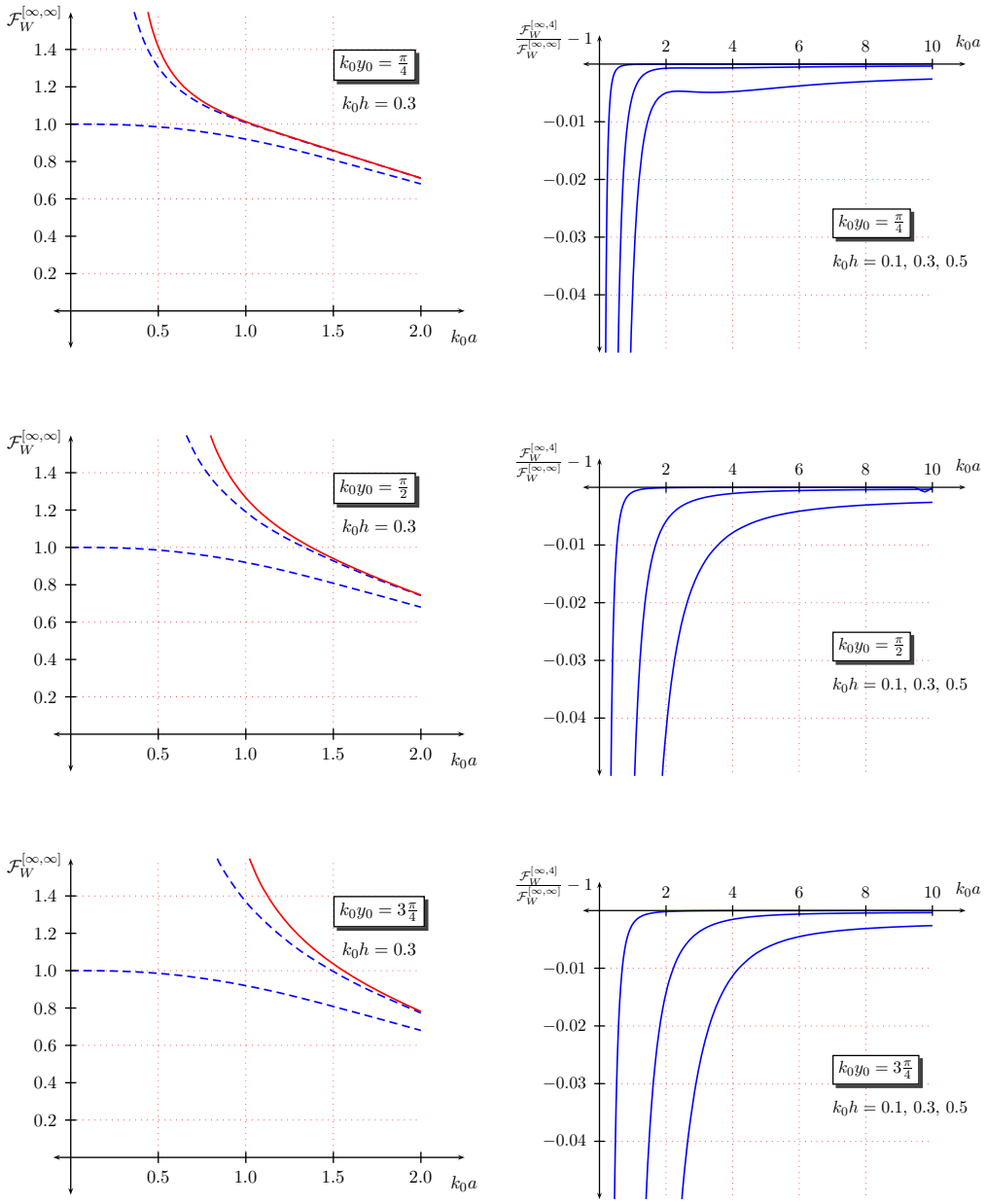

Figure 6.7: Weak coupling limit: The plots on the left show $\mathcal{F}_D^{[\infty,\infty]}$ versus k_0a for various values of k_0y_0 at $k_0h = 0.3$. The dashed curves represents $\mathcal{F}_D^{[\infty,2]}$ and $\mathcal{F}_D^{[\infty,4]}$ which is plotted here for reference. In each plot the exact value is greater than the value estimated by $\mathcal{F}_D^{[\infty,4]}$. The plots on the right show the fractional error in the perturbative result. In each plot the higher values of k_0h have larger errors.

another paper [70] has covered dielectrics in electromagnetism. Starting from the central formula in [69] (alternatively using eq. (6.19), for the weak coupling limit) we will have

$$\frac{E_W}{L_x} = -\frac{\lambda_1\lambda_2}{32\pi^3}\int_{-\infty}^{\infty} dy \int_{-\infty}^{\infty} dy' \frac{1}{(y-y')^2 + a(y,y')^2}, \tag{6.94}$$

where $a(y,y') = a + h_2\sin[k_0 y'] - h_1\sin[k_0(y+y_0)]$. Changing variables, $y - y' \to y$, $y + y' \to 2\theta/k_0$, and making substitutions very similar to those made after eq. (6.86), we have

$$\frac{E_W}{L_x L_y} = -\frac{\lambda_1\lambda_2}{32\pi^2}\frac{1}{2\pi^2}\int_{-\infty}^{\infty} dy \int_{0}^{2\pi} d\theta \frac{1}{y^2 + [a - r(k_0 y)\cos\theta]^2}, \tag{6.95}$$

where $r(k_0 y)^2 = h_1^2 + h_2^2 - 2h_1 h_2\cos(k_0 y + k_0 y_0)$, which is different from the expression for r in the PFA case, presented after eq. (6.86), in the dependence in the argument of the cosine function. Nevertheless, the θ integral can still be performed using eq. (6.88) to yield

$$\frac{E_W}{L_x L_y} = -\frac{\lambda_1\lambda_2}{32\pi^2}\frac{1}{\pi}\int_{-\infty}^{\infty}\frac{dy}{y}\,\mathrm{Re}\left[\frac{1}{(y+ia)^2 + r(k_0 y)^2}\right]^{\frac{1}{2}}, \quad \text{for} \quad |h_1| + |h_2| < a. \tag{6.96}$$

Using the above expression in eq. (6.10) we calculate the lateral force per unit area in the weak coupling limit to be

$$\frac{F_{\mathrm{Lat,W}}}{L_x L_y} = -\frac{\lambda_1\lambda_2}{32\pi^2\, a^2}\frac{h_1}{a}\frac{h_2}{a}(k_0 a)^4\frac{1}{\pi}\int_{-\infty}^{\infty}\frac{dt}{t}\,\mathrm{Re}\left[\frac{\sin(t + k_0 y_0)}{[(t+ik_0 a)^2 + \{k_0 r(t)\}^2]^{\frac{3}{2}}}\right], \tag{6.97}$$

for $|h_1| + |h_2| < a$. Expanding the denominator in the above expression as a power series in $k_0 r/(t + ik_0 a)$, lets us evaluate the integral using the residue theorem. We can thus write, after letting $h_1 = h_2 = h$, which leads to the simplification, $r(k_0 y_0) =$

$2h\sin[(k_0y+k_0y_0)/2]$,

$$\frac{F_{\rm Lat,W}}{L_xL_y}=\frac{\lambda_1\lambda_2}{32\pi^2\,a^2}(k_0a)^2{\rm Re}\Bigg[\frac{e^{-ik_0y_0}}{(-i)}\sum_{n=0}^{\infty}\frac{1}{[n!]^2}\frac{1}{2n+2}\times\Big(h\frac{\partial}{\partial a}\Big)^{2n+2}\frac{1}{k_0a}\,e^{-k_0a}\sin^{2n}\Big(\frac{k_0y_0}{2}-i\frac{k_0a}{2}\Big)\Bigg],\quad(6.98)$$

which reproduces the leading and next-to-leading results in eqs. (6.54) and (6.83) for the case $n=0$ and $n=1$ respectively. This expression justifies our presumption that the perturbative analysis holds as an asymptotic expansion as $k_0h\to 0$. Expressing the above sum in a closed form, or evaluation of the integral in eq. (6.97), would lead to an exact expression for the lateral force in the weak coupling limit. We have not been able to achieve either, however, so we shall rely on numerical evaluation.

In terms of the notation introduced in eq. (6.92) we can write eq. (6.97) as

$$\mathcal{F}_W^{[\infty,\infty]}=-\frac{(k_0a)^3}{\sin(k_0y_0)}\frac{1}{\pi}\int_{-\infty}^{\infty}\frac{dt}{t}\,{\rm Re}\Bigg[\frac{\sin(t+k_0y_0)}{[(t+ik_0a)^2+\{k_0r(t)\}^2]^{\frac{3}{2}}}\Bigg],\quad(6.99)$$

for $2h<a$. The above non-perturbative expression for the lateral Casimir force on corrugated plates, in the weak coupling limit, has been plotted in figure 6.7. For comparison purposes the perturbative results are plotted as dashed curves in figure 6.7. Actually, we found the numerical evaluation of eq. (6.95), after evaluating the derivative with respect to y_0, easier than that of eq. (6.99). We observe that the perturbative results, when the next-to-leading order is included, compares with the exact result remarkably well for $k_0h\ll 1$ and $2h<a$. The fractional error in the lateral force when the next-to-leading order contribution is included is displayed on the right column in figure 6.7.

Validity of PFA

We shall now compare the PFA result in the weak limit, derived in eq. (6.91), with the non-perturbative result in eq. (6.97). In figure 6.8 we plot the fractional error in the PFA result, for fixed $k_0 h$, and compare it to the fractional error in the perturbative results. We note that PFA is a good approximation for $k_0 a \ll 1$ and perturbative results are valid for $k_0 h \ll 1$. Both the PFA and the perturbative analysis are restricted to $2h < a$. The $2h < a$ restriction is necessary for the force being finite, due to non-overlapping of the potentials for arbitrary offset. For special offsets, the restriction is weaker, and there is no restriction at all, for zero offset. The precise dependence of the restriction on the offset is gotten by referring to eq. (6.91) and observing that the validity regime is $2h \sin(k_0 y_0/2) < a$.

A recent debate, see [64, 65, 66], involved the comparison of the PFA result and the perturbative result. In [53] the authors consider rectangular gratings and for their geometry find 24% deviation from PFA. We earlier noted that the PFA limit is obtained by taking the limit $k_0 a \to 0$ while keeping the ratio h/a fixed. In figure 6.9 we plot the lateral force in the PFA limit and compare it with the non-perturbative result for various values of $k_0 a$. This justifies our presumption that the PFA is a good approximation for $k_0 a \ll 1$. We note that the error in the PFA is less than 1% for $k_0 a \ll 1$ for arbitrary h/a. For $k_0 y_0 = \pi/4$, we observe that the PFA is a very good approximation for $h \sim a$ which satisfies $2h \sin(k_0 y_0/2) < a$. After viewing the plots for various values of $k_0 y_0$ we note that in general the PFA is a good approximation for $h \sim a$ and further beyond for offsets $k_0 y_0 < \pi/4$. It is, in fact, plausible that the PFA holds for large amplitude corrugations for small offsets because the corrugations fit together like fingers in a glove.

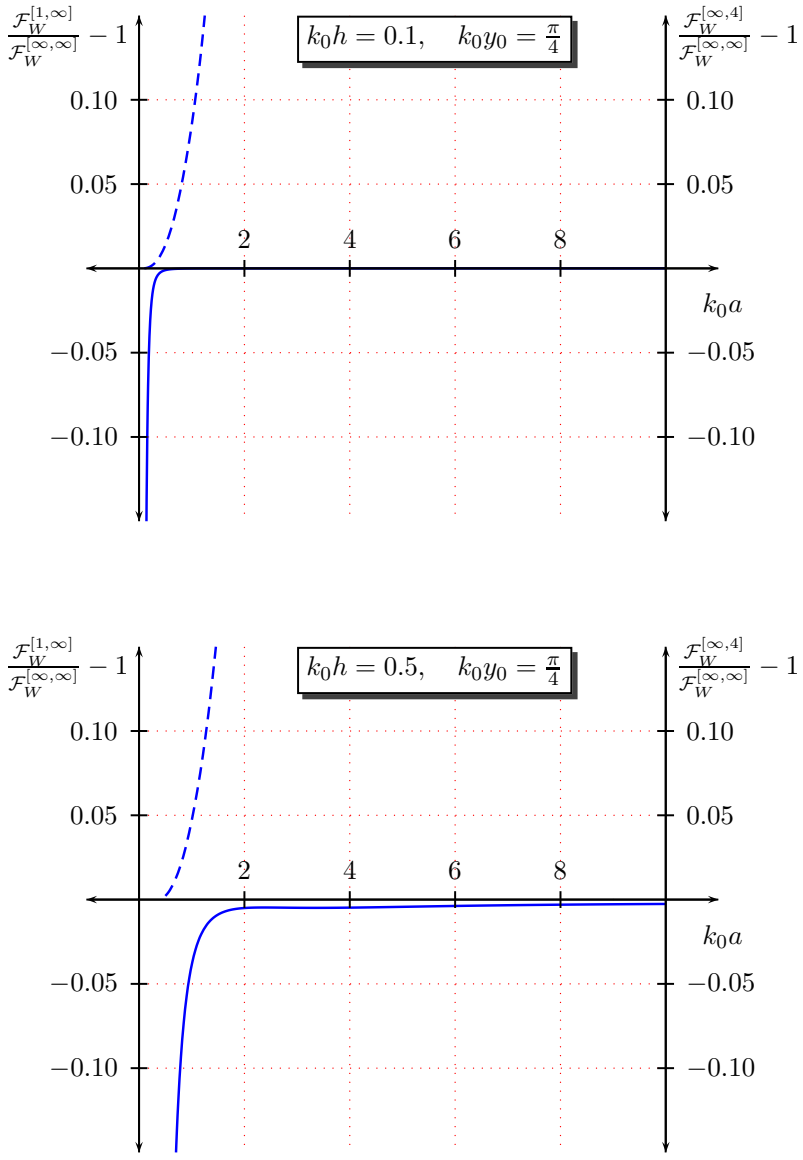

Figure 6.8: Weak coupling limit: Fractional error in PFA is plotted as the dashed curve. The corresponding error in the perturbative result is plotted as the bold curve and is described by the axis on the right.

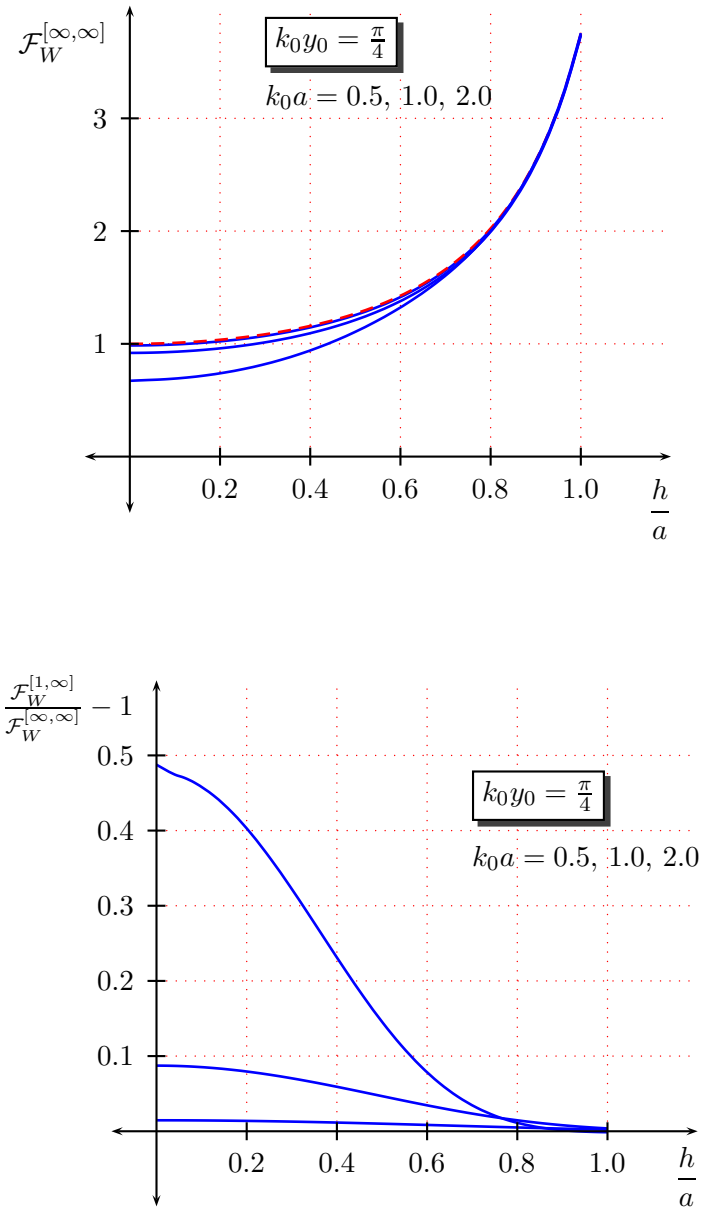

Figure 6.9: Weak coupling limit: On the left the PFA is shown as the dashed curve. The exact results for higher values of $k_0 a$ are seen to deviate from the dashed curve. On the right the fractional error in PFA is shown to increase with higher values of $k_0 a$.

Conclusions

In chapters 1 to 3 we have demonstrated that the Casimir energy is a manifestation of the quantum vacuum and reviewed the case of two parallel plates described by δ-function potentials for the scalar case.

In chapters 4 and 5 we have demonstrated that Casimir energy associated with two parallel plates, including the divergent contributions from single plates, experiences inertial forces on it exactly like a conventional mass. The generalization of this for the case of a cylinder and a sphere is expected to shed light into the intriguing subject of self-stress in these geometries. The classic example being the repulsive force on a sphere [71].

In chapter 6 we have evaluated the lateral Casimir force between corrugated plates up to the next-to-leading order in the corrugation amplitude for the case of sinusoidal corrugations. Generalization of this study to the case of electrodynamics and other geometries should find application in the design of practical nanomechanical devices.

Bibliography

[1] H. B. G. Casimir. On the attraction between two perfectly conducting plates. *Kon. Ned. Akad. Wetensch. Proc.*, 51:793, 1948.

[2] S. K. Lamoreaux. Demonstration of the Casimir force in the 0.6 to 6 micrometers range. *Phys. Rev. Lett.*, 78:5, 1997.

[3] R. L. Jaffe. The Casimir effect and the quantum vacuum. *Phys. Rev.*, D72:021301, 2005, hep-th/0503158.

[4] J. Schwinger. Casimir effect in source theory. *Lett. Math. Phys.*, 1:43, 1975.

[5] T. Emig, N. Graham, R. L. Jaffe, and M. Kardar. Casimir Forces between compact objects: I. The scalar case. *Phys. Rev.*, D77:025005, 2008, 0710.3084.

[6] K. A. Milton and J. Wagner. Multiple scattering methods in Casimir calculations. *J. Phys.*, A41:155402, 2008, 0712.3811.

[7] J. S. Schwinger. The theory of quantized fields. I. *Phys. Rev.*, 82:914, 1951.

[8] J. S. Schwinger. The theory of quantized fields. II. *Phys. Rev.*, 91:713, 1953.

[9] J. S. Schwinger. On the Green's functions of quantized fields. 1. *Proc. Nat. Acad. Sci.*, 37:452, 1951.

[10] J. S. Schwinger. On the Green's functions of quantized fields. 2. *Proc. Nat. Acad. Sci.*, 37:455, 1951.

[11] J. Schwinger. The algebra of microscopic measurement. *Proc. Nat. Acad. Sci.*, 45:1542, 1959.

[12] J. Schwinger. The geometry of quantum states. *Proc. Nat. Acad. Sci.*, 46:257, 1960.

[13] J. Schwinger. Unitary operator bases. *Proc. Nat. Acad. Sci.*, 46:570, 1960.

[14] J. Schwinger. Unitary transformations and the action principle. *Proc. Nat. Acad. Sci.*, 46:883, 1960.

[15] J. Schwinger. The special canonical group. *Proc. Nat. Acad. Sci.*, 46:1401, 1960.

[16] J. Schwinger. Quantum variables and the action principle. *Proc. Nat. Acad. Sci.*, 47:1075, 1961.

[17] J. Schwinger. Exterior algebra and the action principle, I. *Proc. Nat. Acad. Sci.*, 48:603, 1962.

[18] M. Bordag, D. Hennig, and D. Robaschik. Vacuum energy in quantum field theory with external potentials concentrated on planes. *J. Phys.*, A25:4483, 1992.

[19] M. Abramowitz and I. A. Stegun. *Handbook of Mathematical Functions with Formulas, Graphs, and Mathematical Tables*. Dover, New York, 1964.

[20] S. A. Fulling and R. Estrada. Functions and distributions in spaces with thick points. *Internat. J. Appl. Math. Stat.*, 10:25, 2007.

[21] N. Graham, R. L. Jaffe, V. Khemani, M. Quandt, O. Schroeder, and H. Weigel. The Dirichlet Casimir problem. *Nucl. Phys.*, B677:379, 2004, hep-th/0309130.

[22] K. A. Milton. Casimir energies and pressures for delta-function potentials. *J. Phys.*, A37:6391, 2004, hep-th/0401090.

[23] S. A. Fulling, K. A. Milton, P. Parashar, A. Romeo, K. V. Shajesh, and J. Wagner. How does Casimir energy fall? *Phys. Rev.*, D76:025004, 2007, hep-th/0702091.

[24] D. Deutsch and P. Candelas. Boundary effects in quantum field theory. *Phys. Rev.*, D20:3063, 1979.

[25] P. Candelas. Vacuum polarization in the presence of dielectric and conducting surfaces. *Ann. Phys.*, 143:241, 1982.

[26] P. Candelas. Vacuum energy in the bag model. *Ann. Phys.*, 167:257, 1986.

[27] G. Barton. Perturbative Casimir energies of dispersive spheres, cubes and cylinders. *J. Phys.*, A34:4083, 2001.

[28] G. Barton. Casimir energies of spherical plasma shells. *J. Phys.*, A37:1011, 2004.

[29] M. Karim, A. H. Bokhari, and B. J. Ahmedov. The Casimir force in the Schwarzschild metric. *Class. Quant. Grav.*, 17:2459, 2000.

[30] E. Calloni, L. Di Fiore, G. Esposito, L. Milano, and L. Rosa. Vacuum fluctuation force on a rigid Casimir cavity in a gravitational field. *Phys. Lett.*, A297:328, 2002, quant-ph/0109091.

[31] R. R. Caldwell. Gravitation of the Casimir effect and the cosmological non-constant. 2002, astro-ph/0209312.

[32] F. Sorge. Casimir effect in a weak gravitational field. *Class. Quant. Grav.*, 22:5109, 2005.

[33] G. Bimonte, E. Calloni, G. Esposito, and L. Rosa. Energy-momentum tensor for a Casimir apparatus in a weak gravitational field. *Phys. Rev.*, D74:085011, 2006, hep-th/0606042.

[34] K. A. Milton, P. Parashar, K. V. Shajesh, and J. Wagner. How does Casimir energy fall? II. Gravitational acceleration of quantum vacuum energy. *J. Phys.*, A40:10935, 2007, 0705.2611.

[35] K. V. Shajesh, K. A. Milton, P. Parashar, and J. A. Wagner. How does Casimir energy fall? III. Inertial forces on vacuum energy. *J. Phys.*, A41:164058, 2008, 0711.1206.

[36] G. Bimonte, E. Calloni, G. Esposito, and L. Rosa. Relativistic mechanics of Casimir apparatuses in a weak gravitational field. *Phys. Rev.*, D76:025008, 2007, hep-th/0703062.

[37] G. Bimonte, G. Esposito, and L. Rosa. From Rindler space to the electromagnetic energy-momentum tensor of a Casimir apparatus in a weak gravitational field. 2008, 0804.2839.

[38] W. Rindler. Kruskal space and the uniformly accelerated frame. *Am. J. Phys.*, 34:1174, 1966.

[39] K. A. Milton. The Casimir effect: Recent controversies and progress. *J. Phys.*, A37:R209, 2004, hep-th/0406024.

[40] N. R. Khusnutdinov. Zeta-function approach to Casimir energy with singular potentials. *Phys. Rev.*, D73:025003, 2006, hep-th/0511038.

[41] A. A. Saharian, R. S. Davtyan, and A. H. Yeranyan. Casimir energy in the Fulling-Rindler vacuum. *Phys. Rev.*, D69:085002, 2004, hep-th/0307163.

[42] G. Barton and A. Calogeracos. On the Quantum Electrodynamics of a dispersive mirror. I. Mass shifts, radiation, and radiative reaction. *Ann. Phys.*, 238:227, 1995.

[43] A. Calogeracos and G. Barton. On the Quantum Electrodynamics of a dispersive mirror. II. The boundary condition and the applied force via Dirac's theory of constraints. *Ann. Phys.*, 238:268, 1995.

[44] A. D. Helfer. Moving mirrors and thermodynamic paradoxes. *Phys. Rev.*, D63:025016, 2001, hep-th/0001004.

[45] N. Nicolaevici. Quantum radiation from a partially reflecting moving mirror. *Class. Quant. Grav.*, 18:619, 2001, gr-qc/9910098.

[46] J. Haro and E. Elizalde. Physically sound Hamiltonian formulation of the dynamical Casimir effect. *Phys. Rev.*, D76:065001, 2007, 0705.0597.

[47] A. A. Saharian and M. R. Setare. Surface vacuum energy and stresses on a plate uniformly accelerated through the Fulling-Rindler vacuum. *Class. Quant. Grav.*, 21:5261, 2004, hep-th/0404080.

[48] M. R. Setare. Surface vacuum energy and stresses for a brane in de Sitter spacetime. *Phys. Lett.*, B620:111, 2005, hep-th/0505108.

[49] A. A. Saharian and M. R. Setare. Surface Casimir densities on a spherical brane in Rindler- like spacetimes. *Phys. Lett.*, B637:5, 2006, hep-th/0512278.

[50] M. Born. *Ann. Phys. (Leipzig)*, 30:1, 1909.

[51] K. A. Milton, S. A. Fulling, P. Parashar, A. Romeo, K. V. Shajesh, and J. A. Wagner. Gravitational and Inertial Mass of Casimir Energy. *J. Phys.*, A41:164052, 2008, 0710.3841.

[52] C Møller. *The Theory of Relativity*. Oxford University Press, Delhi, 2nd edition, 1972.

[53] A. Lambrecht and V. N. Marachevsky. Casimir interaction of dielectric gratings. 2008, 0806.3142.

[54] H. B. Chan, Y. Bao, J. Zou, R. A. Cirelli, F. Klemens, W. M. Mansfield, and C. S. Pai. Measurement of the casimir force between a gold sphere and silicon surface with nanoscale trench arrays. 2008, 0805.3776.

[55] Yu. S. Barash. *Izv. Vuzov. Ser. Radiofiz.*, 16:1086, 1973.

[56] R. Golestanian and M. Kardar. The mechanical response of vacuum. *Phys. Rev. Lett.*, 78:3421, 1997, quant-ph/9701005.

[57] R. Golestanian and M. Kardar. Path-integral approach to the dynamic casimir effect with fluctuating boundaries. *Phys. Rev. A*, 58(3):1713, Sep 1998.

[58] T. Emig, A. Hanke, R. Golestanian, and M. Kardar. Probing the Strong Boundary Shape Dependence of the Casimir Force. *Phys. Rev. Lett.*, 87:260402, 2001, cond-mat/0106028.

[59] T. Emig, A. Hanke, R. Golestanian, and M. Kardar. Normal and lateral casimir forces between deformed plates. *Phys. Rev. A*, 67(2):022114, Feb 2003.

[60] R. Büscher and T. Emig. Non perturbative approach to Casimir interactions in periodic geometries. *Phys. Rev. A*, 69(6):062101, Jun 2004, cond-mat/0401451.

[61] A. Roy and U. Mohideen. Demonstration of the nontrivial boundary dependence of the casimir force. *Phys. Rev. Lett.*, 82(22):4380, May 1999.

[62] F. Chen, U. Mohideen, G. L. Klimchitskaya, and V. M. Mostepanenko. Demonstration of the lateral casimir force. *Phys. Rev. Lett.*, 88(10):101801, Feb 2002.

[63] F. Chen, U. Mohideen, G. L. Klimchitskaya, and V. M. Mostepanenko. Experimental and theoretical investigation of the lateral casimir force between corrugated surfaces. *Phys. Rev. A*, 66(3):032113, Sep 2002.

[64] R. B. Rodrigues, P. A. Maia Neto, A. Lambrecht, and S. Reynaud. Lateral Casimir force beyond the Proximity Force Approximation. *Phys. Rev. Lett.*, 96:100402, 2006, quant-ph/0603120.

[65] F. Chen, U. Mohideen, G. L. Klimchitskaya, and V. M. Mostepanenko. Comment on "Lateral Casimir force beyond the proximity force approximation". *Phys. Rev. Lett.*, 98:068901, 2007, quant-ph/0702060.

[66] R. B. Rodrigues, P. A. Maia Neto, A. Lambrecht, and S. Reynaud. Rodrigues et al. reply to [65]. *Phys. Rev. Lett.*, 98(6):068902, 2007.

[67] I. Cavero-Pelaez, K. A. Milton, P. Parashar, and K. V. Shajesh. Non-contact gears: I. Next-to-leading order contribution to lateral Casimir force between corrugated parallel plates. 2008, 0805.2776.

[68] I. Cavero-Pelaez, K. A. Milton, P. Parashar, and K. V. Shajesh. Non-contact gears: II. Casimir torque between concentric corrugated cylinders for the scalar case. 2008, 0805.2777.

[69] K. A. Milton, P. Parashar, and J. Wagner. In preparation.

[70] K. A. Milton, P. Parashar, and J. Wagner. Exact results for Casimir interactions between dielectric bodies: The weak-coupling or van der Waals Limit. 2008, 0806.2880.

[71] T. H. Boyer. Quantum electromagnetic zero-point energy of a conducting spherical shell and the casimir model for a charged particle. *Phys. Rev.*, 174(5):1764, Oct 1968.